THE ROLE OF GINGKO BILOBA EXTRACT ON AUTOPHAGY MODULATION, PROTEIN CLEARANCE AND NEURONAL CELL DEATH IN AN *IN VITRO* MODEL OF ALZHEIMER'S DISEASE

by Akile Khoza

Thesis presented in fulfilment of requirements for the degree of Master of Science in the Faculty of Science at Stellenbosch University

Supervisor: Prof Benjamin Loos

April 2019

Declaration

By submitting this thesis electronically, I declare that the entirety of the work contained therein is my own original work, that I am the authorship owner thereof (unless to the extent explicitly otherwise stated) and that I have not previously in its entirety or in part submitted it for obtaining any qualification.

Signature:

Date:2018/12/19

Abstract

Introduction: Alzheimer's disease (AD) is a complex neurological disease, characterized by two protein aggregate forms, namely extracellular amyloid-beta (Aβ) plaques and intracellular neurofibrillary tangles of tau protein. AD is the most common type of progressive dementia and is currently poorly treated, which is associated with poor clinical outcomes. Although significant insight has been gained regarding AD pathology, limited progress has been made in the development of pharmaceutical therapeutics that modify or reverse the debilitating effects of this disease. Autophagy is a vital process involved in cellular survival, as it is essential for organelle and long-lived protein turnover. As such, it is widely accepted that autophagy impairment is a major contributing factor in the development of AD. Gingko biloba (GB) and lithium chloride (LiCl) have been reported to be neuroprotective in the context of neurodegenerative diseases. Even though some countries readily prescribe GB and LiCl to individuals suffering from AD, their mechanism of action, their potency in enhancing autophagy and their ability to clear toxic protein aggregates remains largely unclear. We hypothesized that treatment with GB will exhibit a concentration dependent effect on autophagic activity, and this effect will be further enhanced through combination treatment with LiCl. This effect may then translate in the distinct removal of amyloid precursor protein (APP) and Aβ, preserving lysosomal function and mitochondrial integrity. The aim of the proposed study was therefore to investigate the effect of both GB and LiCl as a single or combination treatment intervention on the modulation of autophagy activity, and the mitigation of Aβ proteotoxicity in an *in vitro* model of AD.

Methods and Materials: Neuroblastomas 2A mouse neural cells, stably expressing AD-related Swedish mutant form of the APP695 plasmid were utilized and cultured under standard conditions. WST-1 assays were utilized to determine suitable drug concentrations. Immunoblotting of LC3-II and p62 protein in the absence and presence of the lysosomal inhibitor bafilomycin A1 (BafA1) were used to assess autophagy activity. Autophagy induction was also characterized using fluorescence microscopy and transmission electron microscopy (TEM). Immunoblot techniques were utilized to assess the clearance effect of key amyloidogenic and mitochondrial fission/fusion was assessed using a combination of immunoblotting and fluorescence microscopy. Lysosomal integrity was assed using an acridine orange stain, while the LAMP2a protein expression profile was assessed through western blotting. Finally, to assess the protective role of GB, western blot analysis probing for cytochrome-c, cleaved caspase-3 and 4HNE was conducted.

Results: 48 hrs butyric acid (BA) treatment and subsequent APP overexpression significantly decreased reductive capacity, however, a 24-hr pre-treatment with LiCl, GB↓ 10µg/ml & GB high (↑:200µg/ml) and GB↓ + LiCl preserved reductive capacity. Significantly increased LC3-II protein levels were observed following GB low (↓:10µg/ml), GB high (↑:200µg/ml), GB low (↓:10µg/ml) + LiCl and GB high (↑:200µg/ml) + LiCl treatment before and after BafA1 exposure. Moreover, a significant reduction in APP, BACE, Aβ and cytochrome-c protein levels was observed following 24 hrs treatment of LiCl, GB low (↓:10µg/ml) and GB high (↑:200µg/ml) in the absence and presence of LiCl. A significant increase in p62 protein levels was observed when cells were exposed to GB high (↑:200µg/ml) followed by BA and BafA1 treatment, in comparison with control and GB low (↓:10µg/ml) treated cells followed by BA and BafA1 treatment, respectively. When the induction of autophagy by GB high (↑:200µg/ml) was inhibited, the protein levels of APP, BACE, Aβ, cytochrome-c and 4HNE were elevated. This scenario led to impairment in mitochondrial and lysosomal function, which was improved by GB treatment in the absence and presence of LiCl.

Discussion and Conclusion: Our results provide clear evidence that GB, and more specifically, GB in combination with LiCl, an FDA approved drug, reduces Aβ pathology, preserves lysosomal and mitochondrial function and thereby attenuates Aβ-induced cell death by upregulating autophagy. In addition, even though both, low and high concentrations of GB result in a similar degree of protection, their effect on protein clearance through autophagy, and autophagy activity itself is distinct, suggesting that autophagy can indeed be finely controlled. We therefore recommend that individuals suffering from AD, or those susceptible to AD, are supplemented with the dose of GB which provides the highest clearance, highest protection and highest flux, which we reported as GB (↑:200µg/ml). Hence a suitably high, yet non-toxic concentration may be recommended as adjuvant treatment. Future research may focus on testing patients by using patient derived cells, such as fibroblasts, to screen and select most suitable drugs to enhance autophagy and protein clearance.

Opsomming

Inleiding: Alzheimer-siekte (AS) is ‘n komplekse neurologiese siekte, gekarakteriseer deur twee proteïen aggregate, naamlik ekstrasellulêre amiloïed-beta (Aβ) plaak en intrasellulêre neurofibrilêre voue van tau proteïen. AS is die mees algemene tipe progressiewe demensie, word huidiglik swak behandel en is bekend vir swak kliniese uitkomste. Alhoewel beduidende kennis opgedoen is wat AS patologie betref, is daar beperkte vordering in terme van die ontwikkeling van farmaseutiese terapie wat die aftakelende uitwerking van die siekte verander of om keer. Outofagie is ‘n noodsaaklik proses betrokke in die oorlewing van selle aangesien dit noodsaaklik is vir organel en langlewende proteïen omset. As sulks word dit oor die algemeen aanvaar dat outofagie disfunksie ‘n groot rolspeler is in die ontwikkeling van AS. Vorige bevindinge dui daarop dat Gingko biloba (GB) en litium chloried (LiCl) ‘n neurobeskermende effek het in die konteks van neurodegeneratiewe siektes. Alhoewel sommige lande geredelik GB en LiCl voorskryf aan individue wat lei aan AS, is dit steeds onduidelik hoe hierdie middele op ‘n meganistiese vlak te werk gaan om die siekte te beveg en tot watter mate hul outofagie versnel en toksiese proteïen aggregate verwyder. Ons stel voor dat behandeling met GB ‘n konsentrasie afhanklike effek op outofagie aktiwiteit sal toon en dat hierdie effek verder versnel sal word in kombinasie met LiCl. Hierdie effek kan moontlik oorgedra word tot die verwydering van amiloïed voorganger proteïen en Aβ wat lei tot die behoud van lisosomale funktionaliteit en mitochondriale integriteit. Die doel van die voorgelegde studie is dus om te ondersoek wat die effek van GB en LiCl, beide op hul eie sowel as in kombinasie, sal wees op die modulasie van outofagie aktiwiteit en op die verlaging van Aβ proteotoksisiteit in ‘n *in vitro* model van AS.

Metodes en materiale: Neruoblastomas 2A muis neurale selle wat die AD-verwante Sweedse mutasie van die APP695 plasmied stabiel uitdruk was gebruik en gekweek onder standaard kondisies. WST-1 toetse was gebruik om geskikte konsentrasies van di middelste bepaal. Immunoblottering van die LC3-II en p62 proteïen in die afwesigheid en teenwoordigheid van die lisosomale inhibeerder bafilomisien A1 (BafA1) was gebruik om outofagie aktiwiteit te ondersoek. Outofagie induksie was ook gekarakteriseer deur gebruik te maak van fluoressensie mikroskopie en transmissie elektron mikroskopie (TEM). ‘n Kombinasie van Immunoblotterings- en fluoressensietegnieke was gebruik om die klaringseffek van sleutel amiloïedogeniese en mitochondriale fisie/fusie te bestudeer. Lisomale integriteit was geannaliseer deur gebruik te maak van ‘n akridien oranje kleurstof terwyl die LAMP2a proteïen uitdrukkingsprofiel geannaliseer is deur westerse blottering. Laastens om die beskermende rol van GB te assesseer was westerse blotteringsanalisie

uitgevoer met die oog daarop om die vlakke van sitochroom-c, gekleefde caspase-3 en 4HNE vas te stel.

Resultate: 48-uur butirielsuur behandeling en daaropvolgende APP ooruitdrukking het die reduksiekapasiteit aansienlik verminder. Deur ‘n 24-uur pre-behandeling met LiCl, GB↓ 10 µg/mol + GB hoog (↑:200 µg/ml) en GB↓ + LiCl is die reduksiekapasiteit egter behou. ‘n Verhoging in die LC3-II proteïenvlakke is waargeneem na behandeling met GB laag (↓:10 µg/ml), GB hoog (↑:200 µg/ml), GB laag (↓:10 µg/ml) + LiCl en GB hoog (↑:200 µg/ml) + LiCl voor en na BafA1 blootstelling. Verder is ‘n verlaging in APP, BACE, Aβ en sitochroom-c proteïen vlakke waargeneem na 24-uur behandeling met LiCl, GB laag (↓:10 µg/ml) en GB hoog (↑:200 µg/ml) in die afwesigheid en teenwoordigheid van LiCl. ‘n Verhoging in die p62 proteïenvlakke is waargeneem met die blootstelling van selle aan GB hoog (↑:200 µg/ml) gevolg deur BA en BafA1 behandeling in vergelyking met die kontrole en met GB laag (↓:10 µg/ml) behandelde selle gevolg deur BA en BafA1 behandeling onderskeidelik. In die geval waar die induksie van outofagie deur GB hoog (↑:200 µg/ml) geïnhibeer was, was daar ‘n verhoging in die proteïenvlakke van APP, BACE, Aβ, sitochroom-c en 4HNE. Hierdie scenario het gelei tot ‘n verswakking in die mitochondriale en lisosomale funksie wat verbeter is deur behandeling met GB in die afwesigheid en teenwoordigheid van LiCl.

Bespreking en afsluiting: Die resultate verskaf bewyse dat GB, en meer spesifiek GB in kombinasie met LiCl, ‘n FDA goedgekeurde middel, Aβ patologie verlaag, lisosomale en mitochondriale funksie onderhou en daarby Aβ-geïnduseerde seldood verlaag deur outofagie te opreguleer. Alhoewel lae en hoe konsentrasies van GB lei tot ‘n soortgelyke vlak van beskerming, is hul effek op proteïenklaring deur outofagie en outofagie-aktiwiteit nie dieselfde nie wat daarop dui dat outofagie fyn beheer kan word. Ons stel dus voor dat individue wie ly aan AS, of wie vatbaar is vir AS, aanvullings meet krymet die dosis GB (↑:200 µg/ml) wat die hoogste klaringsvlak verskaf, die hoogste beskerming en die hoogste fluksuasie-koers bied. Dus ‘n geskikte hoë, nie-toksiese konsentrasie kan voorgestel word as ‘n bykomende middel vir die behandeling of voorkoming van AS. Toekomstige navorsing kan fokus op die toetsing van patiënte deur gebruik te maak van patient-afgeleide selle, soos fibroblaste, om die mees geskikte middel vas te stel om outofagie en proteïen klaring te bevorder.

Acknowledgements

I would like to extend my most gratitude to my supervisor Prof Benjamin Loos, words cannot even begin to express how thankful I am. I would like to thank him for always having his door open; I am a strong and capable student today because of his guidance and his faith in me. He is the best supervisor one could ever ask for. The success of this thesis is vastly through his motivation, support and encouragement.

To Dr Claudia Ntsapi, for always pushing me to be the best I can be and for being patient with me. Every time I had a query whether big or small, her door was always open for me; every conversation I had with her enriched my knowledge and challenged me as a science student. I am immensely grateful for all her assistance in the lab, without her support I would could not have completed this study to the best of my ability.

To the staff of the Central Analytical Facility Lize Engelbrecht and Dumisile Lumkwana, for their assistance in my microscopy work and for helping me generate amazing images.

To the National Research Foundation (NRF) for providing me a study grant.

To Dr Danzil Joseph, the Neuro-Research Group and Tope, for their technical and academic assistance whenever I needed help in the Lab.

To Nelson, my parents and family, for their constant support, encouragement and prayers which kept me going throughout the entire year.

Lastly and most importantly, to my heavenly father, for blessing me with wisdom and understanding, strength, and might, which was my cornerstone and pillar of strength through the entire year. He has been with me through the storm and the fiercest battles this year.

Table of Contents

Declaration ii

Abstract iii

Opsomming v

Acknowledgements vii

Table of Contents viii

List of Figures xiii

List of Tables xv

List of Abbreviations xvi

Units of measurements xviii

CHAPTER 1: LITERATURE REVIEW 1

1 Introduction 1

1.1 AD pathology: basic molecular mechanisms 3

1.2 APP processing, Aβ production and degradation 4

1.3 Mechanisms of Amyloid-Beta-induced toxicity 6

1.4 NFTs and BRAAK staging 8

1.5 Proteolytic systems 8

1.5.1 Autophagy 8

1.6 Lysosomal function 15

1.7 Autophagy and lysosomal dysfunction 15

1.8 Extensive autophagy pathology in AD 17

1.9 Localization of autophagy defects 18

1.10 Autophagy and Amyloid-Beta 19

1.11 The role of mitochondrial dysfunction in AD 20

1.12 Mitochondrial morphology 21

1.13 AD and mitochondrial dysfunction 22

1.14 Cell death and its classical categorization 23

1.14.1 Apoptosis 24
1.14.2 Necrosis 25
1.14.3 Autophagy dependent cell death 26
1.14.4 Cell death dynamics: cross talk between apoptosis, necrosis and autophagy.....26
1.15 Therapeutic interventions 26
1.15.1 Neurotransmitter based therapies 27
1.15.2 Vitamin E, antioxidants and anti-inflammatory agents.....28
1.15.3 Immunotherapy 28
1.15.4 Physical exercise.....28
1.16 Autophagy inducers as promising treatment intervention 29
1.16.1 Rapamycin 29
1.16.2 Rilmenidine 30
1.16.3 Lithium chloride and neurodegeneration 30
1.16.4 Gingko biloba and neurodegeneration 33
1.17 Rationale of the study.....36
1.18 Problem statement 36
1.19 Aims and objectives 37
1.20 Hypothesis 37
CHAPTER 2: MATERIALS AND METHODS.....38
2.1 General consumables and reagents.....38
2.2 Antibodies.....39
2.3 Cell Culture.....41
2.3.1 *In vitro* study design.....41
2.3.2 Maintenance of N2aswe cells 41
2.3.3 Thawing of cells.....41
2.3.4 Seeding of cells for experimental procedures 41
2.5 Treatment groups for autophagy and cell death analysis 42
2.5.1 Treatment reagents 42
2.5.2 GB treatment.....42

2.5.3 Lithium chloride (LiCl) treatment 42
2.6 Experimental procedures 43
2.6.1 Cellular Viability assays 43
2.7 The effects of GB and LiCl on autophagy and amyloidogenic processing 44
2.7.1 Protein extraction 45
2.7.2 Protein determination and sample preparation 45
2.7.3 Sodium dodecyl-sulphate polyacrylamide gel electrophoresis 45
2.8 Cell death analysis 46
2.8.1 Transient transfection 47
2.8.2 Mitochondrial assessment 48
2.8.2.1 Tetramethylrhodamine 48
2.9 Immunohistochemistry and confocal microscopy 48
2.10 Acridine orange staining 49
2.11 Transmission electron microscopy 49
2.11.1 Sample preparation 49
2.11.2 TEM sample processing 50
2.12 Liquid chromatography-mass spectrometry based quantitative analysis 51
2.13 Statistical analysis 51
CHAPTER 3: RESULTS 52
Section 3.1: The effect of Ginkgo biloba (GB) and lithium chloride (LiCl) treatment on cell viability 52
3.1.1 Dose response of lithium chloride and Ginkgo biloba 52
3.1.2 Concentration-dependent effect of GB on cell viability 53
3.1.3 Combination treatment of GB and LiCl and effects on cell viability 54
3.1.4 Gingko biloba pre-treatment confers neuroprotection against amyloid-βeta mediated proteotoxicity 55
Section 3.2 Characterisation of GB modulation on autophagy and protein cargo clearance and its effects on amyloid processing. 59
3.2.1 Gingko biloba treatment in the presence and absence of LiCl modulates autophagic flux 59

3.32.2 Immunofluorescence analysis of p62.....63

Section 3.3 The effects of Gingko biloba treatment on lysosome abundance.....65

3.3.1 The effects of Gingko biloba treatment on the lysosomal acidic compartment under neurotoxic conditions.....66

3.3.2 The effects of Gingko biloba treatment on the neuronal ultrastructure under neurotoxic conditions.....68

Section 3.4 The effect of Gingko Biloba treatment on the clearance of amyloidogenic proteins under neurotoxic conditions.....70

Section 3.5 The effect of Gingko biloba treatment on apoptosis onset under neurotoxic conditions 73

Section 3.6 The effect of Gingko Biloba treatment on mitochondrial fission and fusion dynamics 75

3.6.2 The effect of Gingko biloba treatment on mitochondrial morphology.....78

Section 3.7 Autophagy activity (flux) under neurotoxic conditions 80

Section 3.8 The effect of Gingko Biloba treatment on autophagy flux and APP processing 84

3.8.A Inhibition of autophagy leads to the accumulation of APP 84

3.8.B Inhibition of autophagy leads to the accumulation of BACE.....86

3.8.C Inhibition of autophagy leads to the accumulation of Aβ.....87

Section 3.9 The effect of Gingko Biloba treatment on autophagy and apoptosis 89

3.9.A The role of Autophagy inhibition on cell death onset 89

3.9 B The role of Autophagy on oxidative stress.....90

Section 3.10 The compositional analysis of GB.....92

CHAPTER 4: DISCUSSION.....93

4.1 Gingko biloba pre-treatment confers neuroprotection against amyloid-beta proteotoxicity 94

4.2 Gingko biloba treatment and LiCl modulate autophagic flux.....95

4.3 Gingko biloba treatment preserves lysosome function 98

4.4 Gingko biloba treatment clears amyloidogenic proteins under neurotoxic conditions 101

4.5 Gingko biloba treatment prevents amyloid-beta induced apoptosis.....102

4.6 Gingko biloba treatment preserves mitochondrial fission and fusion dynamics 103

4.7 Robust autophagy flux is vital under neurotoxic conditions to maintain cellular homeostasis 105

4.8 Inhibition of autophagy leads to the accumulation of amyloidogenic proteins 106

4.9 Autophagy upregulation by GB attenuates amyloid-beta mediated cell death 108

4.10 The role of autophagy in oxidative stress 109

CHAPTER 5: SUMMARY AND CONCLUSION 110

5.1 Summary diagram 112

5.1.1 Molecular defects in AD 112

5.1.2 Proposed protective mechanism of GB in the presence and absence of LiCl. 112

FUTURE RECOMMENDATIONS AND LIMITATIONS OF THE STUDY 113

REFERENCES 115

Appendix 126

List of Figures

Figure 1.1: Amyloidogenic and non-amyloidogenic pathway of APP processing

Figure 1:2: Regulation of autophagy

Figure 1.3: Autophagy metabolism

Figure 1.4: Schematic diagram of the fate of Galectin-3

Figure 3.1.1: Relative reductive capacity of N2aswe cells after 24 hrs treatment exposure to various concentrations of lithium chloride

Figure 3.1.2: Relative reductive capacity of N2aswe cells after 24 hrs treatment exposure to various concentrations of Gingko biloba

Figure 3.1.3 A: Relative reductive capacity of N2aswe cells after 24 hrs treatment exposure to Gingko biloba

Figure 3.1.3 B: Morphological assessment of N2aswe cells after 24 hrs treatment exposure to Gingko biloba

Figure 3.1.3 A: Relative reductive capacity of N2aswe cells following exposure to Gingko biloba

Figure 3.1.3 B: Micrographs representing N2aswe cells following exposure to Gingko biloba

Figure 3.2.1 A: Relative protein expression levels of LC3

Figure 3.2 B: Relative protein expression levels of p62

Figure 3.2.2. Fluorescence micrographs of p62 abundance

Figure 3.3.1: Relative protein expression levels of LAMP2a

Figure 3.3.2: Lysosomal acidic compartment (LAC) detection using Acridine Orange (AO) staining.

Figure 3.3.3: Representative Transmission electron micrographs

Figure 3.4: Relative protein expression levels of (A) APP and (B) BACE (C) Aβ

Figure 3.5: Relative protein expression levels of (A) Cytochrome-c and (B) Cleaved-Caspase-3

Figure 3.6.1: Relative protein expression levels of (A) MNF1 (B) DRP1

Figure 3.6.2: Representative micrographs of N2aswe cells stained with TMRE

Figure 3.7 A: Relative protein expression levels of p62 following BA exposure in the presence and absence of BafA1

Figure 3.7 B: Relative protein expression levels of LC3-II following BA exposure in the presence and absence of BafA1

Figure 3.8 A: Relative protein expression levels of APP following BA exposure in the presence and absence of BafA1

Figure 3.8 B: Relative protein expression levels of BACE following BA exposure in the presence and absence of BafA1

Figure 3.8 C: Relative protein expression levels of Aβ following BA exposure in the presence and absence of BafA1

Figure 3.9 A: Relative protein expression levels of cytochrome-c following BA exposure in the presence and absence of BafA1

Figure 3.9 B: Relative protein expression levels of 4HNE following BA exposure in the presence and absence of BafA1

List of Tables

Table 2.1 List of reagents and sources

Table 2.2 List of primary antibodies

Table 2.3 Treatment compounds

Table *2*.4 Lipofectamine 3000 transfection solution components

Table 3.1 Treatment groups based on cell viability results

Table 3.10 The compositional analysis of GB

List of Abbreviations

AD	Alzheimer's disease
ALP	Autophagic-lysosomal pathway
APOE-ε4	Alipoprotein ε4
Aβ	Amyloid-beta
APP	Amyloid Precursor Protein
APP-CTF	APP C-terminal fragment
ATG	Autophagy-related
Atg	Autophagy-related genes
ATP	Adenosine triphosphate
AV	Autophagic vacuole(s)
BACE	Beta-site APP-cleaving enzyme
BAF	Bafilomycin A1
Bcl-2	B-cell lymphoma-2
DMEM	Dulbecco's modified Eagle's medium
DMSO	Dimethyl sulfoxide
EOFAD	Early onset familial Alzheimer's disease
ER	Endoplasmic reticulum
FBS	Fetal bovine serum
FDA	Food and drug administration
Fis1	Fission protein
GB	Gingko Biloba
GFP	Green fluorescent protein
GSK3	Glycogen synthase kinase 3
HD	Huntington's disease
IGF-1	Insulin-like growth factor-1
IP3	Inositol triphosphate
IRS-1	Insulin receptor substrate-1
JNK1 c-	Jun N-terminal kinase 1
LC3	Microtubule-associated light chain-3
LiCl	Lithium chloride
LOAD	Late onset Alzheimer's disease
Mfn	Mitofusin protein
mTOR	Mammalian target of rapamycin

ND	Neurodegeneration
NFT	Neurofibrillary tangles
PD	Parkinson's disease
PI3K	Phosphatidylinositol 3-kinase
PI-3-P	Phosphatidylinositol-3-phosphate
PIP3	Phosphatidylinositol (3,4,5)trisphosphate
PKA	Protein kinase A
PSEN	Presenilin
UPS	Ubiquitin proteasome pathway
PVDF	Polyvinydilene difluoride
RIPA	Radioimmunoprecipitation assay buffer
ROS	Reactive oxygen species
sAPPα	Soluble peptide APPα
SDS-PAGE	Sodium-dodecyl-sulfate-polyacrylamide gel electrophoresis
SQSTM1 Sequestome 1	p62
TCA	Tricarboxylic acid
TEM	Transmission electron microscopy
TMRE	Tetramethylrhodamine ethyl ester
TNF	Tumour necrosis factor
Tris-HCl	Trisaminomethane hydrochloride
TSC	Tuberous sclerosis complex
ULK-1	Unc-51 like autophagy activating kinase 1
v-ATPase	vacuolar H^+-ATPase
WST-1	Water soluble tetrazolium salt 1

Units of measurements

%	percentage
°C	degrees Celsius
µM	micromolar
µg	microgram
µl	microlitre
µm	micrometre
cm	centimetre
hr	hour
hrs	hours
l	litre
min	minute(s)
ml	millilitre
mm	millimetre
mM	millimolar
ng	nanogram
nM	nanomolar
nm	nanometre
rpm	rotations per minute
sec	second
V	volt

CHAPTER 1: LITERATURE REVIEW

1 Introduction

Neurodegeneration (ND) describes the process of steady and progressive degeneration and loss of neuronal cells, resulting in the malfunction of the central nervous system. Impaired proteostasis, protein misfolding and abnormal protein aggregation are common features of most neurodegenerative diseases, invariably leading to neuronal toxicity and cell death onset. Hence, there is an urgent need for novel therapies to either halt or reverse the progression of neurodegenerative diseases such as Alzheimer's disease (AD) and Parkinson's disease (PD), which continue to impose a tremendous societal and economic burden (Alzheimer's Association, 2016). Despite the availability of extensive data from both *in vitro* and *in vivo* model systems, the precise pathogenic mechanisms leading to the development of neurodegenerative diseases remains unclear. To this end, the mechanistic understanding of the major molecular and pathological processes implicated in the progression of neurodegenerative diseases, may aid in the development of novel disease modifying therapeutics. AD is a severe neurodegenerative disease and the most common form of senile dementia amongst the elderly, affecting over 46.8 million people globally (Alzheimer's Association, 2016). Age is a major risk factor for the development and progression of AD, with the number of people aged 60 years and older projected to more than double in the next 35 years and with the prevalence of AD and PD expected to increase by a drastic 7.1 million newly diagnosed cases by 2025 (United Nations, 2015). AD is a growing concern in developing countries such as South Africa (SA), where the provision of services is poor (de Jager *et al*., 2017). In SA, an estimated 187 000 elderly individuals were reported to be living with dementia (Alzheimer's Association, 2016). This prevalence is expected to rise to 250 000 by 2030, with the population concurrently increasing in the number of elderly individuals (60 years and older). This is likely to pose an even greater societal and economic challenge to resource poor countries, with already-severely stretched health and social care systems.

Although research efforts have intensified in the last decade, AD remains greatly understudied and poorly documented in the context of SA. The lack of AD-related research focus in SA may be attributed, at least in part, to the high burden of Human immunodeficiency virus infection/acquired immune deficiency syndrome (HIV/AIDS) pandemic and Tuberculosis (TB), which are currently classified as diseases of major national priority. Hence, available resources are largely dedicated to the study and prevention of these diseases, while non-communicable diseases such as AD remain largely neglected. AD is a complex neurological disease, and the most common type of progressive dementia

associated with poor clinical outcomes (Wimo et al., 2017). AD remains an unmet clinical challenge and is characterized by the progressive degeneration and eventual loss of neurons, particularly in the hippocampal and cerebral cortex region (Jack et al., 2013). Clinically, dementia is diagnosed when normal daily living is severely compromised following progressive cognitive impairment. Although insight has been shed regarding AD pathology, limited progress has been made in the development of pharmaceutical therapeutics that modify or reverse the debilitating effects of this disease. Currently, all approved treatment options for AD are primarily symptomatic. This includes acetylcholinesterase inhibitors, as well as N-methyl-D-aspartate (NMDA)-receptor antagonist which treat symptoms but not the underlying molecular dysfunction and cause (Anand et al., 2014). Despite advances in unravelling the biological underpinnings of AD pathology, to date there are still no disease-modifying therapies available for those affected. This highlights the substantial need for dedicated research efforts toward the development of better targeted AD therapeutic interventions that are strongly aligned with the molecular defect and may potentially modify the progression of the disease. In this literature discussion, I will therefore provide an in-depth background of the molecular mechanisms that have been identified to play a key role in the disease onset and progression. These may present novel targets, which may hold potential for the development of therapeutic interventions in the treatment of neurodegenerative diseases such as AD, PD etc.

Recently, the role of proteotoxicity and macro-autophagy (hereafter referred to as autophagy) in the context of neurodegeneration has received major attention. The autophagy process will be discussed in greater detail in the context of proteolytic systems. Therefore, in particular the molecular mechanisms that govern protein degradation and neuronal cell death will be highlighted. It is in this context, that two drugs, namely Gingko biloba (GB) and lithium chloride (LiCl) have been reported to be neuroprotective (Kanowski, et al., 1996; Baldessarini et al. 1999). Importantly, in some countries, both drugs are often prescribed to individuals suffering from AD, however, their mode of action of action remains largely unclear. LiCl is a promising compound that has been shown to modulate the activity of the autophagy pathway (Sarkar et al., 2005), and has been approved and used clinically, primarily in the treatment of depression. However, drugs that modulate autophagic activity, and thereby impact the removal of toxic protein aggregates have not been fully explored for translation at the clinical level, largely due to limited knowledge about drug concentration ranges that affect and control autophagy. Similarly, GB is currently recommended as a supplement for AD patients, but questions related to its clinical application in the context of AD remain unclear. GB is known to have beneficial neuroprotective properties, but it is currently unclear to what extent it induces autophagic activity. Interestingly, these two drugs have been shown to impact

proteolytic clearance of toxic proteins such as amyloid beta (Aβ) by modulating the autophagy pathway, thus making these drugs favourable candidate compounds for therapeutic intervention in AD. However, it is unclear which concentration of GB or LiCl would maximize protein degradation and hence favour neuronal cell survival. It is also not clear whether a combination of both drugs could further enhance protein degradation through enhanced autophagic activity. In order to understand the underlying molecular mechanisms which are involved in steering the onset and progression of AD, it is important to focus on the physiology of functioning neurons with their distinct dependence on protein degradative pathways, and the precise control and regulation of these pathways. Accordingly, the basic molecular mechanisms, proteolytic production and Aβ degradation will first be discussed.

1.1 AD pathology: basic molecular mechanisms

In the year 1906, the neuroscientist Alois Alzheimer, studied post-mortem brains of women who had died from gradual behavioural and cognitive dysfunction (Hardy and Higgins 1992). In 1968, a relationship between the magnitude of Aβ plaques in brain tissue of the elderly and the risk of developing dementia was first described (Hardy and Higgins 1992). It has been suggested that prior to the deposition of Aβ1-42 peptides in the formation of amyloid plaques, Aβ initially forms oligomers and later forms insoluble fibrils (Ahmed et al., 2010). The regions that are characterized by an accumulation of amyloid plaques have been shown to be surrounded by neurons that contain neurofibrillary tangles (NFTs). Controversy exists about the order of events in the pathogenesis of AD, and the molecular mechanisms that govern the relationship between NFTs and amyloid plaques. For many years, the amyloid cascade hypothesis (ACH) has been suggested as a key underlying mechanism for AD pathology, which suggests that the presence of Aβ may be the first histological feature in AD, with other secondary features arising later in disease progression (Hardy and Higgins, 1992). The ACH suggests that the deposition of amyloid plaques (mainly containing Aβ peptides) is the causative factor in AD pathology, and that the formation of NFTs, vascular damage, neuronal cell loss and dementia occur due to increased Aβ deposition (Hardy and Higgins 1992).

Pathologically, AD is characterized by the presence of senile plaques, composed mainly of Aβ peptides and NFTs composed of hyperphosphorylated cleaved forms of microtubule-associated protein tau (Paradis, Koutroumanis and Goodyer, 1996). However, the accumulation of Aβ peptides in the brain appears to be the main contributor to the pathogenesis of AD. Moreover, the aggregation of toxic proteins has shown to be critical in most neurodegenerative diseases, including PD and Huntington's disease (HD). Protein aggregation is defined as the clumping of misfolded, aggregate-prone proteins (Hartl and

Hayer-Hartl, 2009). Interestingly, very recently these protein aggregates have also been proposed to offer protective properties (Swart et al., 2014). Moreover, whether neurotoxicity originates from the misfolded protein intermediates or the aggregate bodies themselves remains unknown. One hypothesis is that misfolded proteins become toxic, and therefore are predisposed to aggregation in brain areas mostly implicated in AD (Swart et al., 2014).

Although the majority of AD cases manifests as a late onset sporadic form (LOAD), the role of genetic factors in the pathophysiology of AD is increasingly recognised in early onset AD (EOAD) or Familial AD cases (Alzheimer's Association, 2016). Familial AD occurs before the age of 65 and is thought to be a rare form of the disease which is usually due to hereditary mutations (Alzheimer's Association, 2016). LOAD accounts for more than 95% of all AD cases and occurs in individuals older than 65 years. In Familial AD, genetic mutations in coding genes of proteins participate in the breakdown of amyloid precursor protein (APP) and production of Aβ (i.e. the APP gene, the presenilin1 (PSEN1) gene and the presenilin 2 (PSEN2) gene) (Folch et al., 2015). These mutations favour and trigger the formation of neurotoxic species of the Aβ peptide, primarily Aβ42 peptide. PSEN1 mutations have also been shown to cause autophagy defects (Chong et al., 2018). The sporadic form of AD is influenced by both genetic and environmental factors (i.e. epigenetic factors), which impact the clearance of neurotoxic Aβ peptides, and may thereby contribute to the complex pathology of AD.

The ACH suggests an imbalance between the production and clearance of Aβ, with a decrease in the clearance of Aβ in sporadic AD and increased Aβ production in the familial form of AD (Hardy and Higgins 1992). Familial and sporadic AD patients have been shown to be clinically indistinguishable, and increased Aβ deposition and neurotoxicity is thought to represent the most consistent feature, suggesting that both AD forms may share common underlying molecular mechanisms (Bali et al., 2012). Amyloids are defined as tissue deposits of extracellular fibrils (Hardy, 1997), which are present in low quantities under physiological conditions, and play an important role in synaptic physiology (O'Brien and Wong, 2011). Strikingly, the role of its precursor protein, APP remains unclear, although it has been shown that the expression of APP confers overall beneficial effects such as neuronal growth and increased cellular viability (O'Brien and Wong, 2011). Consequently, studies have focused on the production and the degradation of Aβ with AD progression (Hyttinen et al., 2014).

1.2 APP processing, Aβ production and degradation

APP can be metabolized rapidly in a series of complex processes by a group of secretase enzymes (Fig.1.1) (Hardy and Higgins, 1992). APP is sorted in the Golgi apparatus and the endoplasmic reticulum, and further transported to the axon, where it is delivered to the

synaptic terminals (cell surface) by the trans-Golgi network, which is a crucial site for the processing of APP (Lodish et al., 2000). Following transport along the trans-Golgi network, APP can further be transported directly to endosomal compartments or to the surface of the cell (Lodish et al., 2000). The precise intracellular localization of APP processing is a vital factor determining whether Aβ is produced. Following the amyloidogenic pathway, APP is incorporated into endosomal components through clathrin-coated vesicles and is initially cleaved by beta-site APP-cleaving enzyme 1 (BACE1) (Hardy and Higgins, 1992). This cleavage, results in the generation of a soluble N-terminal fragment termed sAPPβ. The C-terminal fragment of APP (C99), which is bound to the cell membrane, is further cleaved by the y-secretase-presenilin complex at Aβ sites between Aβ40-Aβ44 (Hardy and Higgins, 1992). This process leads to the production of Aβ peptides and the intracellular APP domain (AICD) (Takahashi et al., 2002). Several peptide isoforms ranging in length from 39 to 43 amino acids are formed during the amyloidogenic cleavage of APP, with Aβ40 and Aβ42 being the most-commonly found isoforms. Aβ42 is the more neurotoxic isoform, as it aggregates more rapidly and forms insoluble plaques that lead to neuronal cell death and cognitive defects (Kellett and Hooper, 2009). In the context of AD, the abnormally increased production of Aβ occurs through the amyloidogenic processing of APP. It is important to note that the formation of Aβ peptides is an ongoing, gradual process, thereby explaining why AD-associated pathology is evidenced decades prior to its clinical manifestation (Alzheimer's Association, 2015).

Alternatively, APP can be metabolized through the non-amyloidogenic pathway, where it is initially cleaved by α-secretases (Fig.1.1) (Kellett and Hooper, 2009). During this process, APP is sorted in the Golgi apparatus and the endoplasmic reticulum, and further transported to the axons' surface where it is cleaved by γ-secretase to form non-pathogenic soluble products, including P3 fragments (O'Brien and Wong, 2011). α-secretase cleavage occurs in the Aβ domain of APP, thereby inhibiting the production of Aβ. Notably, the target protein sequence identified by α-secretase is closer in proximity to the cell surface than those of BACE1, as a result the non-amyloidogenic pathway is generally more favoured under physiological conditions (O'Brien and Wong, 2011).

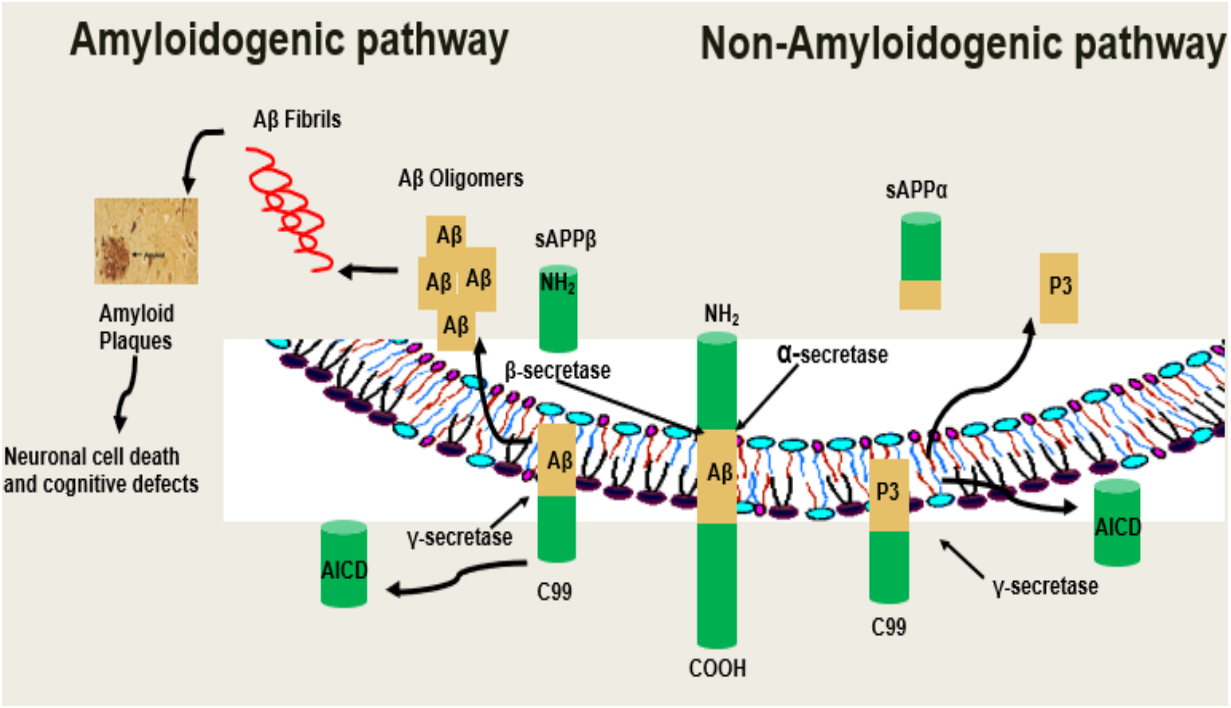

Figure 1.1: Amyloidogenic and non-amyloidogenic pathway of APP processing. APP is internalized into the endosome membrane where it is cleaved by BACE1 releasing CTF- and insoluble APPβ. The latter is subsequently cleaved by γ-secretase that releases AICD+Aβ. Consequently, the insoluble APPβ is released to the extracellular space via exocytosis. Thereafter, Aβ peptides that are 42 amino acids long aggregate into plaques and induce neurotoxicity. Abbreviations: **Aβ** = amyloid-beta, **APP** = amyloid precursor protein, **AICD** = intracellular APP domain, **C99** = C-terminal fragment, **COOH** = carboxylic acid terminal, **NH_2** = NH_2 terminal (Adapted from Ntsapi et al., 2017).

Estus and colleagues suggest that APP can also be processed by the endosomal-lysosomal pathway, after recycling of membrane-bound APP and possibly via an intracellular metabolic route (Estus et al., 1992). The endosomal-lysosomal pathway has been shown to be involved in the processing of APP following the recycling of the membrane-bound APP (Wirak et al., 1991). This alternative processing pathway of APP can produce carboxyl-terminal segments comprising the complete Aβ peptide, which may ultimately lead to increased Aβ deposition (Estus et al.,1992). This points towards the importance of the lysosomal system in the context of APP processing, which is important since lysosomal dysfunction is also a hallmark of AD.

1.3 Mechanisms of Amyloid-Beta-induced toxicity

The contribution of Aβ in the progression of AD is well established. However, studies have shown that Aβ peptide also mediates several physiological process, such as calcium and potassium regulation (Kellett and Hooper, 2009). Kellet and Hooper further highlighted the

fact that Aβ only becomes toxic when its levels increase above physiological levels, due to the imbalance in production and clearance, as evidenced in AD. In sporadic forms of AD, the amyloidogenic processing of the APP pathway is accelerated as a result of increased protein expression and enhanced BACE1 activity (O'Brien and Wong, 2011). Since BACE1 is the rate-limiting step in the production of Aβ, an increase in its protein expression and activity influences the protein levels of Aβ peptide. In a neuroblastoma 2A (N2a) mouse neural cell line that stably expresses the AD-related Swedish mutation (APPswe), the levels and activity of BACE1 were shown to increase markedly following treatment with APP-transgene inducer, butyric acid. Consequently, the expression of the APP was increased, resulting in increased production of Aβ (Shin et al., 2016).

Studies have extensively reported several molecular disruptions as a direct result of increased Aβ protein levels (Behl et al., 1994). In an *in vitro* study by Behl et al. (1994), absolute cell death was demonstrated in cultured rat pheochromocytoma PC12 cells and rat cortical neurons exposed to exogenous Aβ fibrils for 24 hrs. This finding revealed that Aβ fibrils are acutely neurotoxic (Behl et al., 1994). Mouse models overexpressing mutant human APP displayed increased Aβ deposition within four to six months and manifested sequential injury of neuronal cells, synaptic dysfunction and inflammatory damage (O'Brien and Wong, 2011). In these mouse models, numerous caspases (3, 6, 7, and 9) were shown to be activated, contributing to the demonstrated death of neuronal cells via apoptosis. Aβ has also been shown to directly contribute to tau pathology, which is also a major hallmark in AD pathology (Mawuenyega et al., 2011). Studies have shown that soluble Aβ promotes hyperphosphorylation and cleavage of tau, resulting in the generation of NFTs. Furthermore, extracellular Aβ has been shown to activate Glycogen synthase kinase 3 beta (GSK3β), which is a key regulator for tau phosphorylation (Hyttinen *et al.*, 2014). The intracellular NFTs are composed of hyperphosphorylated microtubule-associated tau protein aggregates present in several neurons (Perl and Perl, 2010). Tau protein is vital in the stabilization of the microtubule network of the cytoskeleton (Fontaine et al., 2015), and its phosphorylation regulatory process have been shown to be controlled by the activity of GSK3. In AD states, GSK3 activity has been demonstrated to increase, resulting in the hyperphosphorylation and aggregation of tau (Avila et al., 2004). A more recent study revealed that the reduction of Aβ peptides prevents the development of spatial memory impairment and inhibits tau pathology (Vanden et al., 2017). Taken together, these studies suggest that Aβ neurotoxicity may be a mediator of tau pathology in AD.

1.4 NFTs and BRAAK staging

Although the diagnostic criteria for AD was initially developed by Alois Alzheimer (Alzheimer, 1911), it was pioneering work by Braak and Braak (1991) that led to the establishment of a staging system to monitor the progression of the disease. This monitoring system is termed the “Braak staging of Alzheimer disease-associated neurofibrillary pathology” and is based on the progressive region-specific protein aggregation (Braak and Braak, 1991). The progression of AD is typically slow and develops in three-sub-divided stages, namely mild (early-stage), moderate (middle-stage), and severe (late-stage) (Alzheimer’s Association, 2015). Early in the AD stages, the hippocampus undergoes atrophy (Caselli and Reiman, 2013), leading to failure in cognitive function, specifically memory formation. This contributes to the significant link between AD and dementia.

1.5 Proteolytic systems

1.5.1 Autophagy

The disruption of proteostasis and the dysregulation in protein degradative pathways is associated with the onset of AD (Komatsu et al., 2006). The presence of protein aggregates in AD illustrates a failure in the neuronal cells’ protein quality control systems (Hyttinen et al., 2014). Therefore, the maintenance of proteostasis and a tight equilibrium between protein synthesis and degradation is vital in the removal of abnormal, aggregate-prone proteins (Sarkar et al., 2009). Neuronal cells rely heavily on protein quality control systems to meet their metabolic demands during periods of energy/ nutrient deprivation (Rubinsztein, 2006). The maintenance of proteostasis is accomplished by two degradative processes, including the ubiquitin-proteasome pathway (UPP) and the autophagy-lysosomal pathway (ALP). The UPP primarily targets short-lived cytosolic and nuclear proteins whereas the ALP degrades long-lived cytoplasmic proteins and impaired organelles (Mizushima et al., 2010). Given that 99% of intracellular proteins are long-lived, the maintenance of proteostasis depends primarily on ALP in neuronal cells (Mizushima et al., 2010).

The ALP comprises of three sub-divisions based on how cargo is transported for degradation to the lysosome. The sub-types include microautophagy, autophagy, and chaperone-mediated autophagy (CMA) (Mizushima et al., 2010). CMA involves the selective recognition and delivery of cytosolic proteins harbouring a pentapeptide amino acid sequence (the CMA targeting motif - KFERQ) to the lysosomal surface, where upon unfolding, they are internalized through a membrane translocation complex involving lysosome-associated membrane protein type 2A (LAMP-2A) for subsequent degradation by lysosomal proteases (Kaushik and Cuervo, 2015). Microautophagy involves the direct engulfment of cytoplasmic material that is trapped by the vacuole of lysosomes through a process termed membrane

invagination (Nixon, 2011). Finally, autophagy is defined as a process that results in the sequestration of cytoplasmic material into double-membraned vesicles termed autophagosomes, which in turn fuse with lysosomes or late endosomes to acquire hydrolytic activity, forming the autolysosome compartment in which the sequestered cargo is subsequently degraded (Mizushima, 2007). This process leads to the generation of amino acids which can be reused by the cell to adapt to fluctuations in nutrient supply, to produce adenosine triphosphate (ATP) to drive energy-dependent processes such as protein synthesis (Loos et al., 2013). Autophagy also removes damaged organelles such as mitochondria and thereby prevents the stimulation of cell death processes emanating from increased reactive oxygen species, decreased cellular antioxidant mechanisms, as well as protecting cells against proteotoxic stress (Rabinowitz and White, 2010). The turnover of organelles and cellular macromolecules may be indicative of the essential role of autophagy in various physiological processes, including differentiation, normal growth, cellular survival and during starvation (Kabeya et al., 2000). The first direct evidence linking proteostasis control and autophagy in the nervous system came from studies in which genetic deletion of essential autophagy genes Atg5 (Hara et al., 2006) or Atg7 (Komatsu et al.,2006) in the central nervous system caused spontaneous neurodegeneration, promoting extensive neuronal loss, the accumulation of protein aggregates, and premature death in mice. Most cell types show a low level of basal autophagic activity which plays a prominent role in the intracellular turnover of proteins and organelles (Funderburk et al., 2010). However, autophagic activity may be enhanced by diverse stress signals such as nutrient starvation, or hypoxia, or through the use of various pharmaceutical drugs such as rapamycin and spermidine (Rabinowitz and White, 2010).

Disruptions in the autophagy pathway have been shown to enhance abnormal protein aggregation in neurodegenerative diseases, as well as contribute to the development of various pathologies including cancer, cardiovascular diseases and lysosomal storage disorders (Nixon and Yang, 2011). It is important to note that neurons are highly sensitive to fluctuations within the autophagy process due to their post-mitotic characteristics, and thereby require tight regulation of proteostasis. As such, defects within the autophagic system is associated with the onset of neurodegenerative diseases, including AD (Wong and Cuervo, 2010).

1.5.1.1 The autophagy machinery and its regulation

The autophagic process is regulated by a class of conserved autophagy related (Atg) genes that were primarily identified in yeast (Mizushima et al., 2011, Klionsky and Ohsumi, 1999). The autophagy process can be mechanistically organised into several sequential steps, namely: initiation, autophagosome membrane expansion, autophagosome maturation, and

lysosomal degradation, as illustrated in Fig 1.2. Firstly, during initiation, a process termed nucleation occurs. Nucleation results in the formation of a phagophore which matures into an autophagosome (Simonsen and Tooze, 2009). This process involves a multiprotein complex, which consists of a mammalian homolog of Atg6 (beclin1), class III phosphatidylinositol 3-kinase (PI3K). Here the activation of PI3K by ULK/Atg1 complex leads to the association of Atg13-FIP200 members to an isolated membrane (phagophore), thereby forming an autophagosome (Simonsen and Tooze, 2009) (Fig 1.2). The ULK-Atg13-FIP200 complex plays a role in the induction of autophagy.

Next, a ubiquitin ligase (E3), associated with one of the two ubiquitin-like conjugation systems Atg16, is required to complete the formation of an autophagosome (Ohsumi, 2001). The selective process of cargo degradation via autophagy requires the adaptor protein p62 (sequestosome 1/SQSTM1), which selectively binds to ubiquitin-tagged proteins and marks proteins for degradation. The binding of p62 and microtubule-associated protein 1A/1B light chain (LC3) allows the targeted and selective degradation of cytosolic proteins via autophagy. This is followed by the formation of the Atg5-Atg12 complex that then binds to the first of the two ubiquitin-like conjugation systems (Fig 1.2). This process promotes transformation of LC3-I to LC3-II through lipidation with phosphatidylethanolamines (PE) (Ohsumi, 2001). LC3-II associates with the autophagosome membranes, hence the number of autophagosomes is indicative of the extent of LC3 bound to autophagy vesicles (Kabeya et al., 2000).

Autophagosome membrane expansion includes the conjugation of two ubiquitin molecules. In brief, Atg4 processes the C-terminal 22 fragments of LC3-I to generate LC3-II, a soluble form of LC3 which in turn leads to the exposure of the C-terminus glycine segment (Kabeya et al, 2000). The exposed C-terminal of LC3-I is further conjugated by a ubiquitin system, comprising of Atg7 (enzyme E1), Atg3 (enzyme E2) and the Atg12-Atg5-Atg16L complex (enzyme E3) to PE. Finally, for the cargo engulfed by the autophagosomes to be degraded, the autophagosomes are required to fuse with lysosomes which contain hydrolase enzymes and can subsequently degrade the cargo (Fig 1.2). The fusion of autophagosomes with lysosomes results in the formation of autolysosomes (Mizushima, 2007). The autophagosome may either fuse with the lysosome to generate an autolysosome or it can fuse with late endosomes to produce an amphisome. Subsequently, the degradation of engulfed cytosolic contents is initiated by hydrolase enzymes that are contained within the autolysosome. A protein pump termed vacuolar [H*] ATPase is responsible for crucial events including the acidification of autolysosomes, cathepsin protease activation, and effective substrate proteolysis (Yoshimori et al., 1991). This proton pump is located on the lysosomal

membrane. The fusion between lysosomes and autophagosomes is continuous and includes the digestion of contents within the autolysosomes and ultimately lysosomal restoration (Mizushima, 2007).

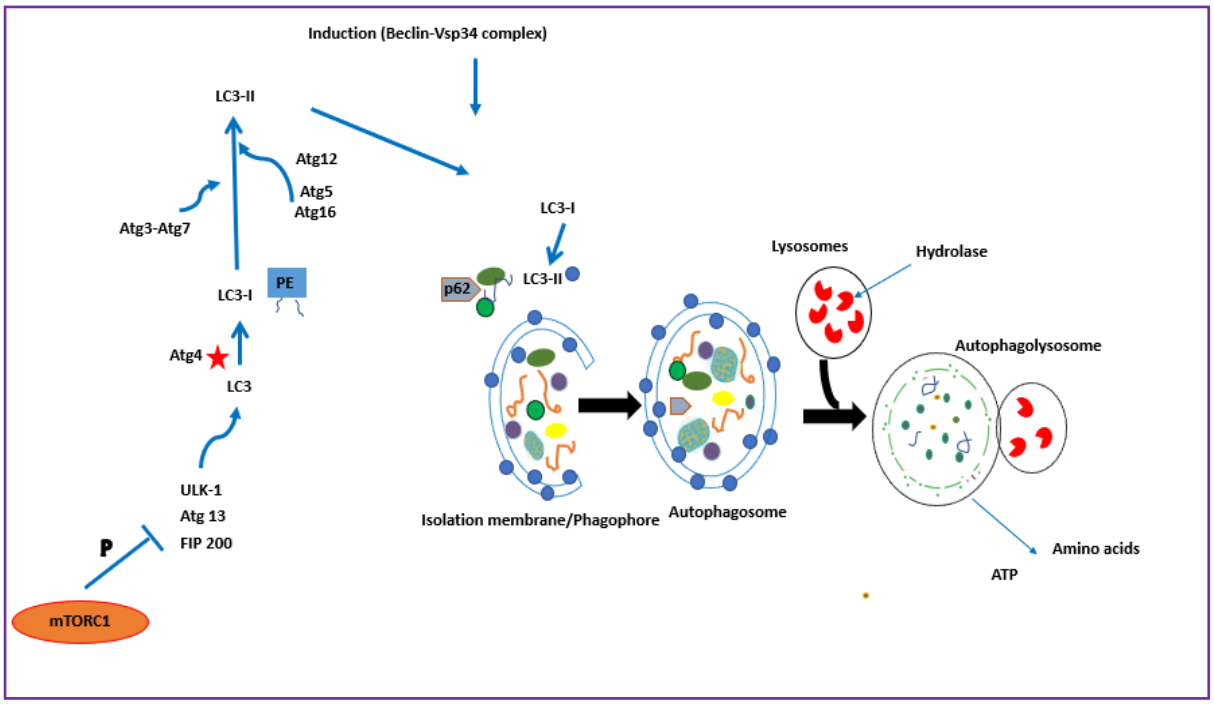

Figure 1:2 Regulation of autophagy. The distinctive stages within the autophagy process are shown to be functionally linked. The formation of autophagosomes (i.e. the initiation phase) and the final steps of the process (i.e. lysosomal restoration) are controlled by mTORC1. Autophagy can be induced by the inhibition on mTORC1, which is mediated by the PI3K signalling pathway. Abbreviations **P**= Phosphorylation, **ATG**=Autophagy-related protein, **LC3 =** microtubule-associated protein 1A/1B light chain**, ATP =** Adenosine triphosphate, **mTORC1 =** mammalian target of rapamycin complex**, PE =** phosphatidylethanolamines**, ULK1/UNC-5 like autophagy activating kinase 1 (ULK1)).** (Adapted from Meléndez and Levine, 2009).

1.5.1.2 Autophagy and metabolism

One of the primary roles of the autophagic process is to supply nutrients and metabolic substrates to cells especially during adverse conditions such as nutrient starvation, in order ensure cell survival. This is achieved mainly through the metabolism of endogenous nutrient reserves which may be used in the production of ATP (Loos et al., 2013). Starvation-induced autophagy is mainly regulated by the (mammalian target of rapamycin) mTOR signalling. The mTOR nutrient signalling pathway has been widely studied and shown to be a major regulator of the autophagic process (Ravikumar et al., 2010). mTOR is a conserved protein kinase that plays a key role in controlling a balance between protein synthesis and degradation and interacts with several proteins to form two distinct complexes: the mTOR

complex 1 (mTORC1) and mTOR complex 2 (mTORC2) (Tchevkina and Komelkov, 2012). mTORC1 consists of Rag, a protein belonging to the family of Ras-like small GTPases which are key mediators of amino acid–induced mTORC1 activation, bound together with a regulator protein called RAPTOR (Rabinowitz and White, 2010). Several stimuli, including amino acids, growth factors (insulin) and energy (in the form of ATP) can cause the activation of mTORC1 which in turn inhibits the initiation of autophagy (Ravikumar et al., 2010). Controlled proteostasis is vital for neuronal functioning, and mTORC1 signalling has been shown to play a pivotal role in controlling this process since mTORC1 promotes anabolic cellular metabolism to supply the necessary building blocks for cell growth and proliferation. mTORC2 is insensitive to rapamycin (Wullschleger et al., 2006), but the molecular mechanism of mTORC2 regulation by upstream effectors is largely unknown. However, mTORC2 has been implicated in the control of cellular morphology through the modulation of actin function (Cuervo et al., 2005). Increasing studies have revealed that aging is associated with the augmentation of abnormal proteins, and that this can be caused by a decline in the autophagic activity (Cuervo et al., 2005).

Under low energy levels, the autophagic process serves as an energetic sensing mechanism (Loos et al., 2013). This is achieved through three main pathways involved in the sensing of energy, linked to the autophagic machinery. These pathways include protein kinase A (PKA), adenosine monophosphate-activated protein kinase (AMPK) and mTORC1, and act as important regulators of metabolism, energy sensing and consequently vulnerability to cell death (Loos et al., 2013). The activation of mTORC1 inhibits autophagy, promotes protein synthesis and nucleotide synthesis as illustrated in (Fig 1.3). An increase in energy in the form of ATP causes a reduction in the AMPK signalling pathway which in turn causes an increase in the activity of mTORC1. In turn, activated AKT directly phosphorylates and thereby inhibits tuberous sclerosis tumour suppressor complex1/2 (TSC1/2), resulting in dissociation of TSC1/2 from the lysosome, where Rheb is localized, promoting formation and activation of the TSC/Rheb complex. Since Rheb is an activator of mTORC1, inhibition of TSC1/2 by AKT dependent phosphorylation results in mTORC1 activation. mTORC1 can also inhibit transcription factor EB (TFEB), a master transcriptional regulator of lysosomal and autophagy genes which inhibits the biogenesis of lysosomes which in turn negatively regulates the autophagy process (Rabinowitz and White, 2010). DNA damage activates p53 which subsequently triggers TSC2 and thereby activates autophagy. Subsequently, extracellular signal-regulated kinase 2 **(**ERK1/2) is activated, which inhibits TSC2, thereby activating mTORC1, resulting in the down-regulation of autophagy activity (Ravikumar et al., 2010). This pathway is stimulated when insulin binds to the receptor on the cell surface,

resulting in the activation of mTORC1 and thereby the inhibition of autophagy (Fig 1.3) (Sarkar, 2013).

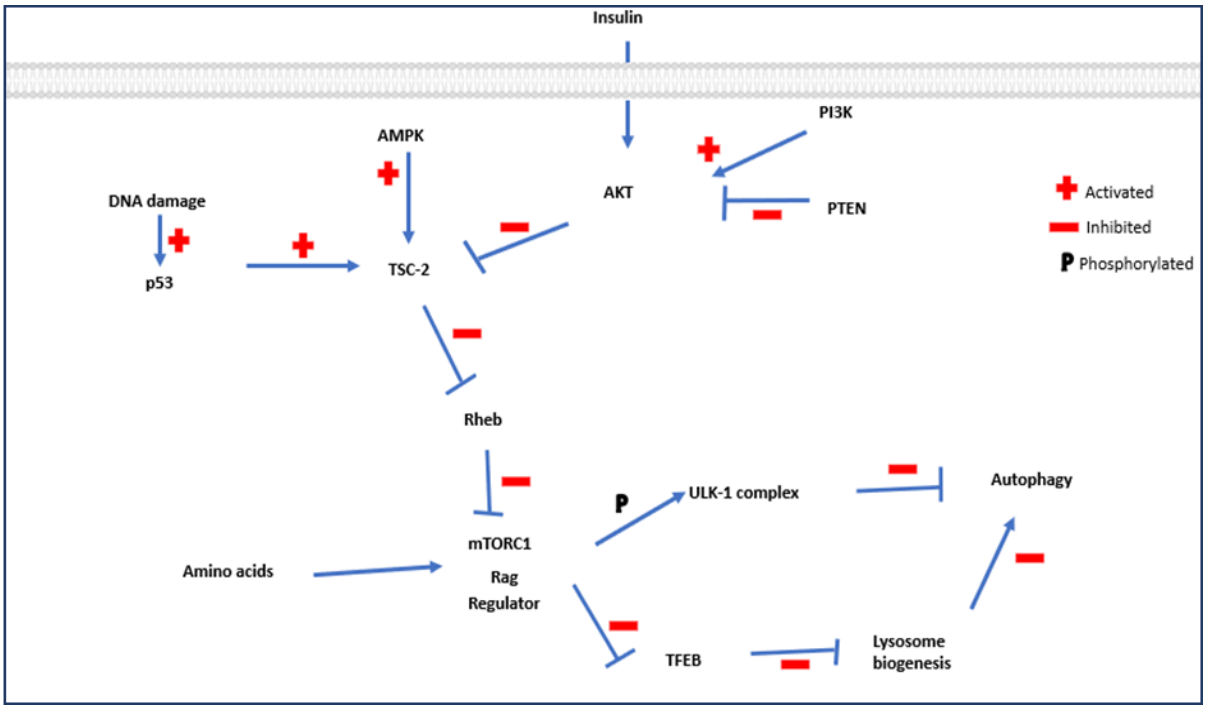

Figure 1.3: Autophagy metabolism is regulated by three main pathways involved in the sensing of the energic status of the cell. These include, protein kinase A, adenosine monophosphate-activated protein kinase (AMPK) and mTORC1 which inhibits the ULK1 complex by phosphorylating complex components. These pathways are important regulators of metabolism, energy status and thereby impact vulnerability to cell death (Adapted from Loos et al., 2013). Abbreviations: **AMPK** = adenosine monophosphate-activated protein kinase**, TSC2 = tuberous sclerosis complex 2, AKT/PKB =** Protein Kinase B**, TFEB =** Transcription factor EB, **PTEN =** Phosphatase and tensin Phosphatase and tensin homolog deleted on chromosome 10, **ULK1 =** Serine/threonine-protein kinase UNC-5 like autophagy activating kinase**, mTORC =** mammalian target of rapamycin complex**, PI3K= phosphatidylinositide 3-kinase.**

1.5.1.3 Current techniques to measure autophagic flux

The autophagic flux is defined as the rate of protein degradation through the entire autophagy pathway (Klionsky et al., 2016; du Toit et al., 2014). Increased or decreased autophagic flux may be associated with a higher or lower autophagosome pool size. The selective process of cargo degradation via autophagy requires the adaptor protein p62, which interacts with cargo targeted for degradation. For example, p62 binds to LC3 through the LC3 interacting region (LIR), which is necessary for degradation of the protein. Hence, the total expression of p62 within a cell may be inversely correlated to the status of the autophagic flux.

There are a wide range of tools and techniques used to assess autophagy. In *in vivo* and *in vitro* studies, autophagy can be induced through treatment with pharmacological drugs such as rapamycin (Boland et al., 2008). Stress signals such as nutrient deprivation or hypoxic

conditions also induce autophagic activity. Subsequently, the level of autophagic activity can be inferred by measuring the difference in LC3II levels between samples in the presence and absence of autophagy fusion inhibitors (Mizushima and Yoshimori, 2007). Such autophagy inhibitors include lysosomal protease inhibitors E64d and pepstatin A, as well as the vacuolar H^+-ATPase inhibitor bafilomycin A1, which directly affects lysosomal pH and thereby inhibits the fusion of autophagosomes and lysosomes (Mizushima and Yoshimori, 2007). Western blotting techniques can be used to assess LC3-I to LC3-II conversion due to the distinct electrophoretic mobility of these LC3 isoforms as the abundance of LC3-II reflects the number of autophagosomes. The “flux” of LC3 puncta, as in the immunoblotting-based assay, can also be determined using fluorescence microscopy, where the increase in the number of LC3 puncta in the presence, compared to that in the absence of a autophagosome/lysosome fusion inhibitor, represents the number of autophagosomes that would have been degraded during the treatment period (Klionsky et al., 2016). Importantly, upstream inhibitors, such as 3-Methyladenine, would not work, as they would just decrease the synthesis.

Autophagosomes have been shown to be present at low levels within healthy neurons (Boland et al., 2008). Initially it was thought that this was due to low autophagic activity within neurons. Mizushima and colleagues developed transgenic mice that systemically express green fluorescent protein (GFP) attached to LC3 and used fluorescence microscopy techniques to analyse the extent of autophagy induction by nutrient starvation in different tissues (Mizushima et al., 2004). This is an excellent technique to assess autophagy activity in *in vivo* studies as it facilitates the visualization of autophagosomes. Using this approach, autophagy induction was found to be distinct in different organs (tissues) in response to nutrient starvation, suggesting that autophagy is constitutively active in tissues and highly efficient in healthy neurons (Mizushima et al., 2004). However, it should be noted that although LC3-II is a good marker for autophagosomes, the amount of LC3-II itself at a given time point does not necessarily estimate the autophagic activity, because not only autophagy activation but also inhibition of autophagosome degradation greatly increases the amount of LC3-II. It is therefore necessary to measure the autophagic flux.

Electron microscopic (EM) analyses have also been used to examine autophagy in *in vivo* and *in vitro* model systems. Regrettably, this method is time consuming and requires various skills, and it is sometimes challenging to morphologically distinguish autophagic vacuoles from other structures. However, EM may be used to assess the degradation of organelles such as mitochondria, which can be visualised in the nervous system, ideally employing the perfusion fixation to avoid changes in autophagy (Davis et al., 2014). Although EM-based techniques do not allow to assess the dynamic nature of the autophagy pathway, flux can be

inferred by fixing tissue at different time points in the presence, compared to that in the absence of an inhibitor (Klionsky et al., 2016). Transmission electron microscopy (TEM), can also be employed to semi-quantitively measure autophagy. TEM allows to measure the number of autophagosomes that are produced and allows to quantify the surface area of autolysomes (Eskelinen et al., 2011).

Recently, a new probe referred to as the GFP-LC3-RFP-LC3ΔG probe, which is a fusion protein of GFP-LC3 and RFP-LC3 was developed by Kaizuka et al. (2016) to assess autophagic flux. In brief, this protein is translated as one fusion protein, and is subsequently cleaved by endogenous ATG4 proteases and produces equal amounts of GFP-LC3 and RFP-LC3ΔG proteins in the cytosol. RFP-LC3ΔG serves as an internal control by remaining stable in the cytosol, while GFP-LC3 is degraded through the autophagic process. This probe offers simple quantitative evaluation of the autophagic flux (Kaizuka et al., 2016). Interestingly, studies are currently underway to develop mice strains stably expressing GFP-LC3-RFP-LC3ΔG to monitor both basal and induced autophagy, the currently available mice have only been shown to sufficiently express GFP-LC3-RFP-LC3DG in muscles (Kaizuka et al., 2016).

1.6 Lysosomal function

Lysosomes are specialized membrane-enclosed organelles that digest large molecules using an array of hydrolytic enzymes (Settembre et al., 2015). These vesicles are vital in the functional execution of protein and organelle degradation through the autophagy pathway. The lysosomal membrane consists of transport proteins that enable transportation of proteins found inside and outside of the cell, and also control lumen acidification and the fusion of this vesicle with other lysosomal structures such as autophagosomes (Settembre et al., 2015).The role of lysosomes in the degradation of substrates or cellular waste is well established (Settembre et al., 2013). However, lysosomes have recently been implicated in several physiological processes such as the repair of the plasma membrane, signalling mechanisms and energy metabolism (Saftig and Klumperman, 2009).

1.7 Autophagy and lysosomal dysfunction

Given the essential role of functional lysosomal activity in the autophagy process, these organelles are increasingly recognised as pivotal role players in the regulation of many cellular processes. Thus, the effective functioning of lysosomes is crucial in the context of health and disease **(**Settembre et al., 2013). In a study by Maejima et al. (2013), suppression of autophagy has been shown to block the biogenesis of lysosomes under conditions of injured lysosomes *in vitro.* This highlights that autophagy is also able to sequester damaged

lysosomes, a process termed lysophagy, to control lysosomal biogenesis (Maejima et al., 2013). The degradative capacity and low pH of injured lysosomes is recuperated in an autophagy-dependent manner. Pathogenic invasion of cells can cause lysosomes to rupture, leading to oxidative stress, and the onset of apoptotic or necrotic cell death (Maejima et al., 2013). The rupture of lysosomes causes cellular contents to leak, including the leakage of cathepsins from the lysosomal lumen into the cytosol (Boya and Kroemer, 2008). LAMP1 and LAMP2 are specific lysosomal membrane associated proteins which prevent the lysosomal membrane from being digested by the hydrolase enzymes because they are glycosylated (Eskelinen, 2006). The permeabilization of lysosomal membranes leads to the liberation of proteases into the cytosol from the lumen, which further triggers cell death onset. Under these conditions, proteases are released from the lysosomal lumen, which in turn results in the activation of a controlled mode of cell death (Terman et al., 2006).

Several cellular processes which are dependent on functional lysosomal activity, are also affected by lysosomal rupture, which also leads to DNA damage, and a decrease in the lysosome's degradative capacity (Boya and Kroemer, 2008). The rupture of lysosomes also stimulates the nucleotide-binding domain and leucine-rich repeat (NLRP3) inflammasome, which causes the secretion of pro-inflammatory cytokines such as IL-1B, thereby enhancing inflammation and promoting disease pathogenesis (Maejima et al., 2013). Hence, the rupture and injury of lysosomes is harmful and induces cellular stress. Several *in vivo* studies have demonstrated how cytosolic substrates including Aβ, bacteria and lipids can contribute to the impairment of lysosomal membranes. The lysosomal membrane has been shown to be impaired by various elements including mineral crystals and lysosomotropic compounds. These compounds are involved in the pathology of many diseases, including neurogenerative diseases such as AD (Boya and Kroemer, 2008). Galectin-3 (Gal-3) is a recently discovered marker for damaged endomembranes, including lysosomes (Paz et al., 2010). Gal-3/Mac-2 forms part of the Galectin family members, which belongs to the family of lectin proteins (Paz et al., 2010). These protein families are recognized by a preserved sequence and by their high affinity for β-galactosides. While Gal-3 is found in the nuclear region as well as the cytosol, only β-galactose-containing glycoconjugates are present on the surface of cells and in the lumen of the Golgi apparatus, the post-Golgi secretory apparatus and endocytic components. Therefore, the rupture of endosomal membranes permits the release of Gal-3 to enter the glycoproteins present in the lumen of these compartments (Paz *et al.*, 2010). In a study by Boya and Kroemer (2008), it was shown that lysosomal damage caused by oxidative stress leads to the recruitment of Gal-3 to LAMP1 and increased colocalization with LC3 (Fig 1.4), suggesting that Gal-3 may be effectively used as a common marker of lysosomal damage.

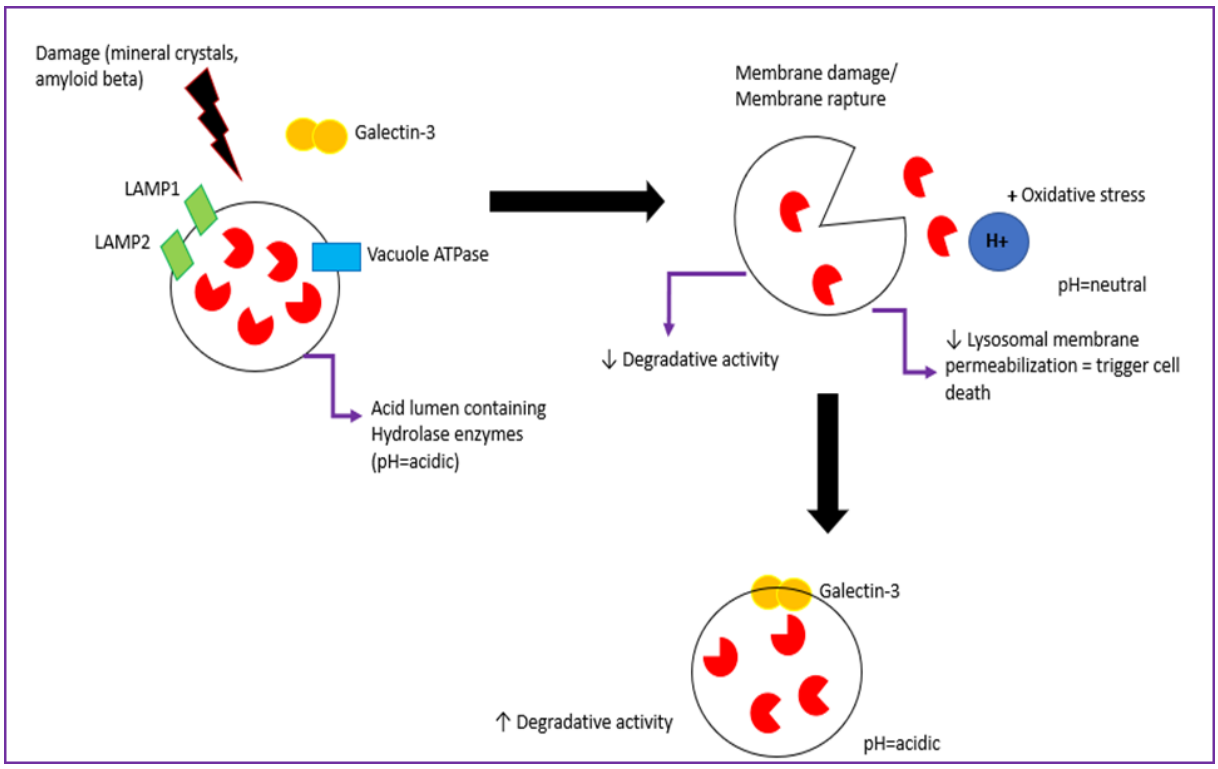

Figure 1.4: Schematic diagram of the fate of Galectin-3 following its recruitment to damaged lysosomes. Abbreviations: **LAMP = lysosomal** associated membrane proteins**, ATPase =** adenylpyrophosphatase**, H^+=** hydrogen ion**.** Adapted from (Maejima et al., 2013).

1.8 Extensive autophagy pathology in AD

It is widely accepted that autophagy impairment is a major contributing factor in the development of AD (Nixon, 2007). Increasing evidence indicates that autophagy is compromised in ageing, and this impairment in turn contributes to further deterioration of biological functions (Hyttinen *et al.*, 2014). Defects in the autophagy process are associated with a rise in the vulnerability of the cell to undergo cell death (Ntsapi et al.,2017). The relationship between autophagy dysfunction, the changing rate of protein degradation in the specific pathology, and the aggregate prone behaviour of specific candidate proteins remains unclear. The maintenance of the equilibrium between protein synthesis and degradation of aggregate-prone cytotoxic proteins is vital for proper functioning and growth of the cell (Ntsapi et al., 2017).

In an electron microscopy study on post mortem human brain samples from patients with AD, Nixon et al. (2005) revealed the massive accumulation of autophagic vacuoles that appeared to accumulate in dystrophic neurites. The dystrophy in neurons was shown to be associated with amyloid plaques (Nixon and Yang, 2011). The accumulation of autophagic vacuoles can be the result of enhanced autophagy induction, impairment of autophagosome maturation, or impaired fusion of lysosomes with autophagosomes, which is linked to a reduction in the

formation rate of autophagosomes (Nixon and Yang, 2011). In AD patients, the expression of beclin-1, which is an important regulator of autophagy induction, was found to be decreased (Pickford et al., 2008). Since beclin-1 expression is an essential protein in autophagy initiation and induction, a decrease in its expression causes an impairment in autophagy induction, thereby contributing to the build-up of toxic protein aggregates and contributes to AD pathology. Furthermore, in neurons isolated from PS1-deficient mice, substrate proteolysis and autophagosome clearance during autophagy was found to be prevented and impaired due to the selective impairment of autolysosome acidification and cathepsin activation (Lee et al., 2010).

Furthermore, in AD brains, electron-dense autolysosomes were shown to accumulate, suggesting a failure in lysosomal function within the proteolytic pathway (Lee et al., 2010). The use of lysosomal inhibitors and the suppression of certain cathepsins was found to result in the accumulation of autophagic vacuoles due to the inhibition of lysosomal proteolysis. Most importantly, the critical role of the autophagy process in neuronal function is highlighted in Atg5 or atg7 knockout mouse models (Komatsu et al., 2006, 2007). In these studies, the occurrence of neurodegeneration was shown to occur independent of the presence of cytotoxic proteins. This highlights the role of dysfunctional autophagy in neuronal disease progression and pathology. The ongoing removal of cytoplasmic constituents via basal autophagic activity is vital to avert the build-up of misfolded, aggregate-prone proteins which may interfere with proper neuronal functioning, and consequently result in neurodegeneration (Hara et al., 2006). The accumulation of autophagic vacuoles has been ascribed to a deficiency in autophagic vacuole removal rather than a marked induction of autophagy (Boland et al., 2008). In contrast, during the early stages of AD, induction of autophagy has been demonstrated to be upregulated (Ginsberg et al., 2010). Accumulated autophagic vacuoles represent a common feature in AD, and represent the presence of undigested, or partially degraded protein clumps which are an immense burden to the autophagy system. Of note, the accumulation of misfolded undigested proteins is also a central theme in lysosome storage disorders (Mizushima et al., 2008).

1.9 Localization of autophagy defects

It has been argued that during early stages of lysosomal system abnormalities, the response of the endoplasmic pathway is dysfunctional, while in later stages there is a gradual impairment of the autophagy process (Lipinski *et al.*, 2010). This leads to an immense augmentation of undegraded materials in dystrophic neurons. Current evidence demonstrates a failure in the impaired autophagosome-lysosome fusion resulting in disturbances in substrate proteolysis (Nixon and Yang, 2011). Immunogold labelling and

ultrastructural studies on neocortex biopsies of AD patients have shown that dystrophic neurites consist of dense lysosomes that are composed of different autophagic vacuoles, including autophagosomes (Nixon and Yang, 2011). These represent the intermediate stages in autophagy progression, suggesting that in AD, the autophagic process is insufficient to mediate clearance. The ability to pinpoint the site or stages at which the autophagy process may be impaired has led to the suggestion that the precise modulation of localized dysfunctional stages within this process may serve as a promising therapeutic intervention in AD pathology.

The inhibition of lysosomal proteolysis in AD has been reported to selectively impair transportation of autophagy-associated vesicles along axons. This leads to AD-type axonal dystrophy, which is characterized by selective accumulation of autophagic vacuoles (Nixon and Yang, 2011). In the brain of healthy individuals, the presence of autophagic vacuoles in neurons is not apparent (Nixon et al., 2005). Since autophagosomes are intermediate structures in the autophagy process, their presence in cells is indicative of the dynamic balance between their rate of sequestration (formation) and degradation by lysosomes (Nixon and Yang, 2011). If the rate of autophagosome clearance is greater, or matches the rate of autophagosome formation, the presence of autophagic vacuole intermediates is barely detectable (Boland et al., 2008). Therefore, the pathology of autophagy reflected in AD is thought to be caused by the disrupted degradation of autophagic vacuoles instead of rapid induction of autophagy alone (Boland et al., 2008). Therefore, targeting the late stages of the autophagy process may be a promising therapeutic target in AD.

1.10 Autophagy and Amyloid-Beta

Autophagy is a vital process in cellular survival, as it is essential for organelle and long-lived protein turnover. In the PS1/APP mouse model of Aβ-amyloidosis, the extracellular deposition of Aβ has been shown to occur following impaired neuronal autophagy induction in early stages of AD (Yu et al., 2005). Sequentially in dystrophic dendrites, late autophagic vacuoles and autophagosomes accumulate and thereby the ‘maturation of autophagosomes and subsequent fusion with lysosomes’ is impaired. In post-mortem studies assessing the brains of AD patients, autophagosomes have been identified as a site for intracellular Aβ production and subsequent accumulation through immunolabelling techniques (Yu et al., 2005). In a study by Caccamo et al. (2010), it was demonstrated that the accumulation of Aβ causes an increase in mTORC1 signalling, while the expression of Aβ was reduced when mTORC1 signalling was decreased, suggesting that Aβ levels may modulate autophagy induction. Indeed, when the production of Aβ was blocked by inhibiting the γ-secretase activity in 7PA2 cells, the kinase activity of mTORC1 was restored (Caccamo et al., 2010).

These results suggest that Aβ and not APP intermediates may increase mTORC1 signalling, thereby decreasing autophagy activity (Caccamo et al., 2010). In agreement, studies conducted on microglia and neuronal cells have demonstrated that the increase in PI3K-AKT signalling pathway is stimulated by Aβ levels, and thereby modulates mTORC1 activity (Wullschleger et al., 2006). It has particularly been shown that an increase in the PI3K-AKT signalling pathway may be caused by Aβ oligomers and not monomers. Indeed, autophagy impairment is associated with the formation of Aβ aggregates, and this association is thought to play a role in AD pathology.

1.11 The role of mitochondrial dysfunction in AD

Mitochondria generally occur as a reticular network to create an interconnected system which provides energy and metabolites for the cell (Lee et al., 2004). Extensive studies have reported that mitochondrial irregularities associated with their form or distribution may play a role in the progression of neurodegenerative diseases such as AD. Mitochondria are cytosolic double membraned organelles which serve as essential modulators of many signalling pathways, and have several functions including the maintenance of synaptic plasticity, generation of neurotransmitters, and energy production in the form of ATP (Pagani and Eckert, 2011). Mitochondria generate ATP through oxidative phosphorylation and the tricarboxylic acid (TCA) cycle. Through a series of enzymatic reactions, the TCA cycle leads to the generation of photons from NADH and FADH (Laura et al., 2014). This is followed by redox reactions comprising of protein complexes (complex I, complex II, complex IV and complex V) that generate a proton gradient. The last step of oxidative phosphorylation results in the generation of ATP (via the phosphorylation of ADP to ATP). This step is regulated by complex V through the ATP synthase machinery. Mitochondrial function is necessary for cellular metabolism, as sustained ATP synthesis is integral to maintaining normal cellular function, cellular viability and homeostasis. In addition, important physiological functions, such as regulating calcium concentration, scavenging free radicals, triggering cell death and regulating variations in redox reactions in the cell are key features of mitochondrial activity (Pagani and Eckert, 2011).

The unique physiological features of neuronal cells and high energy demands make them extremely dependent on the normal functioning of mitochondria (Palmer et al., 2011). Fundamentally, any functional abnormalities in mitochondria may be detrimental to the functioning of neurons. Current literature supports a role for mitochondrial dysfunction and oxidative damage in the pathogenesis of AD, indicating that mitochondrial dysfunction plays an early and prominent role in AD (Pagani and Eckert, 2011). According to the mitochondrial cascade hypothesis, mitochondrial dysfunction is the primary event that causes Aβ

deposition, synaptic degeneration, and NFT formation (Pagani and Eckert, 2011). Pathophysiological events such as dysregulation of calcium homeostasis, production of free radicals and respiratory chain uncoupling which are a consequence of dysfunctional mitochondria, contribute to the triggering of neuronal cell death (Pagani and Eckert, 2011). Mitochondria are central in the execution of intrinsic apoptosis. This process is triggered by inherent protein signals such as caspase activation, which leads to the permeabilization of the mitochondrial membrane, causing the mitochondrial permeability transition pore to open. Similarly, the mitochondrial membrane potential declines, resulting in the production of free radicals (Kerr et al., 1972). Dysfunctional mitochondria are also central role players in bioenergetic sensing (Kroemer et al., 1998). During the distressed state, this can result in the activation of necrosis or apoptosis, both of which will be discussed at a later stage.

1.12 Mitochondrial morphology

The regulation of mitochondria through fusion and fission reactions enables these dynamic organelles to undergo continuous remodelling. Several biological processes such as cellular metabolism, proliferation and cell death are regulated by mitochondria (Laura et al., 2014). Therefore, the maintenance of mitochondrial homeostasis is essential for the resultant fate of the cell and is regulated by the opposing fission and fusion events. Fission state is defined as when a single organelle like mitochondria divides into more independent constitutions and fusion is the opposite reaction (Westermann, 2010). These processes are crucial not only for the preservation of mitochondrial function, but also the removal of damaged mitochondria (Laura et al., 2014). The fusion of an impaired mitochondrion to an adjacent healthy mitochondrion prevents the deleterious effects associated with mitochondrial dysfunction (Laura et al., 2014). This process permits the mixture of healthy mitochondrial DNA and the exchange of macromolecules (proteins, lipids, metabolites), which thereby dilutes the impaired mitochondria population. In contrast, the removal of damaged mitochondria may be achieved through the fission process whereby damaged mitochondria are separated into smaller fragments, thereby making it simpler for these organelles to be targeted for degradation through autophagy, in a process referred to as mitophagy (Laura et al., 2014). It is important to note that the fusion of mitochondria can be prevented by the loss of the mitochondrial membrane potential, which may be the result of a high population of impaired mitochondria. The fusion event thus relies on the internal potential of the mitochondrial membrane which ultimately allows the cell to undergo these processes (Laura et al., 2014).

During the fission state, mitochondria take up a rod or spherical shape caused by fragmentation and are transported by the tubulin network. When the mitochondria are healthy, there is an equilibrium between the fusion and fission state, which enables their

intracellular movement (Laura et al., 2014). Mitochondrial fusion favours the distribution of ATP in metabolically active cells making fusion events beneficial to the cell. In contrast, the fission events of mitochondria are more evident in quiescent cells (Westermann, 2010). The fragmentation of mitochondria during fission is a trigger for cell death, whereas the fusion of mitochondria facilitates the preservation of a healthy pool of mitochondria and proper functioning of mitochondria (Chan, 2006).

The dynamic network of mitochondria is regulated by distinct proteins which are part of the dynamin family. The primary set of proteins responsible for the fission events are dynamin related protein 1 (DRP1) and fission protein 1 (Fis1) (Reddy, 2009). DRP1 is prominently found in the cytoplasm, however, the fragmentation of mitochondria is promoted by the interaction of DRP1 with the outer membrane of mitochondria. Fis1 is confined to the mitochondrial outer membrane and is stimulated by free radicals which in turn induces the fission of mitochondria. The mitofusin (Mfn) proteins are primarily responsible for the regulation of the fusion events. These proteins include Mfn1 and Mfn2, which are both localized on the outermost mitochondrial membrane (Reddy, 2009). Opa1, an additional fusion protein, is present on the innermost mitochondrial membrane. Mfn1 facilitates the interaction process between Mfn compounds next to mitochondria, resulting in fusion of adjacent mitochondria (Reddy, 2009). Fission is favoured during apoptosis, moreover, Fis1-deficient cells have been shown to be resistant to apoptotic cell death and display a high degree of fusion states instead (Reddy, 2009). Several studies have demonstrated that cells deficient in fusion proteins (i.e. Mn1) are susceptible to apoptotic cell death, and such cells display mitochondria that favour the fission state, hence extensive fragmentation (Lee et al., 2004).

1.13 AD and mitochondrial dysfunction

Recent research in sporadic AD cases suggests that APP expression, processing of APP, and Aβ accumulation are all affected by the functioning of mitochondria (Swerdlow et al., 2014). Aβ protein aggregates are implicated in the pathology of AD and appear to impair mitochondrial function (Diana et al., 2008). Indeed, Aβ was shown to be targeted to mitochondria, consequently resulting in the onset of apoptosis, and eventually leading to neurodegeneration (Diana et al., 2008). This process is initiated by the accumulation of Aβ within the mitochondrial membrane, which further disrupts the functioning of the mitochondria, by either damaging mitochondrial enzymes or by impairing mitochondrial DNA (Pagani et al., 2011). Subsequently, these events lead to an increase in mitochondrial membrane permeabilization and lipid peroxidation, which causes the production of reactive oxygen species that further disturb synaptic function (Pagani et al., 2011). This eventually

leads to the unwanted generation of NFTs, ultimately causing the synapse to fail, causing apoptosis, and eventually neurodegeneration (Pagani et al., 2011). Aβ can also target components of the electron transport chain, such as the mitochondrial matrix TCA cycle enzymes which further disturb metabolic processes associated with the mitochondria. Aβ has been reported to promote the activity of mitochondrial fission protein Fis1, causing the fragmentation of mitochondria (Pagani and Eckert, 2011).

1.14 Cell death and its classical categorization

Current literature suggests that the progressive loss of neurons in vulnerable brain regions, such as the hippocampus and cortex, is a key feature of AD (Stadelmann et al., 1999). However, the exact mechanism of neuronal loss remains unclear. Neuronal cell loss in certain regions of the brain, including the hippocampus, is thought to occur via the induction of apoptosis (Stadelmann et al., 1999). The clinical presentation of AD has been shown to correlate with the extent of neuronal loss in certain brain regions including the hippocampus and neocortex. *In vitro* studies of AD reveal that hippocampal neurons subjected to exogenous Aβ peptides indeed display primarily features of apoptotic cell death (Calissano, et al., 2009). *In vivo*, these features are accompanied by synaptic failure, protein aggregation and macroscopic changes such as enlarged ventricles and an atrophied hippocampal region (Apostolova et al., 2012).

Cell death has traditionally been categorized into three modes, including: apoptosis, necrosis and autophagic cell death (ACD) (Galluzzi et al., 2017). They are respectively categorized as type I, II or III modes of cell death (Clarke, 1990). These forms of cell death are highly dependent on the cell's ability to withhold or mitigate the encountered stress and its ability to recuperate (Fulda et al., 2009). In the past twenty years, intensive research efforts have been directed towards the study of cell death, because of the involvement of this process in pathophysiological diseases such as cancer and neurodegenerative diseases. Very recently, the Nomenclature Committee on Cell Death (NCCD) has established widely accepted definitions and classifications of cell death from biochemical, functional and morphological viewpoints (Galluzzi et al., 2017). This has caused a shift from the traditional separation of the cell death modalities. Previously, necrosis and apoptosis were highlighted as the major forms of cell death. However, each cell death type was studied separately, and thereby considered to inherently operate independently. Current operational definitions, classify apoptosis, autophagy dependent cell death (ADCD), and necrosis as regulated cell death (RCD) (Galluzzi et al., 2017). RCD is caused by the activation of signal transduction regulators and can thus be modulated genetically or pharmacologically (Galluzzi et al., 2017). RCD has been shown to play a chief role in multiple physiological conditions,

including inflammation, embryo development, tissue homeostasis, and neurodegeneration (Delbridge et al., 2016). Details of the underlying RCD mechanisms and their involvement in AD progression will be subsequently discussed.

1.14.1 Apoptosis

Apoptosis is typically termed programmed cell death, as this process frequently occurs during development and in response to cell injury during morphogenesis (Kerr et al., 1972). For cell demise to be morphologically categorized as apoptotic, nuclei fragmentation, membrane blebbing, chromosomal DNA cleavage, and cell shrinkage should be evident (Edinger and Thompson, 2004). It was further shown that mitochondrial morphology remains unchanged. During apoptotic cell death, the cell is eventually removed through phagocytosis, and thereby no immune response is elicited. The apoptosis process relies on a series of molecular events and can be further distinguished into intrinsic and extrinsic pathways but concludes in the same execution process (Bibel and Barde, 2000). Apoptosis is regulated by a family of cysteine proteases termed caspases, including caspase 8 and 3 (Song et al., 2017).

The activation of the death receptors including, tumour necrosis factor-alpha (TNFα) and Fas (CD95/APO1) located on the cell surface, leads to the transmission of cell death signals which in turn activate the signalling of intracellular pathways (Elmore, 2007). This process represents the extrinsic pathway. These death receptors further interact with their ligands and form clusters. Subsequently, the formation of a death-inducing signalling complex (DISC) occurs, triggering the autocatalytic activation of pro-caspase 8 which forms caspase 8 (Elmore, 2007). The execution of the extrinsic pathway is stimulated by caspase 8. Finally, the interplay and the execution of both the intrinsic and extrinsic pathway is the activation of caspase 3. This process results in the fragmentation and condensation of DNA, and cleavage of Poly ADP-ribose polymerase (PARP) (Tewari et al., 1995). Interestingly, in neurodegeneration, caspase 3 has been shown to play a key role in the execution of apoptosis, with caspase 3 activity being reported to be involved in the processing of APP (Gervais et al., 1999). Importantly, the intrinsic pathway involves the functioning of mitochondria (Kroemer et al., 2007). Stimuli, including hypoxia, free radicals and toxins serve as positive signals for the activation of intrinsic apoptosis. During intrinsic apoptosis, inherent protein signals such as caspases are activated by certain stress signals leading to the permeabilization of the mitochondrial membrane, causing the mitochondrial permeability transition pore to open (Friedlander, 2003). This damages the mitochondria and leads to cytochrome c release into the cytosol, which serves as a proapoptotic signal (Green, 2005). Next, the cytoplasm and nucleus begin to condense (pyknosis), leading to mitochondrial aggregation (Friedlander, 2003). Similarly, the mitochondrial membrane potential declines,

resulting in the production of free radicals (Kerr et al., 1972). Next, cytochrome c binds and triggers the formation of a complex, termed the apoptosome, involving apoptotic protease activating factor 1 (Apaf1), pro-caspase 9 and ATP utilization. The latter leads to the activation of caspase 9. The members of β-cell lymphoma 2 (Bcl-2) play an essential role in the regulation and control of apoptosis. These members serve as a survival mechanism as they inhibit the activation of pro-apoptotic proteins Bak/Bax, which act on the mitochondrial membrane potential (MMP) and lead to the release of cytochrome c, further leading to the generation of ROS (Behl, 2000). The Bcl-2 family, which includes Bcl-2 and Bcl-xl, serves as anti-apoptotic proteins which in turn together with BH3 inhibit the activation of pro-apoptotic proteins (Behl, 2000).

1.14.2 Necrosis

Necrosis is triggered during an acute ischemic state or neuronal cell injury in the central nervous system (Emery et al., 1998). It involves a cascade of events, including the osmotic swelling of cells, swelling of mitochondria, release of cytoplasmic substances into the extracellular space and, at a late stage, nuclear pyknosis. During the process of necrosis, Los et al. (2002) showed that cell death could be triggered intrinsically through an inflammatory response and via the release of the pro-inflammatory cytokine interleukin-1 beta (IL1β) (Zong and Thompson, 2006). The formation of excitotoxins and production of free radicals emanating from sudden biochemical disruptions contribute to the morphological cellular changes evident in necrosis (Friedlander, 2003). The mitochondria are highly affected by the sudden biochemical disruptions and tend to swell as a result (Aranovic et al., 2012). The ATP produced by mitochondria also serves as the initial activator of the inflammasome response during necrosis (Iyer et al., 2009). Subsequently, the nucleus also swells, as a result, the chromatin network surrounding the nucleus begins to condense (Friedlander, 2003). This process can further cause the nucleus to rupture (karyorhexis), and the DNA becomes degraded; collectively causing the plasma membrane to rupture and well (Schweichel and Merker, 1973). Since necrosis does not typically occur during development or results via activation of caspases, it has not been identified or considered as a programmed cell death mode. However, Proskuryakov et al. (2003) described a process termed necroptosis which suggests a ‘programmed’ process of necrosis, whereby cells exhibit features of both necrosis and apoptosis. This notion is supported by a study that found that neurodegenerative diseases display cell death onset in the form of necroptosis, which results following an ischemic state or several infections (Nikoletopoulou et al., 2013). It is now generally accepted that necroptosis is indeed a *bona fide* cell death modality (Galluzzi et al., 2017).

1.14.3 Autophagy dependent cell death

Autophagy is active in atrophic and homeostatic conditions, and thereby forms part of the normal physiological process. In contrast, autophagy dependent cell death (ADCD) can be defined as unregulated form of autophagic activity which fails to terminate the cell before it collapses leading to unregulated degradation of cellular contents (Lockshin and Zakeri, 2004). This leads to the production of many undigested autophagic vacuoles. Moreover, when the induction of autophagy is not controlled, beclin1 and Atg1 can be overexpressed in mammalian cells and *Drosophila* (Scott et al., 2007), which could indicate ADCD due to the cells' inability to endure untargeted degradation of huge substances found in the cytoplasm. However, the concept of ADCD remains controversial, as several studies have demonstrated that increased autophagy prior to cell demise acts as a pro-survival mechanism to prevent cell death onset (Shen et al., 2012).

1.14.4 Cell death dynamics: cross talk between apoptosis, necrosis and autophagy

The notion that apoptosis, necrosis and autophagy occur in isolation has become increasingly controversial. Several studies suggest that these pathways are linked through intrinsic factors and molecular interplay mechanisms. Indeed, apoptotic cell death has been shown to initiate with autophagy, and autophagic failure can in turn induce apoptosis (Lockshin and Zakeri, 2004). Autophagy has been implicated as the crucial link between necrosis and apoptosis through its ATP production role (Edinger et al., 2004). Distinctive to apoptosis, necrosis is noted to be the end result of ATP depletion above a threshold level at which the cell cannot manage or recuperate from. A reduction in ATP by 50% has been reported to induce necrosis and activation of apoptosis is ATP dependent. Indeed, autophagy can postpone the occurrence of either necrosis or apoptosis, depending on how much ATP is generated (Loos and Engelbrecht, 2009). Autophagy has also been shown to induce apoptosis by preventing the stimulation of apoptosis-associated caspases, which in turn decreases cellular injury (Song et al., 2017). Autophagy is also reported to assist in inducing apoptosis through the activation of apoptosis-related proteins. Moreover, the inhibition of autophagy through the activation of apoptosis-related proteins has been shown to degrade Atg proteins such as Atg4, Atg5 and Beclin1 (Song et al., 2017).

1.15 Therapeutic interventions

The prevalence of AD significantly rises with age. As a result of improved medical care, the global elderly population has increased, particularly in developing countries such as SA (Honig and Boyd, 2013). Although extensive research in the AD field is ongoing, no

treatment interventions have been proven to stabilize, reverse or modify the progression of this disease (Honig and Boyd, 2013). AD is currently poorly treated and has a very poor clinical outcome. The following factors contribute to the susceptibility of AD: age, cerebrovascular disease, family history, level of education/literacy, vascular complications, previous head injuries/trauma and genetic mutations (e.g. presence of the APOE-4 allele). Importantly, low levels of education play an additional role in the development of AD in countries such as SA (de Jager *et al*., 2017). The available treatment options are however limited, with treatment only improving cognitive and behavioural symptoms, but not modulating the underlying molecular dysfunction causing the pathology.

The US Food and Drug Administration (FDA) has approved five treatment therapies for the management of AD (Alzheimer's and Dementia, 2016). These medications offer moderate improvement in cognitive and behavioural functions. The approved FDA medications include, four acetylcholinesterase inhibitors (based on neurotransmitter agents) and an NMDA-receptor antagonist (Honig and Boyd, 2013). Other, more recent and promising therapeutics include the use of pharmaceutical drugs which upregulate autophagic activity (e.g. rapamycin), but these drugs are not prescribed to AD patients. Hence, there is still a major need for more targeted therapeutic interventions that can modify the progression of the disease upstream and downstream of the molecular mechanisms. A brief outline of the therapeutic options that are presently available will be provided, supplemented with the disconnection that exists between the therapeutic action and the molecular dysfunction that underlies AD pathology.

1.15.1 Neurotransmitter based therapies

Reduction in cortical choline acetyltransferase activity is associated with cognitive decline in AD (Lleó, 2007). This led to the development of acetylcholinesterase inhibitors (AChEIs) as a treatment option in this context. This treatment is based on the cholinergic hypothesis, developed about two decades earlier. The AChEIs act by suppressing cholinesterases, and thereby enhance the availability of acetylcholine for brain synaptic processing (Lleó, 2007). Clinical trials have clearly demonstrated that these compounds are beneficial for both cognitive and behavioural defects in AD patients. Between 1993 and 2001, the U.S. FDA approved and standardized four AChEIs compounds for AD treatment: donepezil, galantamine, rivastigmine and tacrine. Of those four, tacrine hydrochloride has received the least attention because it exhibits hepatotoxic side effects (Lleó, 2007). Donepezil hydrochloride is frequently prescribed as it is only taken once daily. Later, galantamine hydrobromide and rivastigmine tartrate were also approved, and used in a once daily dosage. Another recommended drug is memantine hydrochloride that blocks chronic hyper-activation of NMDA receptors, thereby acting as a NMDA antagonist (Honig and Boyd,

2013). Memantine offers further beneficial symptomatic effects when combined with AChEIs inhibitors. The overactivation of the NMDA type glutamate receptors or overexposure to the neurotransmitter glutamate leads to neuronal cell demise, and disproportionate influx of calcium (Lipton, 2004). Although these drugs offer improved cognitive, behavioural and functional properties; they are limited as they only target symptomatic factors and fail to target the progression of the disease. Yet, to date, the only prescribed medications to AD patients are neurotransmitter-based drugs (Chou, 2014). These data indicate that while current treatment options offer transient symptomatic relief to those affected, they offer little targeting of the molecular defects in AD and have not yet been successfully exploited for the overall treatment of the disease.

1.15.2 Vitamin E, antioxidants and anti-inflammatory agents

The build-up of free radicals and the existence of oxidative stress are triggers of AD and common features in the brains of AD patients. This has led to the assumption that antioxidants may be used as a potential treatment option for AD. A widely used antioxidant-based therapeutic approach involves the use of vitamin E (α-tocopherol). A dose of 2000 IU/day is recommended for AD patients; however, this high dose is associated with an increase in mortality (Valory et al*.,* 2009). Hence, the safety of this concentration and the overall efficacy of vitamin E in the treatment of AD has been questioned and is not widely used.

1.15.3 Immunotherapy

The anti-amyloid therapy aims to improve the removal of Aβ deposits by using a vaccine approach. In transgenic mouse models of AD, Aβ42 immunization has been shown to prohibit the presence of Aβ pathology and prevents memory defects (Schenk et al., 1999). In transgenic AD mice models, the overexpression of APP has been shown to be decreased when immunized with Aβ. In some clinical cases, patients displayed improved cognitive, behavioural effects and a reduction in Aβ deposits, while other patients experienced autoimmune reactions (Morgan, 2011). This treatment option has only been implemented as part of clinical trials and has not been approved by the FDA.

1.15.4 Physical exercise

Epidemiological studies have shown an inverse proportional relationship between the extent of exercise/physical activity and the risk of suffering from neurodegenerative diseases such as AD (Paillard et al., 2015). Indeed, physical activity has been reported to enhance cognitive function (Hillman et al., 2008). Moreover, autophagy has been shown to be activated by exercise in peripheral tissues, the brain, skeletal muscle, pancreas, adipose tissue, and the liver (Levine et al., 2012). Interestingly, aerobic exercise has been shown to encourage

angiogenesis and to trigger the release of neurotrophic factors, which in turn facilitates synaptogenesis and neurogenesis, and memory is linked to cognitive function (Paillard et al., 2015). The efficacy of exercise as a treatment intervention is however still being researched (He et al., 2012a; García-Mesa et al., 2011).

1.16 Autophagy inducers as promising treatment intervention

The underlying molecular mechanisms governing AD progression have been widely studied and are increasingly understood. Accumulating evidence suggests that the production of Aβ oligomers is a major feature in AD pathology and triggers several events which result in synaptic failure and neuronal dysfunction (Selkoe and Hardy, 2016). Therefore, the development of drugs should be directed towards targeting the clearance of Aβ, which may be promising in modifying disease progression and AD pathophysiology. Hence, this approach should centre around increasing the clearance or decrease the generation of Aβ. The latter can be achieved by modulating the APP processing in favour of the non-amyloidogenic pathway, while the former can be enhanced by inducing autophagy activity above basal levels with disease progression (Salminen et al., 2013). This approach has recently received major attention.

1.16.1 Rapamycin

Rapamycin is an antibiotic that targets mTORC1 by inhibiting its kinase activity and thereby induces autophagic activity. It exerts its inhibitory effect by directly inhibiting the mTORC1 (Cai and Yan, 2013). By inhibiting mTORC1, rapamycin treatment *in vivo* has been shown to mitigate tau and Aβ pathology in transgenic mice (Caccamo et al., 2010). It has been demonstrated that administration of 2 mg/ml of rapamycin for 15–48 hrs displays protective effects in cell culture models of neurodegenerative diseases, including AD (Berger et al., 2006). Rapamycin is also used as an immune-suppressant and has been approved by the FDA (Cai et al., 2012). Rapamycin treatment has been shown to protect hippocampal neurons from Aβ-induced synaptotoxicity by increasing the activity of pre-synapses (Ramírez et al., 2014). Autophagy induction has been shown to markedly decrease the accumulation of neurotoxic protein aggregates, including Aβ, and promotes the removal of mutant proteins such as mutant HD protein (Rubinsztein, 2004). Therefore, the upregulation of autophagy by rapamycin can modulate the metabolism of APP, and thereby reduce the levels of Aβ in favour of neuroprotection. Although, rapamycin treatment has shown promising results *in vivo* no successful human trails have been reported to date. Importantly, as rapamycin is also an immune-suppressant, it may in turn be harmful to the immune system when used for an extended period. The use of rapamycin as treatment agent for AD is still in its infancy (Caccamo et al., 2010). However, it remains a promising treatment option.

1.16.2 Rilmenidine

The screening of drugs approved by the US FDA for their autophagy-inducing potential led to the identification of rilmenidine as a potential treatment for HD and other neurodegenerative diseases (Rose et al., 2010). Rilmenidine is a safe, and efficient drug currently used to treat hypertension. In a HD mouse model and primary neuronal culture, rilmenidine has been shown to attenuate toxicity caused by polyglutamine peptides (Rose et al., 2010). The protective effect of this drug is achieved through its autophagy inducing properties, possibly acting in an mTOR independent manner. Rilmenidine has also been shown to lower the levels of cAMP (Rose et al., 2010). A clinical study on individuals that clinically manifested HD, revealed that treatment with rilmenidine was relatively safe and well tolerated (Underwood et al., 2017). This effect was presumed to be mediated by rilmenidine's effect on autophagy activity.

1.16.3 Lithium chloride and neurodegeneration

For the past 50 years, LiCl salts have been extensively used in the treatment of key psychiatric disorders, particularly bipolar and mood related disorders (Baldessarini et al., 1999). LiCl has been shown to pass the blood–brain barrier which makes its use in a clinical setting very important, since many drugs do not pass the blood–brain barrier (Manji and Lenox, 1998). Its mode of action is thought to be mediated through targeting of downstream molecules, resulting in the regulation of autophagy related genes and modulation of intracellular signalling (Forlenza et al., 2012). LiCl is a glycogen synthase kinase-3 beta (GSK3β) inhibitor. GSK3β is a serine-threonine kinase that modulates signalling pathways such as the Notch and Wnt signalling pathways and cell cycle regulation (Forlenza et al., 2012). LiCl can inhibit the enzymatic activity of GSK3β via two mechanisms, firstly via direct inhibition by competing at the cationic binding site for magnesium, which is necessary for its enzymatic stimulation (Chalecka-Franaszek and Chuang, 1999); and secondly, via indirect inhibition, by PKB activation via the Akt pathway which responds to insulin signalling or growth factors. LiCl's collective effects on several intracellular signalling pathways eventually leads to the inhibition of apoptosis, the enhancement of neurotrophic factor synthesis and the facilitation of synaptic plasticity mechanisms and neurogenesis (Fornai et al., 2008). This is also associated with memory enhancement in animal studies (Fornai et al., 2008). LiCl's inhibitory effect on inositol monophosphatase (IMPase) was shown to result in the depletion of free inositol, thereby leading to a reduction of myoinositol-1,4,5-triphosphate (IP3) levels (Sarkar et al., 2005). This effect was later shown to upregulate autophagy activity. Although LiCl's autophagy inducing potential may not be relevant in the treatment of mood disorders, this effect is critical in the treatment and prevention of neurodegenerative diseases (Sarkar et al., 2005).

Moreover, in human studies, LiCl dietary supplementation has been shown to enhance neuroprotective factors such as brain-derived neurotrophic factor (BDNF) synthesis, anti-apoptotic gene expression, thickening of the cortical region, oxidative stress inhibition and enlarged hippocampal and grey matter density (Forlenza et al., 2012). A recent clinical trial with amnestic mild cognitive impaired patients, revealed that long-term supplementation with LiCl, potentially slowed the progressive decline in functional and cognitive capabilities, and further attenuated tau hyperphosphorylation (Forlenza et al., 2012). Although reports from clinical trials appear promising thus far, further studies are necessary, particularly large-scale clinical trials to evaluate LiCl's potential neuroprotective effects in the treatment of cognitive deficits among elderly individuals.

1.16.3.1 Neuroprotective effects of Lithium chloride: evidence from preclinical and clinical studies

Treatment with LiCl has also been shown to attenuate Aβ induced cell death in neuronal cells and animal studies that were exposed to exogeneous Aβ peptide (Su et al., 2004). The increase in GSK3β enzymatic activity is an early hallmark of AD pathophysiology, which stimulates various downstream cellular events, in turn resulting in the enhancement of Aβ production and tau hyperphosphorylation. LiCl treatment also enhances anti-apoptotic protein expression such as Bcl-2 which results in the inhibition of cytochrome c release from the mitochondrial membrane, thereby regulating mitochondrial permeability and maintaining calcium homeostasis (Chen et al., 2006). These cellular events are vital for the maintenance of cellular integrity, and cell survival. Treatment with LiCl has also been demonstrated to modulate the processing of APP and to reduce the generation of Aβ through the suppression of GSK3β in APP-mutated transgenic mice (Phiel et al., 2003). Moreover, LiCl has been shown to possess anti-inflammatory properties, as evidenced by a reduction in interleukin-1β and tumour necrosis factor-α production in glial cells exposed to LiCl treatment (Li et al., 2011). Therefore, LiCl holds therapeutic potential in the mitigation of inflammatory cell responses.

A clinical study was conducted in patients with mild to moderate AD, to evaluate the efficacy of LiCl, the results were negative in the initial studies (Dunn et al., 2005). In fact, patients that were treated with LiCl were found to have a greater risk for developing dementia, with an increase in risk associated with an increase in the dosage of LiCl prescribed (Dunn et al., 2005). In a clinical trial of a single-blind placebo-controlled group consisting of 71 AD patients, 10-week treatment duration with LiCl was demonstrated to not have any significant benefits on cognitive function (Hampel et al., 2009). GSK3β enzymatic activity was not significantly inhibited by LiCl, and Aβ42, tau protein and cerebrospinal fluid (CSF) biomarker levels were not altered. However, a reduction in the levels of CSF phosphorylated tau was

displayed in the LiCl group. LiCl has also been studied in other neurodegenerative diseases including PD, HD and amyotrophic lateral sclerosis (ALS). In the context of ALS, supplementation with LiCl has revealed neuroprotective effects associated with autophagy activation, an increase in mitochondrial number in motor neurons and inhibition of reactive astrogliosis (Fornai et al., 2008).

As detailed in the sections above, the long-term neuroprotective effects of LiCl supplementation have been widely documented in treatment of psychiatric disorders and AD model systems. However, the use of this drug in a clinical setting may be challenging as there are safety precautions concerning long-term usage amongst the elderly. However, further research is required to confirm the efficacy, safety and long-term use of LiCl to achieve the best therapeutic outcomes possible.

1.16.3.2 Lithium chloride and autophagy

LiCl has been demonstrated to induce autophagy in a mTOR-independent manner. This induction process occurs through the inhibition of IMPase and inositol transporters and receptors (IP3R). Suppression of IMPase activity leads to a reduction in free inositol levels, resulting in lowered IP3 and myo-inositol-1,4,5 triphosphate levels (Sarkar et al. 2005). Additionally, activation of IP3 and its respective receptor has been shown to inhibit autophagy (Criollo et al. 2017). However, Sarkar and colleagues (2008) have further investigated the inducing effects of LiCl on autophagy and observed that LiCl-induced autophagy can also occur in an mTOR-dependent manner. LiCl has also been shown to promote the removal of mutant huntingtin and α-synuclein protein (Sarkar et al., 2005). The mTOR-independent induction of autophagy has been demonstrated in response to co-treatment with rapamycin and LiCl, which revealed greater reduction of pathological prion proteins in murine neuroblastoma cells compared to cells only treated with rapamycin alone (Sarkar et al.,2005). However, the observed reduction was comparatively less significant than cells treated only with LiCl. LiCl induced autophagy holds much promise as a therapeutic avenue in the removal of aggregate prone-proteins involved in the pathology of many neurodegenerative such as AD (Heiseke et al., 2009). This is reflected in a study where LiCl induced autophagy resulted not only in the reduction of pathological prion proteins, but also in a slight reduction in cellular prion protein levels (Heiseke et al., 2009). This was reflected by an increase in LC3-II protein levels in cells treated with LiCl. The reduction in pathological prion proteins was observed in a dose- and time-dependent manner in murine neuroblastoma cells, where the clearance of pathological prion proteins was revealed at a concentration of 10 mM of LiCl treatment (Heiseke et al., 2009).

In N2aswe cells either untreated or treated with LiCl for 24 hrs and analysed for endogenous levels of LC3-II, an increased amount of LC3-II protein levels was observed in cells treated with LiCl (Heiseke et al., 2009). To exclude the possibility that the observed increase in LC3-II levels upon LiCl treatment did not result from impaired autophagosome-lysosome fusion (also leading to an increased level of LC3-II protein expression), the amount of LC3-II was measured in the presence and absence of bafilomycin A1 treatment (Yamamoto et al. 1998). This led to an increase in LC3-II protein signal, indicating that LiCl indeed upregulates autophagic activity above basal levels.

1.16.4 Gingko biloba and neurodegeneration

Gingko biloba (GB) is a phytopharmacon and is commonly cultured for its leaf and for its nuts. The GB-producing tree can tolerate urban and industrial environments and has great resistance against fungal, viral and bacterial infection (Oken et al., 1998). The GB leave extract has been used for decades in traditional Chinese medicine for various purposes. GB has successfully been used as treatment and in the prevention of vascular and cerebral disorders including AD. The main properties of GB include gingko-flavanols (mainly in the form of isorhamnetin, kaempferol and quercetin) which make up to 22–27% and 5–7% terpenoids (Augustin et al., 2009). The terpenoids comprise of bilobalide and the ginkgolides A, B, C, J and M; which are synthesized from 20 carbon cage molecules enclosed by six 5-membraned rings (Oken et al., 1998). The ginkgolides have several physiological properties and ginkgolide B is a platelet-activating factor (PAF) antagonist. PAF has been shown to directly affect the function of neurons. In the hippocampal region, ginkgolide J has been shown to protect cells against neuronal cell death and irregular hippocampal long-term potentiation which is induced by Aβ accumulation (Vitolo et al., 2008). Ginkgolide B has specifically been shown to inhibit Aβ25–35 induced neurotoxicity via the upregulation of BDNF expression in hippocampal neurons (Xiao et al., 2010).

Flavonoids are the main components of the GB extract and lend their anti-oxidant properties and ability to scavenge free radicals. This makes GB a suitable natural treatment for cellular oxidative stress related diseases, including AD (Chan et al., 2007). In numerous studies GB has been demonstrated to decrease lipid peroxidation in cell membranes, protect neuronal cells against peroxidation induced oxidative stress and reduce injury of neurons following ischemia (Wieraszko et al., 1993). Earlier studies have shown that in AD, supplementation with EGb761 (standardised GB leave extract) is associated with anti-oxidative properties, scavenging of free radicals, anti-amyloidogenic properties, regulation of neurotransmitters and anti-apoptotic properties (Horakov et al., 2003). Therefore, EGb761 can be viewed as a multivalent agent with the potential to serve as preventive treatment for diseases with complex aetiology such as AD (Bastianetto et al., 2000). In a study by Stark and Behl (2014),

the proteasome catalytic activity and the protein degradative activity was found to be enhanced by EGb761 treatment in cultured cells. The authors further investigated this effect in the context of an HD cell culture model using cells that expressed pathologic variants of polyglutamine protein. In this context, treatment with EGb761 was found to lead to an increase in proteasome activity, thereby stimulating enhanced degradative capacity of short-lived proteins (Stark and Behl 2014). These findings could suggest that EGb761 promotes the degradation of short-lived, misfolded proteins via the proteasome degradative pathway. However, since most intracellular proteins are long-lived, to more efficiently target the degradation of protein aggregates in neurodegenerative diseases would require a better-quality control system such as the autophagy pathway. However, further studies are warranted to clarify the role of EGb761 in neuroprotection as variable results have been reported on the beneficial properties of EGb761 in the treatment of neurodegenerative diseases (Moosmann and Behl 2002; DeKosky et al., 2008).

1.16.4.1 Gingko biloba and AD

It is well established that ageing is a major contributor to AD pathophysiology. Due to its ability to combat age-associated oxidative stress and inflammation, GB can be used as an effective treatment of AD (Tchantchou et al., 2009). This is due to GB's anti-inflammatory and antioxidant properties, evident from several clinical studies reporting the efficacy of EGb761 in the treatment of dementia and AD (Le Bars et al., 2000; Kanowski, et al., 1996). However, work by DeKosky et al. (2008) revealed that treatment with GB (120 mg) twice a day did not significantly decrease the overall incidence rate of AD or dementia. Although standardized GB extracts have been shown to be neuroprotective in the context of neurodegeneration, the mechanism of actions remain unclear. In AD transgenic mice, Aβ aggregation and oxidative stress induced by Aβ has been shown to be attenuated by EGb761 supplementation (Shi, 2010). Recent *in vivo* studies have demonstrated that genes encoding proteins implicated in the pathogenesis of AD are influenced by short-term treatment with EGb761 (Watanabe et al., 2001). This is exemplified in work by Schindowski et al. (2001) which demonstrate that treatment with EGb761 *in vivo* and *in vitro* has anti-inflammatory, antioxidant properties and leads to enhanced cerebral blood flow. In addition, treatment with EGb761 has also been shown to attenuate Aβ aggregation (Luo et al., 2002) and oxidative stress induced by Aβ (Smith and Luo, 2003) in transgenic cells and animal models. In the brain tissue of transgenic mice, chronic treatment with EGb761 (300 mg/kg) has been shown to differentially influence protein levels involved in the processing and metabolism of APP (Augustin et al., 2009). This study also revealed that long-term EGb761 dietary supplementation leads to a significant decrease in human APP levels in the cortex and hippocampus regions, which could potentially indicate that APP is molecularly targeted

by EGb761. Augustin and colleagues ultimately concluded that supplementation with EGb761 did not affect the levels of APP expression in young mice, suggesting that the duration of GB treatment and/or the animal's age may impact the efficacy of treatment (Augustin et al., 2009).

1.16.4.2 Gingko biloba and autophagy

GB dietary supplementation results in robust autophagic induction, as revealed by an increase in LC3-II protein levels and beclin1 expression in the brains of APP-transgenic mice (Liu et al., 2015). Similarly, in microglia cells the protein expression of LC3-II and beclin1 was elevated and associated p62 levels were decreased following GB EGb761 treatment, suggesting that GB treatment upregulates autophagy activity. Another GB extract (EGb1212) consisting of a greater quantity of bilobalide and ginkgolide B has been reported to inhibit autophagy in the ischemic brain (Yin et al., 2013). However, the overall extent of autophagic flux modulation in response to GB treatment remains unknown.

1.17 Rationale of the study

Two distinct features of proteotoxicity are observed in the brains of AD patients at autopsy, namely extracellular deposits of senile plaques composed of Aβ peptide deposition, and intracellular aggregation of NFTs composed of hyperphosphorylated tau protein, with Aβ deposition being widely recognized as the major contributor to AD pathogenesis (Aging, 2011). Accumulating evidence suggests that autophagy, a major lysosome-based degradation pathway is critical for stress-induced and constitutive removal of long-lived proteins and is the primary pathway responsible for maintaining normal Aβ homeostasis amongst other important physiological functions (Musiek and Holtzman, 2015). The modulation of autophagic activity is therefore thought to be a promising therapeutic strategy towards the alleviation of Aβ-associated neurotoxicity in AD, which is often accompanied by extensive mitochondrial damage. Current literature supports a role for mitochondrial dysfunction and oxidative damage in the pathogenesis of AD, indicating that mitochondrial dysfunction plays an early and prominent role in AD pathogenesis (Pagani and Eckert, 2011). According to the mitochondrial cascade hypothesis, mitochondrial dysfunction is one of the primary events that causes Aβ deposition, synaptic degeneration, and NFT formation. As a result of insufficient degradation of oxidatively damaged macromolecules and organelles through autophagy, neurons progressively accumulate cytotoxic proteins and organelles that could exacerbate neuronal dysfunction (Nixon and Yang, 2011). Since autophagy is the major pathway involved in the degradation of protein aggregates and damaged organelles, there is an intense interest in developing autophagy-related therapeutics given the molecular link between autophagy dysfunction and AD pathogenesis.

1.18 Problem statement

LiCl is a promising modulator of autophagic activity, however, the relationship between its concentration, duration of exposure and potency to induce autophagy is largely unclear as its use has been limited to the treatment of bipolar disorders. Moreover, a fine or precision control of autophagy activity through LiCl treatment has not yet been achieved. Similarly, GB is used as a dietary supplement in AD patients, but it has not been standardized for clinical use. Although it is thought to have positive impact on neuronal proteostasis, it is not known to what extent it can induce autophagy. Moreover, it is not known whether GB exhibits a concentration-dependent effect on autophagy activity and whether a combination approach together LiCl would maximize protein clearance and neuronal protection in an *in vitro* model of Aβ induced neuronal toxicity.

1.19 Aims and objectives

The aim of the proposed study was therefore to investigate the effect of both GB and LiCl as a single or combined treatment intervention on the modulation of autophagy activity, and the mitigation of Aβ proteotoxicity in an *in vitro* model of AD.

We specifically aimed to assess the following parameters:

1. whether GB exhibits a dose-dependent effect on autophagic activity or whether a combination treatment approach with LiCl could further enhance autophagy activity above basal levels
2. whether high and low GB concentrations can attenuate Aβ toxicity distinctively, in the presence and absence of LiCl treatment
3. whether high and low GB concentrations can preserve lysosomal function and mitochondrial network morphology distinctively, in the presence and absence of LiCl treatment

1.20 Hypothesis

We hypothesize that treatment with GB will exhibit a concentration-dependent effect on autophagic activity, and this effect will be further enhanced through combination treatment with LiCl. This effect will translate in the distinct removal of APP and Aβ, by preserving lysosomal function and mitochondrial integrity.

CHAPTER 2: MATERIALS AND METHODS

2.1 General consumables and reagents

Bio-smart Scientific (Edgemead, Cape Town) supplied 15 ml (50015) and 50 ml (50050) falcon tubes, and flat bottom 96 (30096), 48 (30048), 24 (30024) and 6 (30006)-well dishes. NUNC 8-well chambered glass dishes (154534) were supplied by Thermofisher. Sterile cell culture flasks including, 175 cm^2 (431080, 75 cm^2 (708003) and 25 cm^2 (707003), were supplied by White-head Scientific (Stikland, Cape Town). Sterile 5ml (326001), 10 ml (327001) and 25 ml (328001) serological pipettes were supplied by B&M Scientific (Parrow, Cape Town). B&M Scientific (Parrow, Cape Town) also supplied pipette tips and 0.5- and 2-ml Eppendorf tubes.

Table 2.1. List of reagents and sources.

Reagent	Company purchased
2- 2-Mercaptoethanol	Sigma Aldrich (M6250)
APS	Sigma Aldrich (A3678-25G)
Bromophenol Blue	Sigma Aldrich (SAAR1437500CB)
Bovine serum albumin (BSA)	Sigma Aldrich (10735078001)
Cell Scrappers	Nest Biotechnology (710001)
Clarity ECL Western Blotting Substrate	Bio-Rad Laboratories (170501)
Complete Protease Inhibitor	Sigma Aldrich (11573580001)
Coverslips	Sigma Aldrich (Z692263)
Cryovials	Scientific Group (430658)
Dulbecco's modified Eagle's medium (DMEM)	Life Technologies (41965-062)
Dimethyl sulfoxide (DMSO)	Whitehead Scientific (D2650)
Foetal bovine serum (FBS)	Biocom Biotech (FBS-G1-12A)
Glycerol	Merck (SAAR2676520)
Hoechst 33342 Stain solution	Sigma Aldrich (H6024)
Microscope slides	Sigma Aldrich (BR474701)
Mounting Media	Diagnostech (S302380)
NA_3VO_4	Sigma Aldrich (S6508)
NaF	Merck (193270)
NP40	Sigma Aldrich (74385-1L)
n-Pentane	Merck (1.07177.1000)
Opti-MEM Reduced Serum Media	Thermo Fisher Scientific (31985047)

Reagent	Company purchased
PenStrep antibiotic (15140122)	Life Technologies (15140-122)
PMSF	Sigma Aldrich (93482-50ml-F)
Potassium Chloride	Merck (SAAR5042020EM)
Prestained Protein Ladder	Biocom Biotech (PM007-0500)
Running buffer	Bio-Rad Laboratories (161-0772)
Sodium dodecyl sulphate (SDS)	Sigma Aldrich (L3771)
Sodium Chloride	Merck (1.10732.0100)
Sodium hydroxide	Sigma Aldrich (S5881-500G)
Spar Fat Free Long-Life Milk	Local Spar
TEMED	Merck (1.10732.0100)
TGX Stain-free Fast Cast Acrylamide Kit, 12%	Bio-Rad Laboratories (1610185)
Trans-Blot Turbo Midi PVDF Transfer Packs	Bio-Rad Laboratories (1704157)
Triton X-100	Sigma Aldrich (T8787)
Trypsin-EDTA	Life Technologies (25200072)
Tween-20	Sigma Aldrich (P1379)

2.2 Antibodies

The primary antibodies probed for in western blot (WB) and Immunofluorescence (IF) analysis are presented in the table below **(Table 2.2)**. Primary antibodies were either purchased from Cell Signalling Technologies or Abcam. All primary antibodies were diluted in 1x tris-buffered saline (TBS-T) at a dilution factor of 1:1000 and 1:200 dilution in 1x Phosphate Buffered Saline with Tween 20 (PBS-T) solution for WB and IF, respectively. The following secondary antibodies were utilized for WB: anti-rabbit IgG HRP (7074S) and anti-mouse IgG HRP (7076S) purchased from Abcam, anti-mouse IgG (CST7076S) and anti-rabbit IgG (CST7074S) purchased from Cell Signalling.

Table 2.2. List of primary antibodies.

Primary Antibodies	**Host**	**Working Dilution**	**Company purchased**	**Size (kDa)**
anti-SQSTM1/p62(D5L7G)	mouse	1:1000	Cell Signalling Technologies (88588S)	62
APP	rabbit	1:1000	Cell Signalling Technology (2450)	100-140
Amyloid beta (Aβ)	rabbit	1:1000	(Cell Signalling Technologies (2454)	5
cleaved PARP	rabbit	1:1000	Cell Signalling Technology	89
anti-LC3B	rabbit	1:1000	Cell Signalling Technologies, (*2775S*)	16;18
LAMP2a	rabbit	1:1000	Abcam (ab18528)	140
c-Caspase-3	rabbit	1:1000	Cell Signalling (9661)	17;19
Cytochrome c	rabbit	1:1000	Cell signalling (4280)	14
MNF1	mouse	1:1000	Abcam (ab57602)	89
DRP1	mouse	1:1000	Abcam (ab56788)	89
Beta-actin	rabbit	1:1000	Abcam (ab91526)	42
Secondary Antibodies	**Host**	**Working Dilution**	**Company purchased**	**Size (kDa)**
anti-rabbit IgG HRP	Donkey	1:10000	Abcam (7074S)	-
anti-mouse IgG HRP	Donkey	1:10000	Abcam(7076S)	-

2.3 Cell Culture

2.3.1 *In vitro* study design

Neuroblastomas 2A (N2a) mouse neural cells, stably expressing AD-related Swedish mutant form of the APP695 plasmid (N2aswe) were utilized for all experimental procedures. These cells were kindly provided by Professor Sangram Sisodia (Department of Neurobiology, University of Chicago, USA). The N2aswe cell line has been extensively utilized as an *in vitro* model system for the study of AD (Lee et al., 2015).

2.3.2 Maintenance of N2aswe cells

In accordance with the manufacturer's instructions, N2aswe cells were was propagated in tissue culture flasks under a humidified atmosphere containing 5% CO_2 at 37°C. The cultured cells were supplemented with media consisting of (DMEM and Opti-MEM™ at a ratio of 1:1), 1% Penstrep and 5% Fetal bovine serum (FBS). Cells were frozen in media (1 ml FBS, and 10 µl DMSO) containing approximately 1 x 10^6 cells per cryovial and then stored in a liquid nitrogen freezing chamber. To induce the APP transgene expression, N2aswe cells were treated with butyric acid (sodium salt) (BA, 5 mM). The use of 5 mM of BA has been shown to significantly enhance the expression of APP following 12 and 24 hours (hrs) treatment, with no cytotoxic effects reported thus far (Lo et al., 1995; Shin et al., 2016).

2.3.3 Thawing of cells

A volume of 4 ml of pre-heated growth medium were added to a T-25 flask using a sterile 5 ml pipette. Following this, a cryovial containing approximately 1 x 10^6 cells was removed from long-term liquid nitrogen storage and immersed in the water bath (at 37˚C) for ~3 minutes. After ensuring that the cells were adequately thawed, 1 ml of cell-suspension was transferred to a T-25 flask containing 4ml of growth medium. The cells were then incubated at 37˚C in a 5% CO_2 atmosphere. After two hrs of incubation, the growth medium was removed, discarded and refreshed with 4 ml pre-warmed growth medium. For the rest of the experimental procedures, the growth medium was replaced every 48 hrs. Cells were allowed to reach a confluency of 80% prior to experimental procedures.

2.3.4 Seeding of cells for experimental procedures

When the cells reached 80% confluency, the growth media was removed, the cell monolayer was then gently rinsed with prewarmed trypsin-EDTA (2 ml for a T-25 and 3 ml for a T-75). An inverted microscope (Olympus CKX41) was used to determine whether the cells had completely detached from the flask surface. Once the cells had dissociated from the cell surface, an appropriate volume of growth medium (4 ml for a T-25, 12 ml for a T-75, 16-20 ml for a T-175, and 6 ml for 90 cm^2 petri-dishes) was added, and the suspension was

centrifuged at 15000 Revolutions per minute (rpm) for 3 minutes at 37 ˚C. Thereafter, the supernatant was decanted, and the cell pellet was re-suspended in 1 ml of growth medium. Individual cells were counted by using a haemocytometer, and subsequently seeded for experimental procedures at the recommended seeding densities of N2aswe cells based on the surface area of culture vessels. A cell passage number of 10-24 was employed for all procedures.

2.5 Treatment groups for autophagy and cell death analysis

2.5.1 Treatment reagents

BA (H6501) (Sigma) was used to induce APP transgene expression. Gingko biloba (GB) (Flora force) and lithium chloride (LiCl) (Sigma, CAT) were used as the treatment interventions. Bafilomycin A1 (B0025) (LKT Laboratories) was used to inhibit autophagosome-lysosome fusion (Yamamoto et al. 1998). Sterile PBS was used as a solvent to dissolve all the reagents and prepare stock solutions of the treatment compounds.

2.5.2 GB treatment

GB capsules (340 mg) were purchased from Flora Force. For extraction of GB, the 60% acetone extraction (w/v) method was used. Briefly, GB capsules were removed from the bottle and encapsulated powder was retrieved. A total of 0.5 g GB powder was weighed and added to a 60% acetone solution in a volumetric flask. The flask was then placed in an ultrasonic bath at 40 °C for approximately 30 minutes and the GB diluted in acetone solution was filtered using filter paper under a vacuum. Thereafter, a freeze-dried extract method was employed to yield an extracted dry GB residue. The processed GB residue was then weighed and diluted in sterile PBS to prepare the desired stock solutions. Working standard concentrations of 10, 25, 50, 100, 200 and 400 µg/ml GB were prepared by diluting the appropriate volume of stock solutions with prewarmed growth media. All stock solutions were stored at -20 ˚C until further use. GB low concentration (10 µg/ml (↓)) and GB high concentration (200 µg/ml (↑)) were not found to be cytotoxic to the cells, as determined using a colorimetric assay based on the bio-reductive capacity of cells. These concentrations were thus used for all experimental procedures.

2.5.3 Lithium chloride (LiCl) treatment

A stock solution of 1 M of LiCl was prepared immediately prior to each experiment in sterile PBS. Working standard concentrations of 2.5, 5, 10 and 20 mM LiCl was prepared. A final working concentration of 10 mM LiCl was determined using a calorimetric assay.

Table 2.3. describes the treatment groups including the respective treatment intervention period that was used for all the experimental procedures in accordance with the aims of the study.

Table 2.3. Treatment compounds

Treatment intervention	Company	Working Concentration	Time
Butyric acid (BA)	Sigma Aldrich	5 mM	48 hrs
Lithium Chloride (LiCl)	Sigma Aldrich	10 mM	24 hrs
Bafilomycin A1 (BAFA1)	Lkt Laboratories	400 nM	4 hrs
Lysotracker	Thermo-fisher Scientific	75 nM	2 hrs
Hoechst	Thermo-fisher Scientific	1 mg/ml	30 minutes (min)
Silica	Sigma Aldrich	250 mg/ml	3 hrs
TMRE	Abcam	500 nM	30 min

The treatment groups were outlined as follows:

- Control
- 24 hrs LiCl (10 mM) pre-treatment group
- 24 hrs GB (10 and 200 µg/ml) pre-treatment group (GB 10 µg/ml (↓), GB 200 µg/ml (↑))
- 4 hrs BafA1 (400 nM) treatment group
- 48 hrs BA (5 mM) treatment group

2.6 Experimental procedures

2.6.1 Cellular Viability assays

2.6.1.1 Water Soluble Tetrazolium Salts assay to determine viability following Gingko biloba and lithium chloride treatment

The Water-Soluble Tetrazolium Salts (WST-1) bioreductive assay is used to quantify the metabolically active cells in a population, and to ensure that the treatment compounds were not cytotoxic to the cells, thus giving an indication of cellular viability. This colorimetric assay is based on the bioreductive capacity of cells. Metabolically active cells can reduce the water-soluble yellow tetrazolium salt WST-1 to water-insoluble purple formazan crystals of which the absorbance can be detected spectrophotometrically. The principle of this calorimetric assay is based on the cleavage activity of various mitochondrial dehydrogenase enzymes. Therefore, WST-1 can also be used as an indicator of mitochondrial reductive

capacity of metabolically active/living cells. An increase in the absorbance signal indicates an increase in metabolically active/healthy cells, whereas a decrease in the metabolism of healthy cells is accompanied by a decrease in the absorbance signal, indicating the potential cytotoxic effects of the treatment interventions. N2aswe cells were seeded into 48-well plates which contained 200 µ of pre-warmed media and allowed to attach overnight under a humidified atmosphere containing 5% CO_2 at 37°C. The following day culture media was removed from the 48-well plates and cells were exposed to various concentrations of the treatment compounds as described in section (2.3). This was performed in order to relate the intervention concentrations to those known to be therapeutically achievable in humans. After incubation and exposure to various treatment, 10 µl of WST-1 was added to 200 µL culture medium in each well and subsequently incubated for 2 hrs (avoiding exposure to light). Following the incubation period, the absorbance signal was measured at 450 nm using a microplate reader (EL800 universal microplate reader, BioTek Instruments Inc). Under control conditions, cellular viability was considered as 100% and the treated groups were measured against the control groups.

2.7 The effects of GB and LiCl on autophagy and amyloidogenic processing

For western blot purposes, N2aswe cells were seeded at a density of 500,000 cells into 12 T-75 flasks according to each treatment group. WB analysis of the autophagy markers LC3-II and cargo protein p62 was conducted. LC3-II is a functional indicator for autophagic activity (Rubinszstein et al., 2009), and p62 is required for the selective binding of ubiquitinated proteins and marks the proteins for autophagic degradation. However, to investigate the extent of autophagy induction the utilization of autophagosome-lysosomal fusion inhibitors is crucial to accurately interpret results related to autophagy activity (Rubinsztein et al., 2009). To investigate the extent of autophagy modulation by GB, co-treatment with or without bafilomycin A1 was performed (Mizushima and Yoshimori, 2007). This allowed the investigation of the dose-dependent effects of the described treatment groups on autophagic activity, and allowed for the quantification of the rate of autophagic activity. The degradation of cargo through the autophagic pathway was determined by probing for the following proteins: APP and Aβ through WB. The western blot results of autophagy flux and cargo protein levels of cargo, specifically APP and Aβ, allowed us to correlate the relationship between protein degradation through autophagy and the clearance rate of proteinaceous cargo.

2.7.1 Protein extraction

Upon completion of the treatment interventions, N2aswe cells were harvested as follows: T-75 flasks were washed with cold PBS three consecutive times and supplemented with 150 µl of cold radioimmunoprecipitation assay (RIPA) buffer (adjusted to pH 7.4) and supplemented with 10 µl of Protease and Phosphatase Inhibitor Cocktail. A sterile cell scraper was used to gently scrape the cell monolayer and the cell suspension was then transferred to sterile Eppendorf tubes and maintained on ice. The cell lysates were then sonicated for 10 seconds using the ultrasonic liquid processor (Misonix Sonicator 4000, Connecticut, USA) at a frequency of 3 Hertz. Sonification was performed on ice. Subsequently cell lysates were centrifuged at 8000 rpm for 10 minutes at 4 °C until the cell lysates were clarified. The clarified supernatants were carefully collected and transferred to pre-chilled Eppendorf tubes and stored until further analysis at -80 °C.

2.7.2 Protein determination and sample preparation

Protein quantification was performed using the Direct Detect® FTIR Spectrometer (Merck Millipore, USA). The Direct Detect ® infrared spectrometer is an advanced membrane technology, optimized for the detection and quantification of proteins. Briefly, cell lysates are applied in a drop-wise manner directly to a card-based hydrophilic polytetrafluoroethylene (PTFE) membrane that is transparent in most of the infrared spectral region. Once dried, the card-based PTFE membrane is measured by the Direct Detect® system for amide bonds in protein chains, thereby accurately quantifying protein content. A minimum protein concentration of 0.2-5 mg/mL can be accurately determined from a minimal sample volume of 2 µl. RIPA buffer was used as the blank measurement. The card-based PTFE membranes were placed on the spotting tray and 2 µL of blank (RIPA buffer) was added on spot 1. Subsequently 2µL of each sample were loaded onto the assay-free cards and loaded into the loading compartment of the Direct Detect® machine. A protein concentration of 20 µg/ml of each sample were prepared using a blend of β-Mercaptoethanol (150 µl) and Laemmli's sample buffer (850 µl). For further analysis, samples were stored at -80 °C

2.7.3 Sodium dodecyl-sulphate polyacrylamide gel electrophoresis

Using a 12% Bio-Rad Fast Cast Stain Free-gel (Bio-Rad Laboratories, South Africa), equivalent amounts of protein (20 µg) were loaded per lane with a molecular marker being loaded in the first lane to assist with orientation and sizing of separated proteins. Proteins were separated using the sodium dodecyl sulphate polyacrylamide gel electrophoresis (SDS-PAGE; Mini-PROTEAN® Tetra cell, Bio-Rad) system at a constant voltage of 120 V and current of 200 mA (Bio-Rad Power Pac 1000) for approximately 90 minutes. When the migration front reached the bottom of the gel, the gel was carefully placed and activated in

the ChemiDoc imaging system (Chemi Doc MP, Imaging System). Following activation, the gels were immediately transferred onto polyvinylidene fluoride (PVDF) membranes (Immobilon-P® Merck Milipore, IPVH00010, Darmstadt, Germany) using the Bio-Rad electro-transfer system electrotransfer system (Bio-Rad Trans-blot® SD, USA) for 5 minutes. This was followed by the activation of the membranes to obtain the total protein and determine transfer efficiency using the ChemiDoc imaging system. Subsequently, the membranes were rinsed in 100% methanol and allowed to air dry prior to being re-hydrated in 100% methanol until translucent (this was performed to immobilize the proteins on the membranes). The membranes were then incubated for 1 hour in blocking buffer solution (5% fat-free milk diluted in 1x TBS-T).

Each membrane was then cut at the 25 kDa protein marker as the proteins of interest were either visualized higher than 25 kDa and lower than 25 kDa. Following the blocking procedure, the membranes were probed for several proteins of interest using recommended dilutions of **(see Table 2.2 for full details).** With the exception of anti-LC3B which was incubated for two nights, all membranes were incubated overnight at 4°C in primary antibodies. The following membranes were washed in 1x TBS-T three times 10 minutes each, and subsequently incubated in the appropriate HRP-conjugated secondary antibody for an hour at room temperature. The membranes were then washed in 1x TBS-T three times for 10 minutes each (this was performed to avoid formation of isoforms, which was a constant problem in previous WB analyses). The membranes were then exposed to ECL Western Blotting Substrate (Bio Vision, USA, San Francisco Africa) for 1 minute to develop and visualize protein bands using the ChemiDoc imaging system (Chemi Doc MP, Imaging System). The Bio-Rad Image Lab software was used to quantify the band intensities. The percentage band intensity was expressed relative to average β-actin control for each respective protein of interest.

2.8 Cell death analysis

Western blot analysis of the apoptotic marker cytochrome c was performed. The release of cytochrome c into the cytosol serves as a pro-apoptotic molecule (Green, 2005). The aim of this analysis was to investigate if GB or the combination with LiCl could attenuate Aβ induced toxicity, potentially in an autophagy-dependent manner. These results were correlated with the WST-1 cell viability assay findings. Additionally, we aimed to investigate whether GB or the combinational with LiCl could potentially attenuate Aβ induced damage. Western blot analysis of LAMP1 and LAMP2 was collectively assessed to further investigate the hypothesis that Aβ toxicity causes lysosomal damage, whereas/while GB preserves lysosomal function.

2.8.1 Transient transfection

This section aimed to investigate whether APP causes lysosomal damage/leakage by comparing how many cells are Galectin 3 (Gal-3) (+) (damaged cells) and how many cells are LAMP1 (+) (total number of lysosomes). This analysis allowed for the investigation of lysosomal stability. N2aswe cells were transiently transfected with GFP-Galectin3 plasmid. Gal-3 is recruited to damaged lysosomes, and the rupture of endosomal membranes permits the release of Gal-3 to enter the glycoproteins found in the lumen of compartments such as lysosomes (Paz et al., 2010). The Lipofectamine 3000 (Invitrogen, L300000) transfection solution was prepared as described in Table 2.4.

Table 1.4. Lipofectamine 3000 transfection solution components.

Compounds	Eppendorf tube 1	Eppendorf tube 2
GFP-galectin3	(1/773.8 ng/µl) X (800 DNA concentration) = 1µl	NA
P3000	1 µl per well	NA
Serum free media	50 ul per well	50 µl per well
Lipofectamine	NA	0.5 µl per well

Briefly, $5x10^3$ N2aswe cells were seeded in NUNC 8-well chamber dishes and transfected with green fluorescent protein-galectin-3 (GFP-Gal-3) plasmid (expanded and developed at the Department of Human Genetics, Tygerberg, South Africa) (see Appendix for exact protocol followed). This was done prior to treatment by using the Lipofectamine ®3000 transfection reagent (Life Technologies, L30000015). Sufficient transfection efficiency was achieved using a plasmid concentration of 773.8 ng/µL, diluted in Opti-MEM containing P3000 solution (1µL/µg DNA). The DNA-P3000 complex solution was co-incubated with Lipofectamine® 3000 solution in a 1:1 ratio for 30 minutes to allow for stable complex formation. Cells were incubated with Transfection media (10 µL per chamber) for 48 hrs. The efficiency of transfection was verified using the Olympus cell system attached to an Ix 81 inverted fluorescence microscope (Soft imagining system, Olympus Corporation, Tokyo, Japan)

Following transient GFP-Galectin-3 transfection for 48 hrs, N2aswe cells were either treated with BA for 48 hrs or treated with Silicon dioxide (also termed Crystalline silica, found in nature as quartz or sand) (Life technology). Silicon dioxide has been reported to disturb the membrane of lysosomes in alveolar macrophages and trigger inflammation in lungs (Hornung et al., 2008), and this compound was also used as a positive control for lysosomal

injury. Following the treatment procedure, transfected cells were further supplemented with LysoTracker® Red DND-99 (Thermo-Fisher Scientific) which is a red-staining fluorescent dye utilized to label and track organelles that are acidic (such as lysosomes) in live cells. This was followed by nuclei staining using Hoechst (Thermo-Fisher Scientific) to allow for the detection of cell nuclei. Thereafter cells were imaged per group at 100x magnification. Two excitation filters were used to capture the images, including, Oregon Green 488 excitation and DAPI excitation, and the images were captured using the Olympus Cell software (Hamburg, Germany).

2.8.2 Mitochondrial assessment

2.8.2.1 Tetramethylrhodamine ethyl ester treatment and live cell imaging

N2aswe cells (500) were seeded per well into NUNC 8-well chamber dishes and the cells were allowed to attach overnight in a humidified atmosphere containing 5% CO_2 at 37 °C. The following day, the cells were treated with medium (C), LiCl 10mM, GB low (↓:10µg/ml), GB high (↑:200µg/ml), GB low (↓:10µg/ml) + LiCl 10mM, GB high (↑:200µg/ml) + LiCl 10mM for 24 hrs and then further incubated for 48 hrs in BA (5 mM) treatment. This was followed by a refreshment of media comprising of 500 nM tetramethylrhodamine ethyl ester (TMRE; Abcam, #ab113852). TMRE is a fluorochrome that is dependent on the potential of the membrane, and thus used to stain for polarized mitochondria with intact membranes in living cells (Hanley et al., 2002). Cells were stained with Hoechst 33342 at a 1:200 dilution in culture media 1 hr prior to imaging. Two excitation filters were used to capture the images, including Texas Red excitation and DAPI excitation, and the images were captured using the Olympus Cell software (Hamburg, Germany).

2.9 Immunohistochemistry and confocal microscopy

N2aswe (500) cells were seeded into a NUNC 8-well chamber dishes containing 200 µl pre-warmed growth media. The cells were then allowed to adhere overnight. The following day, the cells were treated with medium (C), LiCl 10mM, GB low (↓:10µg/ml), GB high (↑:200µg/ml), GB low (↓:10µg/ml) + LiCl 10mM, GB high (↑:200µg/ml) + LiCl 10mM for 24 hrs and BafA1 treatment for 4 hrs. Following the treatment intervention period, the media was removed, and the cells were rinsed with cold PBS. This was followed by a fixative step, where cells were incubated at 37 ºC for 15 minutes with a 1:1 fixative solution of 4% paraformaldehyde and growth media. The fixative solution was then aspirated, and the cells were washed with PBS three times for 5 minutes. This was followed by a permeabilization process using 0.1% Triton X-100 in sterile PBS for 6 minutes at room temperature (RT). The cells were subsequently washed with 1XPBS three times for 5 minutes and further incubated with 5% Donkey serum (Sigma, D9663) for 1 hour which was used as blocking buffer. The

blocking serum was then removed, and the cells were incubated overnight at 4 °C with the following primary antibodies: ant-APP, anti-Aβ, p62, LC3B, MNF1, DRP diluted in 1XPBS at a 1:200 dilution (see Table 2.2 for details). Approximately 50 µl of primary antibody solution was added to each well. The following day, the primary solution was removed, and the cells were incubated with fluorophore-conjugated secondary antibodies AlexaFluor 568 donkey anti-rabbit (ThermoFisher, 10042) and AlexaFluor 488 donkey anti-mouse (ThermoFisher, A-10037) for 1 hr at RT. This procedure was followed by three times wash step for 5 minutes with sterile 1XPBS. This was followed by a nucleur staining for 10 minutes using Hoechst 33342 diluted in 1XPBS at a 1:200 dilution. After the cells were washed, and allowed to airdry for 10 minutes, Dako® fluorescent mounting medium (Dako Cytomation)) was added to the individual NUNC 8 chamber wells in a dropwise manner and allowed to airdry for 1 hr. Subsequently, the cells were either imaged directly using the Carl Zeiss ELYRA S1 LSM-780 microscope system or stored at -20 °C for further imaging at a later stage.

2.10 Acridine orange staining

Acridine orange (AO) MW (369.94, Sigma) is a fluorescent dye which specifically recognizes acidic compartments, such as lysosomes which stand as an indication of the digestive capabilities (via autophagy) within a cell. Briefly, 500 N2aswe cells were seeded into an 8-chamber dish containing 200 µl pre-warmed growth media. The cells were then treated with medium (C), LiCl 10mM, GB low (↓:10µg/ml), GB high (↑:200µg/ml), GB low (↓:10µg/ml) + LiCl 10mM, GB high (↑:200µg/ml) + LiCl 10mM, for 24 hrs and then then treated for 48 hrs with BA (5 mM). This was followed by a refreshment of media comprising of AO (1:500; Sigma). AO can emit fluorescence after excitation with blue light (466.5 nm) The cells were stained with Hoechst 33342 (1:200 dilution in growth media) prior to imaging. Thereafter, Dako® fluorescent mounting media (Dako Cytomation) was added dropwise to each chamber and left to airdry at -20 ºC overnight. The following day images were acquired using the Olympus CellR system attached to an IX 81 inverted fluorescent microscope equipped with an F-view-II cooled CCD camera (Soft Imaging Systems).

2.11 Transmission electron microscopy

2.11.1 Sample preparation

N2aswe cells were seeded in duplicate into T-75 flasks and allowed to adhere overnight. After reaching a confluency of 80%, cells were treated with medium (C), LiCl 10mM, GB low (↓:10µg/ml), GB high (↑:200µg/ml), GB low (↓:10µg/ml) + LiCl 10mM, GB high (↑:200µg/ml) + LiCl 10mM, and 48 hrs with BA (5 mM). After treatment, 3 ml of trypsin was added to each flask and incubated for 5 minutes to all for complete cell detachment from the flask surface.

Following this, 6 ml of media was added to each flask, and the cell suspension was transferred into 15 ml falcon tubes. The cells were then centrifuged at 1500 RPM for 5 minutes and thereafter the cell pellet was resuspended in 1 ml of pre-warmed 1XPBS. The cell suspension was centrifuged again under the same conditions, and the cell pellet was resuspended in 1 ml of pre-warmed 2.5% glutaraldehyde which was used as a fixative solution. The cell suspension was further centrifuged for 10 minutes and the cell pellet was resuspended in 1 ml 2.5% glutaraldehyde. The cells suspension was then stored at 4°C overnight and TEM analysis were performed at the Tygerberg Hospital by National Health Laboratory Services.

2.11.2 TEM sample processing

The fixative solution was removed, and the cells were washed in 0.1 M sodium phosphate buffer 3 times for 5 minutes. This was accompanied by a centrifugation step (1500 RPM) between each wash step. The cells were then fixed with 1% osmium tetroxide diluted in 0.1 M sodium phosphate buffer for 1 hr. Next, the samples were washed in deionised water 5 times and then transferred to an automated tissue processer, and the samples underwent a series of dehydration steps described as follows:

- 15 min in 10% uranyl acetate
- 10 min in 30% ethanol
- 10 min in 50% ethanol
- 10 min in 70% ethanol
- 10 min in 90% ethanol
- 10 min in 95% ethanol
- 10 min in 100% ethanol
- 10 min in 100% ethanol

Samples were subsequently incubated with a 1:1 solution of 100% ethanol and Spurr's resin for 90 min and then further incubated with 100% Spurr's resin for 120 min. The samples were then embedded for 72 hrs at 60°C in an oven, in 100% Spurr's resin using BEEM Embedding Capsules (Electron Microscopy Sciences). Subsequently, using the Leica EM UC7 ultramicrotome, the resin-embedded samples were sectioned into 200 nm sections. These sections were stretched using chloroform vapor and then placed onto copper grids. Images were acquired using a JEOL JEM 1011 transmission electron microscope and analysed using the iTEM soft imaging analysis program.

2.12 Liquid chromatography-mass spectrometry based quantitative analysis

Liquid chromatography–mass spectrometry (**LC-MS**) **Q-TOF** is a technique that uses analytical chemistry to separate components of an organic compound through the combination of liquid chromatography, allowing the physical separation of elements, and mass spectrometry, used for mass analysis. In order to better understand the Ginkgo extract used in this study, LC-MS was performed. This method enables the precise location and identification of specific terpene lactones and flavonoid glycosides present in acetonic Ginkgo biloba leaf extracts through their different retention times. Upon fragmentation, flavonoid glycosides display cleavage sugar moieties (Beck & Stengel, 2016). Components are separated in a thin column and the machine scans the compound from 5 Delta to 500 Delta and generates a peak before indicating an accurate mass of that specific molecule. With these two parameters, the exact compound can be identified.

2.13 Statistical analysis

Data from at least three independent experiments was analysed by one-way analysis of variance (ANOVA) using the Bonferroni post-hoc test. The GraphPad Prism version 5.02 software was employed to conduct all statistical analysis between treatment groups. A $p<0.05$ was considered as statistically significant. All data are expressed as mean ± standard error of the mean (SEM).

CHAPTER 3: RESULTS

Section 3.1: The effect of Ginkgo biloba (GB) and lithium chloride (LiCl) treatment on cell viability

3.1.1 Dose response of lithium chloride and Ginkgo biloba

One of the main questions in the autophagy field centre around the aspect of whether autophagy activity differs in a concentration dependent manner when using an autophagy inducing agent. Hence, WST-1 viability assays were conducted after incubating N2aswe cells with increasing concentrations of lithium chloride (LiCl) and Gingko Biloba (GB) for 24 hrs respectively, in order to determine a suitable low and high, yet non-toxic concentration. With the guidance of literature, a suitable concentration range was chosen by conducting a dose response to ensure that the desired GB and LiCl working concentrations had no toxic effects to the N2aswe cells.

Literature points to LiCl as a neuroprotective agent (Forlenza & Diniz, 2014). Accordingly, the relative reductive capacity of N2a cells after 24 hrs exposure to various concentrations of LiCl, including 5 mM, 10 mM, 20 mM, 40 mM, 500 mM, were reported (Fig 3.1.1). Exposure to LiCl (10 mM, 20 mM, 40 mM) displayed no significant difference in terms of reductive capacity compared to control conditions [0.61 ± 0.06 ($p < 0.05$)]. These results demonstrated that LiCl has no neurotoxic effects under these concentration ranges. However, we observed that higher concentrations of LiCl (500 mM) appeared cytotoxic by significantly reducing the relative reductive capacity compared to control conditions [0.10 ± 0.02 ($p<0.05$)]. Therefore, a lower concentration of LiCl (10 mM) treatment was utilized for all following experiments.

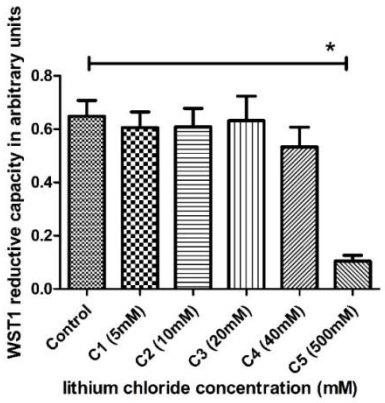

Figure 3.1.1: Relative reductive capacity of N2aswe cells after 24 hrs treatment exposure to various concentrations of lithium chloride (LiCl: 24 hrs 5 mM, 10 mM, 20 mM, 40 mM, 500 mM). * $p<0.05$ vs Control (n=3).

3.1.2 Concentration-dependent effect of GB on cell viability

After incubating N2aswe cells with varying concentrations of GB (10, 25, 50, 100 and 200µg/ml) WST-1 viability assays were performed (Fig 3.1.2). Twenty four hrs supplementation with the respective concentration of GB displayed no significant reduction in the relative reductive capacity: GB 10 µg/ml [1.1 ± 0.08]; GB 25 µg/ml [0.8971 ± 0.01]; GB 50 µg/ml [0.87 ± 0.02]; GB 100 µg/ml [0.71 ± 0.03]; GB 200 µg/ml [0.71 ± 0.04] (Fig 3.1.2). This demonstrated that GB has no neurotoxic effects on N2aswe cells. However, a significant difference decrease was reported between GB 10µg/ml [1.1 ± 0.08]; ($p<0.05$] and GB 100/ 200µg/ml [0.71 ± 0.03; 0.71 ± 0.4 ($p<0.05$)], respectively (Fig 3.1.2). These results showed that N2aswe cells display a degree sensitivity with regards to the reductive capacity when exposed to GB, however, not reaching significance when compared to non-treated control cells. Thus, both a low concentration (10µg/ml: GB↓) and a high concentration (200µg/ml: GB↑) was utilized for subsequent experiments.

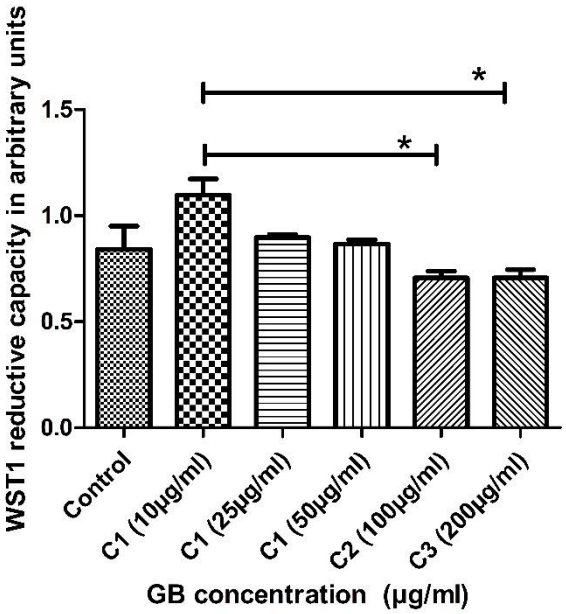

Figure 3.1.2: Relative reductive capacity of N2aswe cells after 24 hrs treatment exposure to various concentrations of Gingko biloba (GB) (10µg/ml, 25 µg /ml, 50 µg /ml, 100 µg /ml and 200 µg /ml). * $p<0.05$, n=3.

3.1.3 Combination treatment of GB and LiCl and effects on cell viability

Light microscopic examination and WST-1 assays were employed to assess the reductive capacity of GB (↓10µg/ml & ↑200µg/ml) in the presence or absence of LiCl (10mM). Treatment with GB↓(10µg/ml) [0.36 ± 0.01]; GB↑ (200µg/ml) [0.33 ± 0.01] and LiCl [0.35 ± 0.01] had no effect on cell viability. Moreover, a similar trend was revealed when the cells were exposed to a combination treatment of both GB concentrations with LiCl [0.32 ± 0.01; 0.32 ± 0.01] (Fig 3.1.3 A). Light microscopic examination revealed no distinguishable differences in the general morphology of the N2aswe cells that were exposed to LiCl, GB (↓10µg/ml & ↑200µg/ml) in the presence and absence of LiCl compared with the control group respectively (Fig 3.1.3 B). Therefore, suitable concentrations were established, and used for subsequent experiments to assess autophagic activity and protein clearance.

(A)

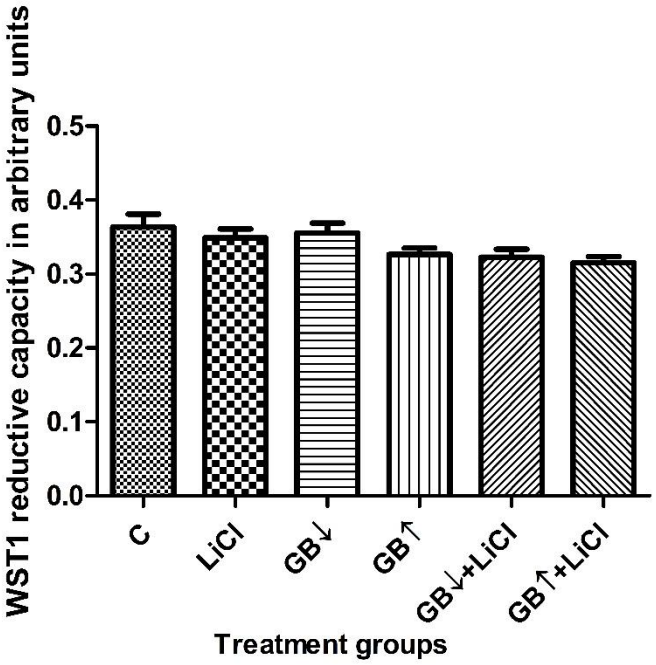

Figure 3.1.3 A: Relative reductive capacity of N2aswe cells after 24 hrs treatment exposure to Gingko biloba (GB↓10µg/ml & GB↑200µg/ml), lithium chloride (LiCl 10 mM) and combination treatment of GB (↓10µg/ml +LiCl) and GB ↑200µg/ml +LiCl (10mM) * $p<0.05$ (n=3).

(B)

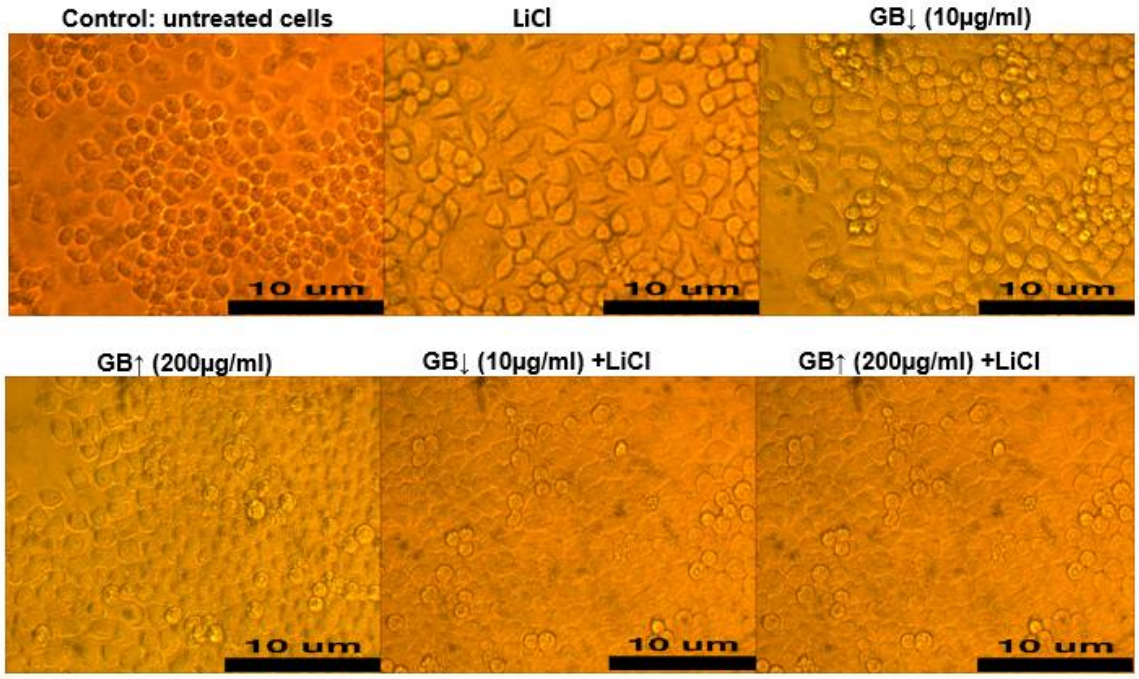

Figure 3.1.3 B: Micrographs representing the morphological assessment of N2aswe cells (Control) after 24 hrs treatment exposure to Gingko biloba (GB↓10µg/ml & GB↑200µg/ml), lithium chloride (LiCl 10 mM) and combination treatment of GB (↓10µg/ml +LiCl) and GB ↑200µg/ml +LiCl (10mM). (n=3). Scalebar: 10µM.

3.1.4 Gingko biloba pre-treatment confers neuroprotection against amyloid-βeta mediated proteotoxicity

In the following section, results that assessed the effect of LiCl and GB in the context of amyloid ß induced neurotoxicity are reported. We hypothesized that supplementation with GB and the combination treatment with LiCl would confer neuroprotection due to their likely role in upregulating autophagy.

3.1.4.1 WST1 Reductive capacity

The relative reductive capacity of N2aswe cells following GB and combination treatment with LiCl prior to BA exposure was assessed using WST1 assays (Fig 3.1.4). BA (5mM) is known to induce the induction APP transgene expression resulting from increased protein expression and activity of BACE, and thereby increasing the production of Aβ (Shin et al., 2016).

A significant reduction in the relative reductive capacity of cells was observed following 48 hrs exposure to BA treatment [0.24 ± 0.01 ($p<0.05$)] (Fig 3.1.4 A) compared to control conditions This result indicates that 48 hrs overexpression of APP impacts cell viability. However, a 24 hrs pre-treatment with LiCl [0.33 ± 0.01 ($p<0.05$)], GB↓ 10µg/ml (0.34 ± 0.01

(p<0.05)] & 200µg/ml [0.34 ± 0.01 (p<0.05)] and GB↓ + LiCl [0.30 ± 0.01 (p<0.05)] prior to BA exposure caused a higher capacity in the relative reductive capacity, compared to BA only treated cells [0.30 ± 0.4 (p<0.05)] (Fig 3.1.4 A). Hence, a rescue effect of LiCl, GB 10µg/ml & 200µg/ml and GB↓ (10µg/ml) + LiCl treatment was observed, and thereby reducing the neurotoxicity caused by the APP overexpression. However, both high and low concentrations of GB equally protected neurons from Aβ-induced neuronal toxicity. Exposure to BA caused prominent cell loss and alteration of cell morphology, compared to control cells as revealed by the corresponding micrographs (Fig 3.1.4 B). In contrast, 24 hrs pre-exposure to LiCl, GB (↓:10µg/ml &↑:200µg/ml) in the presence and absence of LiCl prior to BA treatment displayed an larger number of cells and an improvement in the morphology of cells compared to BA treated cells. In order to further validate the demonstrated neuroprotective role of GB and LiCl, western blot analysis of apoptosis markers, namely: cleaved Caspase 3 and cytochrome C was conducted.

(A)

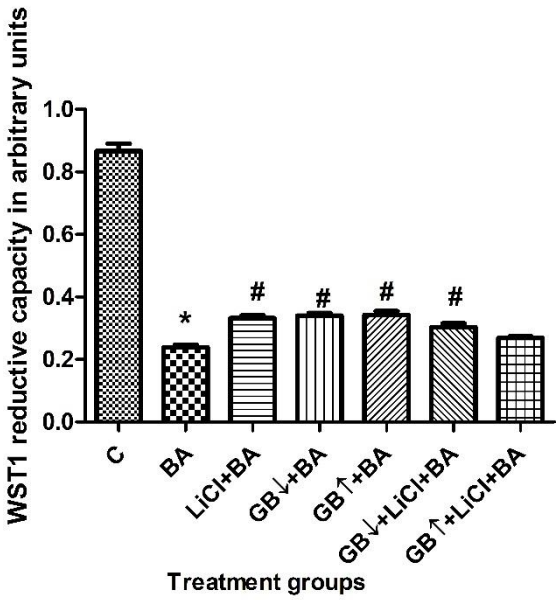

Figure 3.1.4 A: Relative reductive capacity of N2aswe cells following exposure to Gingko biloba (GB) (GB↓10µg/ml & GB↑200µg/ml), lithium chloride (LiCl 10 mM) and combination treatment of GB (↓10µg/ml +LiCl) and GB ↑200µg/ml +LiCl (10mM) followed by butyric acid treatment (BA, 5mM, 48 hrs). * p<0.05 vs control; # p<0.05 vs BA, n=3.

(B)

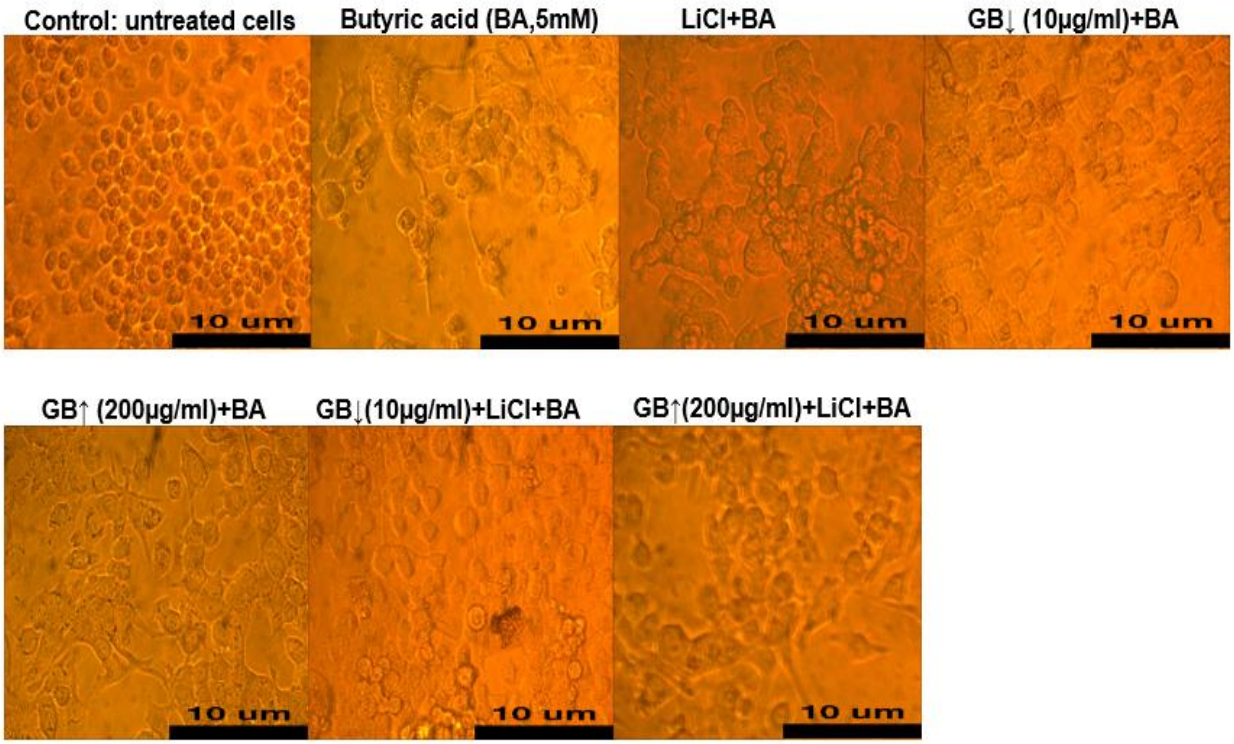

Figure 3.1.4 B: Micrographs representing N2aswe cells (Control) following exposure to Gingko biloba (GB↓10µg/ml & GB↑200µg/ml), lithium chloride (LiCl) and combination treatment of GB (↓10µg/ml +LiCl) and GB ↑200µg/ml +LiCl (10mM) followed by butyric acid treatment (BA, 5mM, 48 hrs). n=3. Scalebar: 10µM.

Treatment groups based on cell viability results

A summary table of the concentrations and intervention times of the six treatment groups of interest which were utilized for all subsequent experiments (Table 3.1)

Treatment	Concentration	Intervention Time
Control (C)	-	-
Lithium chloride (LiCl)	10mM	24 hrs
Gingko biloba low (GB↓)	10µg/ml	24 hrs
Gingko biloba high (GB↑)	200µg/ml	24 hrs
Gingko biloba low + Lithium Chloride (GB↓ + LiCl)	GB10µg/ml + LiCl 10 mM	24 hrs
Gingko Biloba high + Lithium chloride (GB↑ + LiCl)	GB200µg/ml + LiCl 10 mM	24 hrs

Section 3.2 Characterisation of GB modulation on autophagy and protein cargo clearance and its effects on amyloid processing.

Since significant differences were reported between low concentration GB↓ 10µg/ml [1.1 ± 0.08] and high concentration GB↑ 200µg/ml [0.71 ± 0.04] ($p<0.05$)] (Fig 3.1.2 A), we hypothesized that treatment with GB will exhibit a dose dependent effect on autophagic activity, and that this effect may be further enhanced through combination treatment with LiCl. Western Blot analyses were performed to unravel the dose dependent effect of GB and its combination treatment with LiCl on autophagic activity and its potential effect on the distinct removal of APP and Aβ. Firstly, the dose dependent effect of GB and its combination treatment with LiCl on autophagy flux was assessed. Secondly, the protective role of GB treatment under neurotoxic conditions was investigated.

3.2.1 Gingko biloba treatment in the presence and absence of LiCl modulates autophagic flux

In order to asses autophagy, the relative protein expression of LC3-II can be quantitatively measured through the utilization of a lysosomal inhibitor, Bafilomycin A1 (BafA1). The expression of LC3-II is indicative of the abundance of autophagosome vacuoles following BafA1 treatment (Fig 3.2.1. A). BafA1 has only minor effects in control cells, displayed by the non-significant changes in LC3-II protein expression compared to BafA1 untreated cells [144.3 ± 4.72%]. This suggests that these cells have a relatively low basal autophagy flux. Significantly increased LC3-II protein levels were observed for the GB low (↓:10µg/ml) [297.2 ± 14.32% ($p<0.05$)],GB high (↑:200µg/ml) [321.6 ± 14.79% ($p<0.05$)], GB low (↓:10µg/ml) + LiCl 10 mM [237.3 ± 6.48% ($p<0.05$)], and GB high (↑:200µg/ml) + LiCl 10 mM [308.8 ± 19.07% ($p<0.05$)] groups when compared to their corresponding BafA1 negative group. This indicates an increase in autophagosome pool size and an upregulation of autophagy under these treatment conditions. Moreover, the results show an enhanced autophagy activity, compared to basal autophagy. This is revealed by a significant increase in LC3-II protein levels in treated with GB low (↓:10µg/ml) [297.2 ± 14.32% ($p<0.05$)]; GB high in the presence [321.6 ± 14.79% ($p<0.05$)]and absence of LiCl10 mM [308.8 ± 19.07% ($p<0.05$)] followed by BafA1 treatment, in comparison with cells treated only with BafA1 (basal autophagy) group. However, the effect on LC3-II in the combination treatment of GB (↓:10µg/ml) + LiCl 10 mM [237.3 ± 6.48% ($p<0.05$)] was less significant compared to the combination treatment of GB (↑:200µg/ml) + LiCl [308.8 ± 19.07 ($p<0.05$)] in the examined conditions. Although no significant difference in LC3-II expression levels was observed between the different concentrations of GB in the presence of BafA1 [297.2 ± 14.32%, 321.6 ± 14.79%], there was, however, a trend for increased expression in the GB high (↑:200µg/ml) + BafA1 [321.6 ± 14.32%] and the combination treatment of GB high (↑:200µg/ml) + LiCl + BafA1 [237.3

±6.48%] as compared to GB low (↓:10µg/ml) + BafA1 [308.8 ± 19.07%] group. This potentially indicates that GB has a dose dependent effect on autophagic activity.

(A.1)

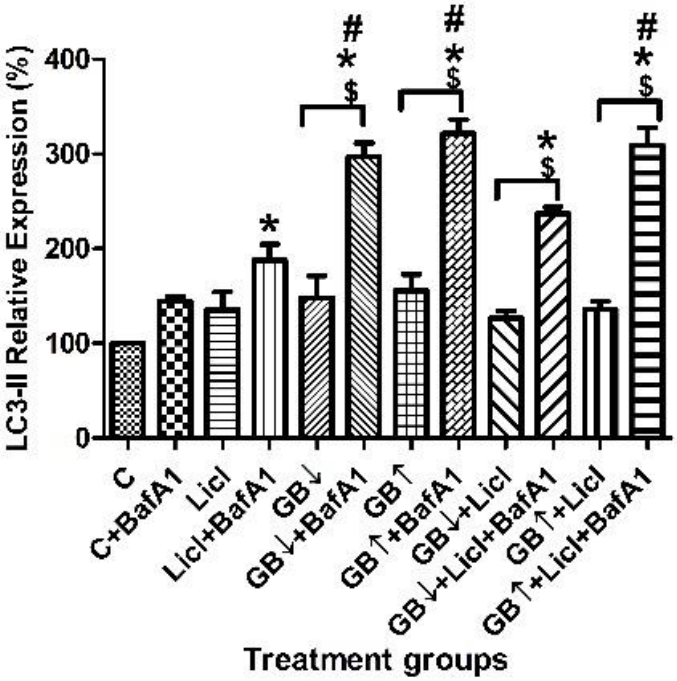

(A.2)

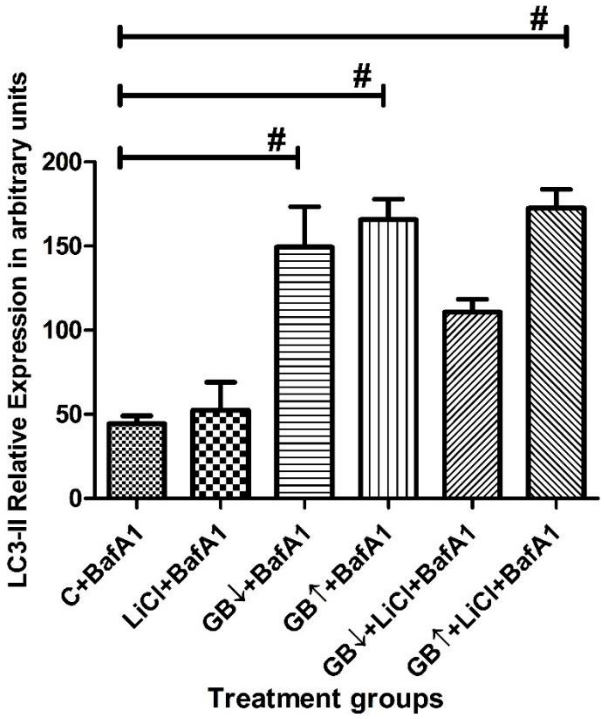

(A.3)

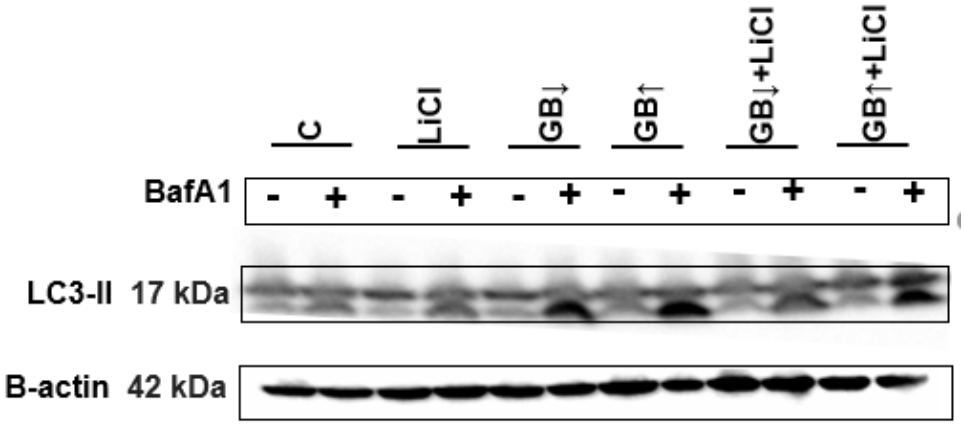

Figure 3.2.1 A: Relative protein expression levels of LC3 and LC3 net Flux in N2aswe cells following treatment with medium (Con), LiCl, GB low (↓:10µg/ml), GB high (↑:200µg/ml), GB low (↓:10µg/ml) + LiCl, GB high (↑:200µg/ml) + LiCl, for 24 hrs before and after Bafilomycin A1 (BafA1;400nM : 4 hrs). Beta-actin (β-actin) was used as a loading control. All data is expressed as means ± SEM (* p-value <0.05 vs control, #p-value <0.05 vs C+BAfA1, $ p-value <0.05 vs corresponding BafA1 negative group. (A.3) A representative blot is shown.

(Fig 3.2.1 B) p62 targets ubiquitinated proteins marked for degradation and thus when autophagy is inhibited using BafA1, an increase in p62 protein level is indicative of its protein clearance through the autophagic pathway. If p62 protein levels do not change upon BafA1 treatment, no clearance and hence no autophagy activity takes place. Hence, like LC3-II, an accumulation of p62 following BafA1 treatment is associated with increased protein degradation through autophagy. Significantly increased p62 protein levels were observed for the GB high (↑:200µg/ml) [170.8 ± 10.60% ($p<0.05$)] when compared to its corresponding BafA1 negative group. This result suggests an induction of autophagy by GB high (↑:200µg/ml). Interestingly, we observed that p62 protein levels were even more elevated when exposed to GB high (↑:200µg/ml) in the presence of LiCl followed by BafA1 treatment when compared to cells treated with GB high (↑:200µg/ml) only [176.6 ± 6.77%) $p<0.05$)]. These results indicate that GB in the presence of LiCl further enhances autophagy compared to GB on its own.

(B.1)

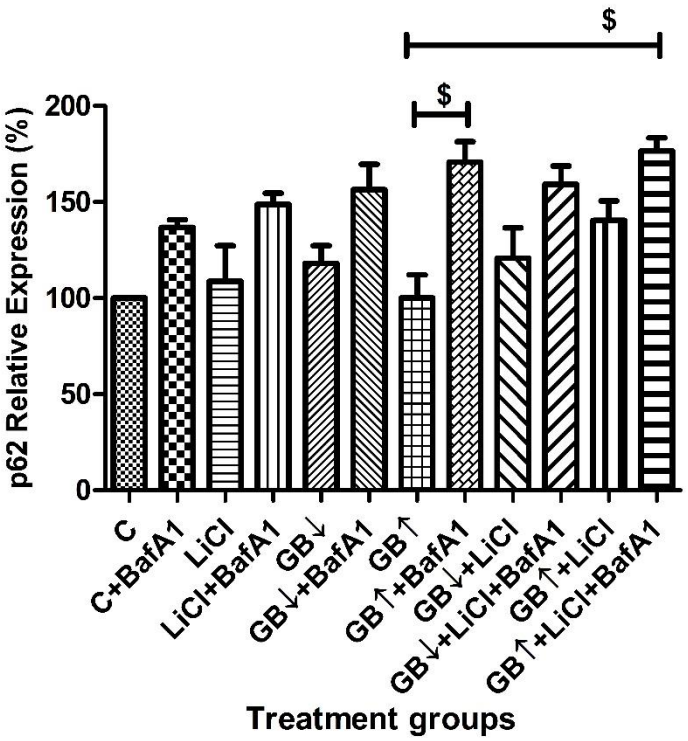

(B.2)

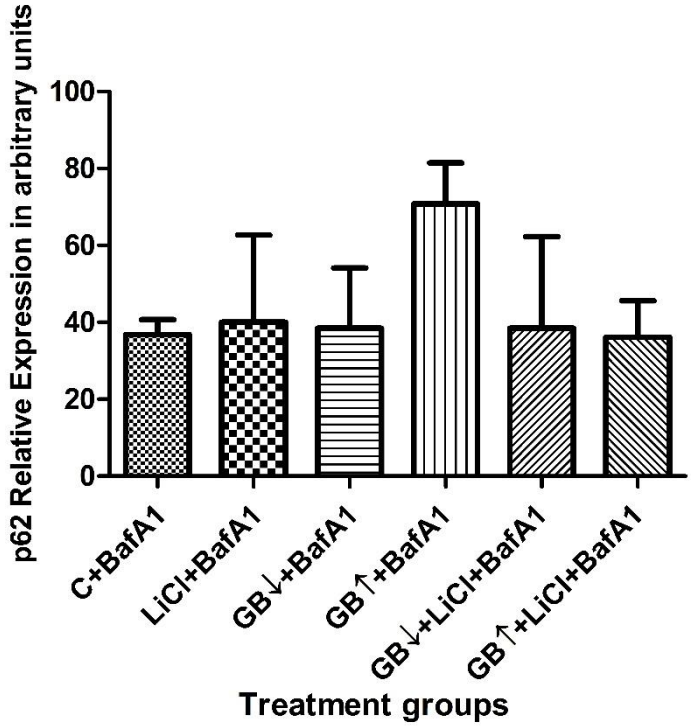

(B.3)

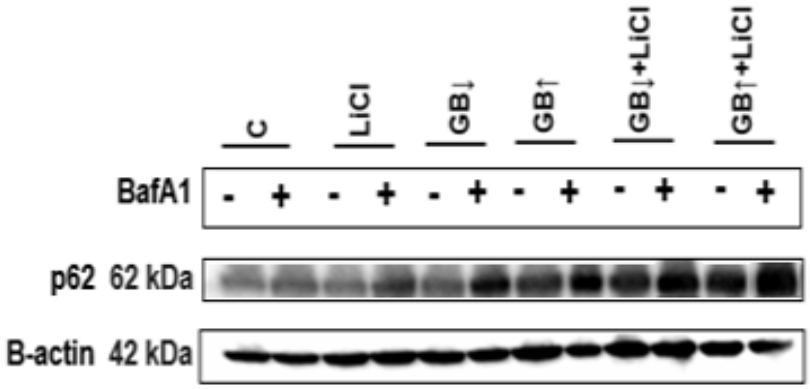

Figure 3.2.1 B: Relative protein expression levels of p62 and p62 net Flux in N2aswe cells following treatment with medium (Con), LiCl 10mM, GB low (↓:10µg/ml), GB high (↑:200µg/ml), GB low (↓:10µg/ml) + LiCl, GB high (↑:200µg/ml) + LiCl, for 24 hrs before and after Bafilomycin A1 (BafA1;400nM : 4hrs). Beta-actin (β-actin) was used as a loading control. All data is expressed as means ± SEM (* p-value <0.05 vs control, #p-value <0.05 vs C+BAfA1, $ p-value <0.05 vs corresponding BafA1 negative group. A representative blot is shown.

3.2.2 Immunofluorescence analysis of p62

In order to further investigate the modulatory role of GB in the absence and presence of LiCl, immunofluorescence analysis of the autophagy adapter protein p62 was conducted. The protein abundance of p62 can serve as a marker to monitor autophagy flux. Suppression of autophagy manifests with increased p62 levels, whereas induction of autophagy results in decreased p62 abundance. Untreated cells served as control cells and displayed a notable abundance of p62 (Fig 3.2.2). Upon exposure to Bafilomycin A1 (BafA1), an increase in red fluorescent signal intensity correlating to higher abundance of p62 clusters was evident (Fig 3.2.2). Thus, the abundance of p62 was increased in BafA1 treated cells compared to control cells indicating the state of basal autophagy of the cells. The results indicate that exposure to GB high (↑:200µg/ml) and a combination treatment of GB high (↑:200µg/ml) + LiCl, followed by four hrs of BafA1, presented the highest abundance of p62 compared to control cells treated with BafA1. Importantly, GB high (↑:200µg/ml) + BafA1 treatment revealed greater abundance of p62 compared to GB low (↓:10µg/ml) + BafA1. This strongly indicates a dose dependent effect of GB on autophagic activity, with the high concentration inducing autophagy more robustly than the low concentration. Moreover, a combination treatment of GB high (↑:200µg/ml) + LiCl followed by four hrs of BafA1 revealed greater abundance of p62, compared to GB low (↓:10µg/ml) + LiCl + BafA1.

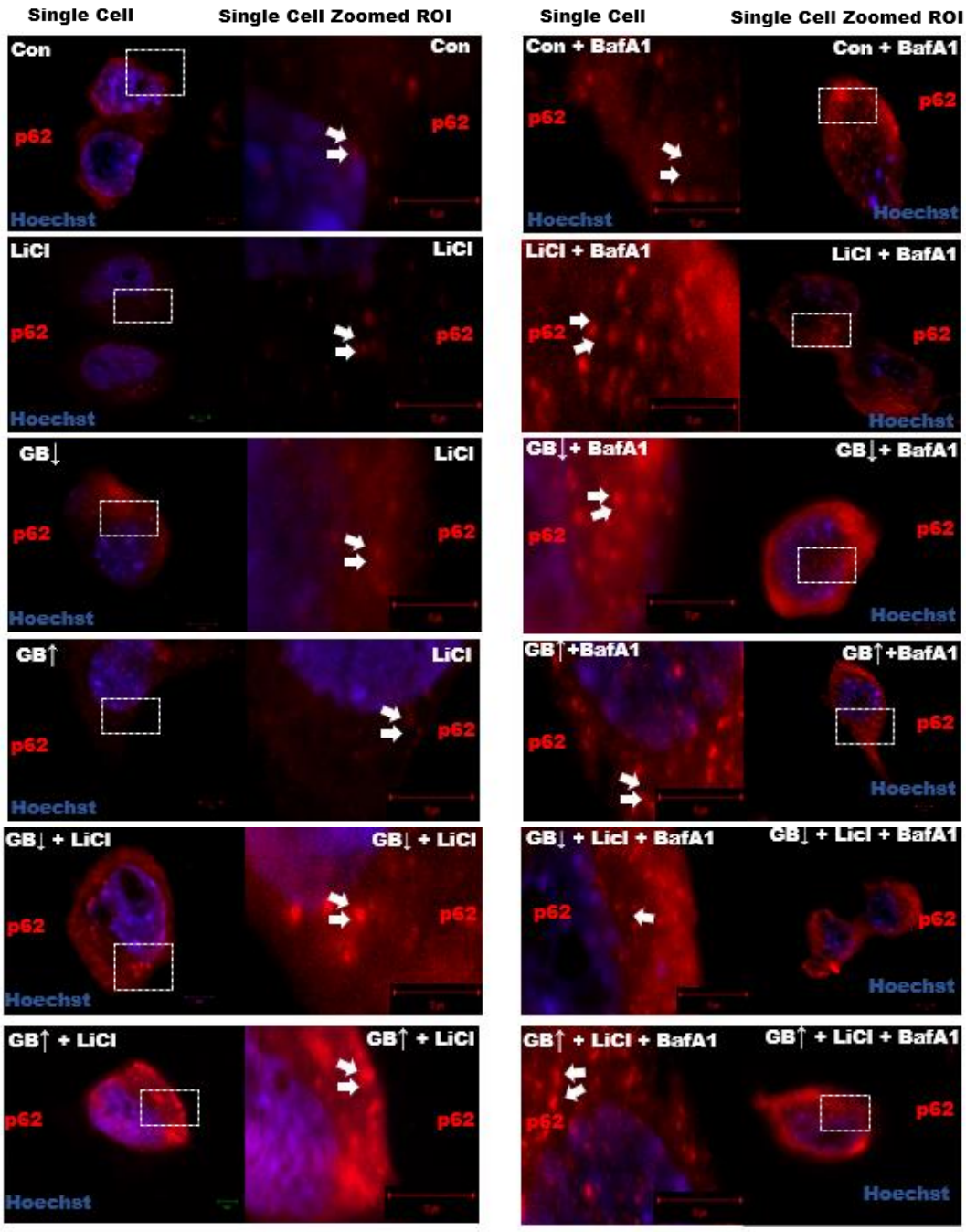

Figure 3.2.2: Fluorescence micrographs of p62 abundance of N2aswe cells that were either untreated, treated with LiCl, GB low (↓:10µg/ml), GB high (↑:200µg/ml), GB low (↓:10µg/ml) + LiCl, or GB high (↑:200µg/ml) + LiCl for 24 hrs and subsequently treated without (left), or with BafA1 (right) (400nM, 4 hrs). First panel represent Single cell and second panel represent single cell zoomed. ROI represents region of interest. Red signal represents p-62 linked to Alexa 561, blue signal represents Hoechst Scale bar: 10 µm. Arrow head indicate p62 clusters.

Section 3.3 The effects of Gingko biloba treatment on lysosome abundance

Western blot analysis probing for of LAMP2a protein levels was performed to assess whether GB supplementation effects the lysosomal compartment and the abundance of lysosomes in the context of APP overexpression. LAMP2a is a specific lysosomal membrane associated protein and its protein expression correlates with the lysosomal abundance in a cell (Eskelinen, 2006). No significant changes were observed in the expression levels of LAMP2a, however, strong trends can be observed (Fig 3.3.1). Relative expression of LAMP2a compared to control was increased with butyric acid treatment [1.08 ± 0.40], decreased in the presence of LiCl [0.33 ± 0.07], GB low (↓:10µg/ml) [0.41 ± 0.16], GB high (↑:200µg/ml) [0.38 ± 0.10], GB low (↓:10µg/ml) +LiCl [0.54 ± 0.22], GB high (↑:200µg/ml) + LiCl [0.64 ± 0.12] and appear increased compared to BA treated cells, when cells were treated with LiCl (10mM) [0.54 ± 0.13] and GB low (↓:10µg/ml) [0.81 ± 0.28] in the presence and absence [1.28 ± 0.47] of LiCl prior exposure to BA. Interestingly, no changes were consistently observed between cells treated with GB high (↑:200µg/ml) and cells co-treated with butyric acid and GB high(↑:200µg/ml) [0.40 ± 0.10], suggesting some, yet, through this method not well quantifiable effect.

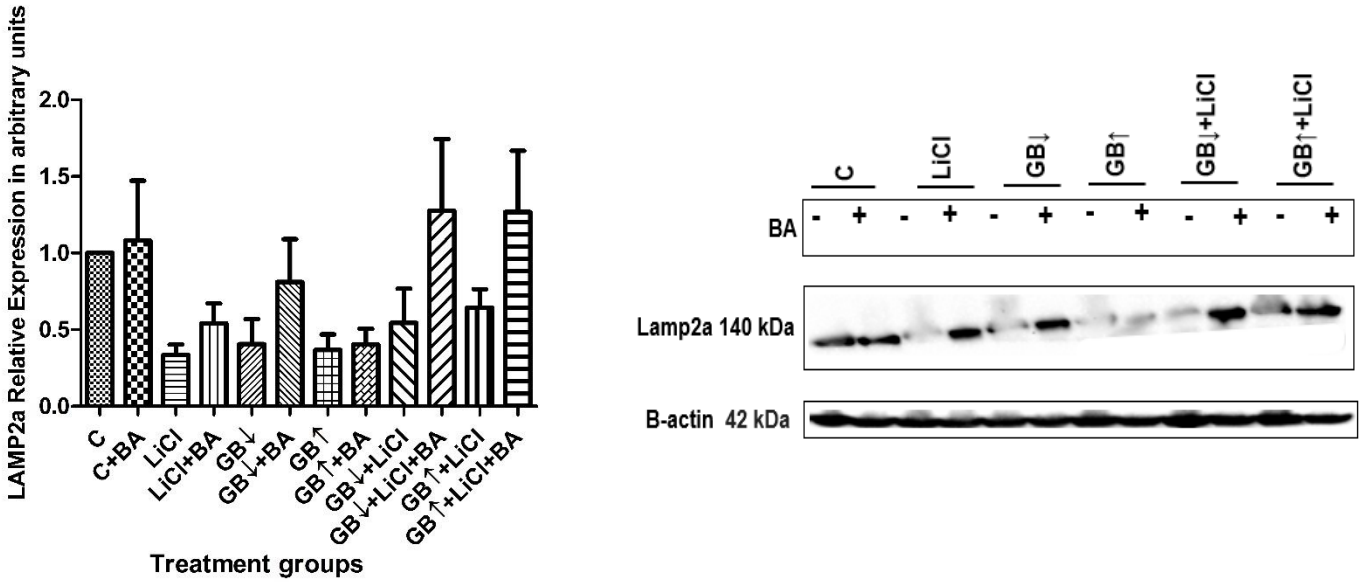

Figure 3.3.1: Relative protein expression levels of LAMP2a in N2aswe cells (C), following treatment with LiCl, GB low (↓:10µg/ml), GB high (↑:200µg/ml), GB low (↓:10µg/ml) + LiCl, GB high (↑:200µg/ml) + LiCl, for 24 hrs and subsequently treated without or with Butyric acid (BA 5 mM; 48H). Beta-actin (β-actin) was used as a loading control. All data are expressed as mean ± SEM. A representative blot is shown.

3.3.2 The effects of Gingko biloba treatment on the lysosomal acidic compartment under neurotoxic conditions

Acridine orange (AO) binds to DNA which emits green fluorescence and fluoresces red in acidic vesicular organelles (AVOs), including lysosomes and autolysosomes. Lysosomes are characterized by an acidic lumen (pH 5) as a result of the concentrated presence of various hydrolase enzymes necessary for cargo degradation. AO has been used as a rapid means to detect the acidic compartment, like lysosomes (Thomé et al., 2016), and indicate lysosomal function. A decrease in red fluorescence emission suggests a decrease in the acidic compartment and hence lysosomal function. Therefore, the AO stain was used to assess the overall lysosomal acidic compartment (LAC) upon treatment with Gingko biloba in the presence and absence of LiCl supplementation under neurotoxic conditions. Untreated N2aswe cells stained with 5 µM of AO for 20 minutes showed clear red puncta and hot spots in the cytoplasm and appeared to be located perinuclear (Fig 3.3.2). All the treatment groups displayed a similar morphology, although a relative decrease in the red signal was demonstrated. Since AO is sensitive to pH changes, exposure to BA is hypothesized to alter the response of AO, as BA causes the cellular condition to become less acidic compared to control conditions. Indeed, treatment with BA (5 mM; 48 hrs) showed changes in nuclear signal and a relative decrease in AO red signal, and hence a reduction in LAC compared to control cells, suggesting decreased lysosomal function. 24 hrs exposure to LiCl prior to BA treatment manifested in a robust increase in AO red signal compared to BA-only treated cells. This was however not the case when the cells were exposed to both GB concentrations prior to BA treatment. The AO red signal under these conditions was similar to BA-only treated conditions. These results suggest that lysosomes are most sensitive to LiCl treatment. Interestingly, a combination pre-treatment of GB and LiCl prior to BA treatment did not affect the AO red signal, in comparison with LiCl-pre-treated cells.

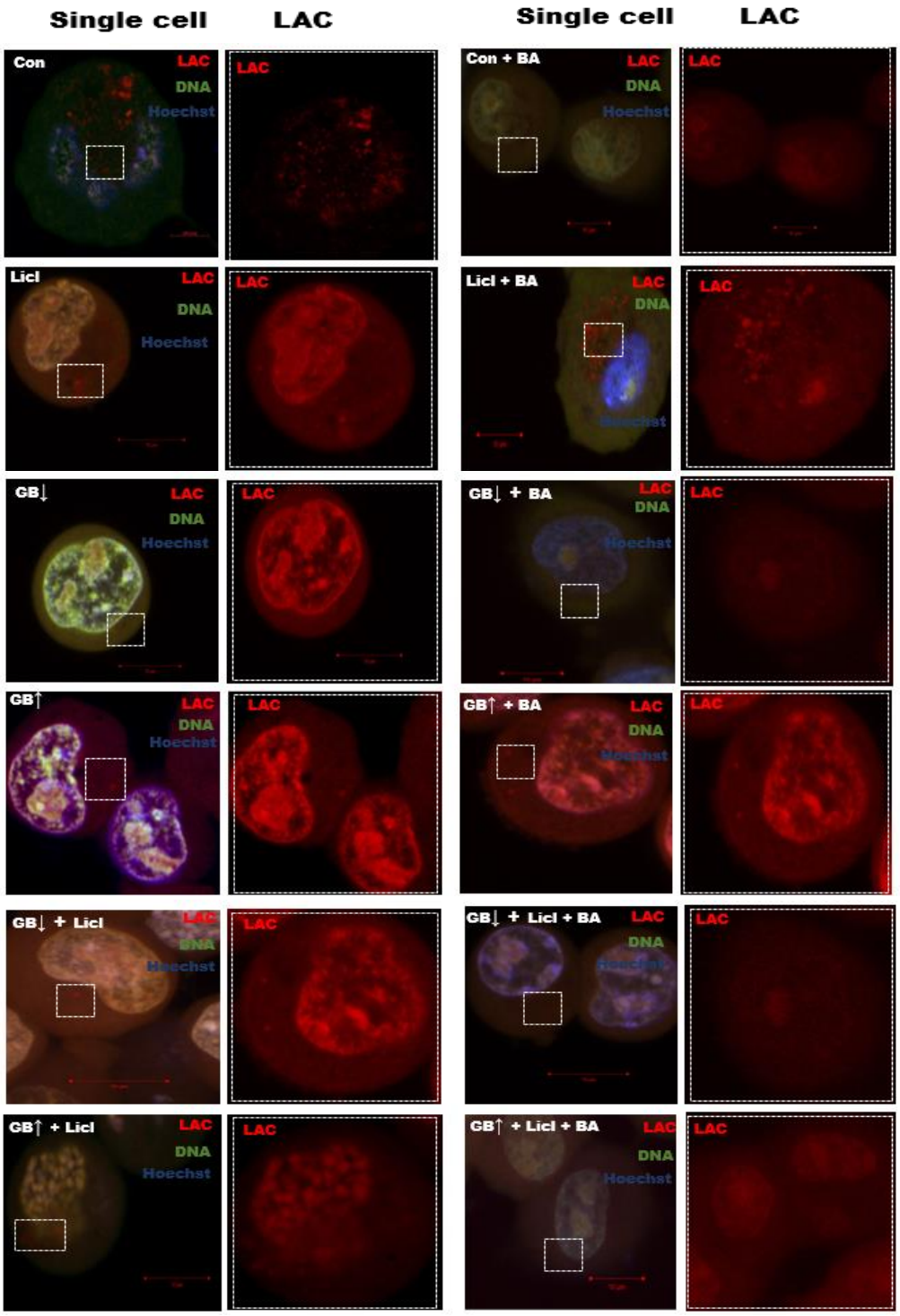

Figure 3.3.2: Lysosomal acidic compartment (LAC) detection using Acridine Orange (AO) staining. (A) Representative micrographs of AO-stained (20min, 5µM) N2aswe cells that were untreated, treated with LiCl, GB low (↓:10µg/ml), GB high (↑:200µg/ml), GB low (↓:10µg/ml) + LiCl, GB high (↑:200µg/ml) + LiCl, for 24 hrs and subsequently treated without (left) or with BA (right) (5mM, 48 hrs). Red (lysosomal acid compartments). Green (DNA). Blue (Hoechst). Scale bar =10µM.

3.3.3 The effects of Gingko biloba treatment on the neuronal ultrastructure under neurotoxic conditions

The ultrastructural morphology of N2aswe cell vacuolar structures, was observed by Transmission electron microscopy (TEM) following treatment with LiCl, GB low (↓:10µg/ml), GB high (↑:200µg/ml), GB low (↓:10µg/ml) + LiCl, GB high (↑:200µg/ml) + LiCl, for 24 hrs and subsequently treated without or with Butyric acid (BA 5 mM; 48 hrs).

Under control conditions, the micrographs revealed regular cytoplasmic components and intact nuclei with distinct chromatin network. Exposure to LiCl, GB low (↓:10µg/ml), GB high (↑:200µg/ml), GB low (↓:10µg/ml) + LiCl, GB high (↑:200µg/ml) + LiCl revealed a similar morphology to control conditions respectively. Moderate vacuolar structures and moderate swirl-like structures with a low electron density was observed under control conditions (Fig 3.3.3). An increase in the number and size of vacuolar structures was observed when the cells were treated with LiCl, GB low (↓:10µg/ml), GB high (↑:200µg/ml), GB low (↓:10µg/ml) + LiCl, GB high (↑:200µg/ml) + LiCl. Moreover, treatment with GB high (↑:200µg/ml) in the absence and presence of LiCl revealed most robust and very large vacuolar structure and the presence of clear distinct electron dense structure (i.e. lysosomes).

BA-treated cells reveal more prominent and larger swirl-like structures compared to control cells, fewer and less defined vacuolar structures and loss of membrane and nuclear integrity. Exposure to LiCl, GB low (↓:10µg/ml), GB high (↑:200µg/ml), GB low (↓:10µg/ml) + LiCl, GB high (↑:200µg/ml) + LiCl prior BA treatment, revealed a more intact nuclear, a mixture of (light and darker vacuolar structures) and increased number of vacuolar structures. Importantly, treatment with GB high (↑:200µg/ml) in the absence and presence of LiCl revealed large vacuolar structures which could contain Aβ peptides targeted for degradation.

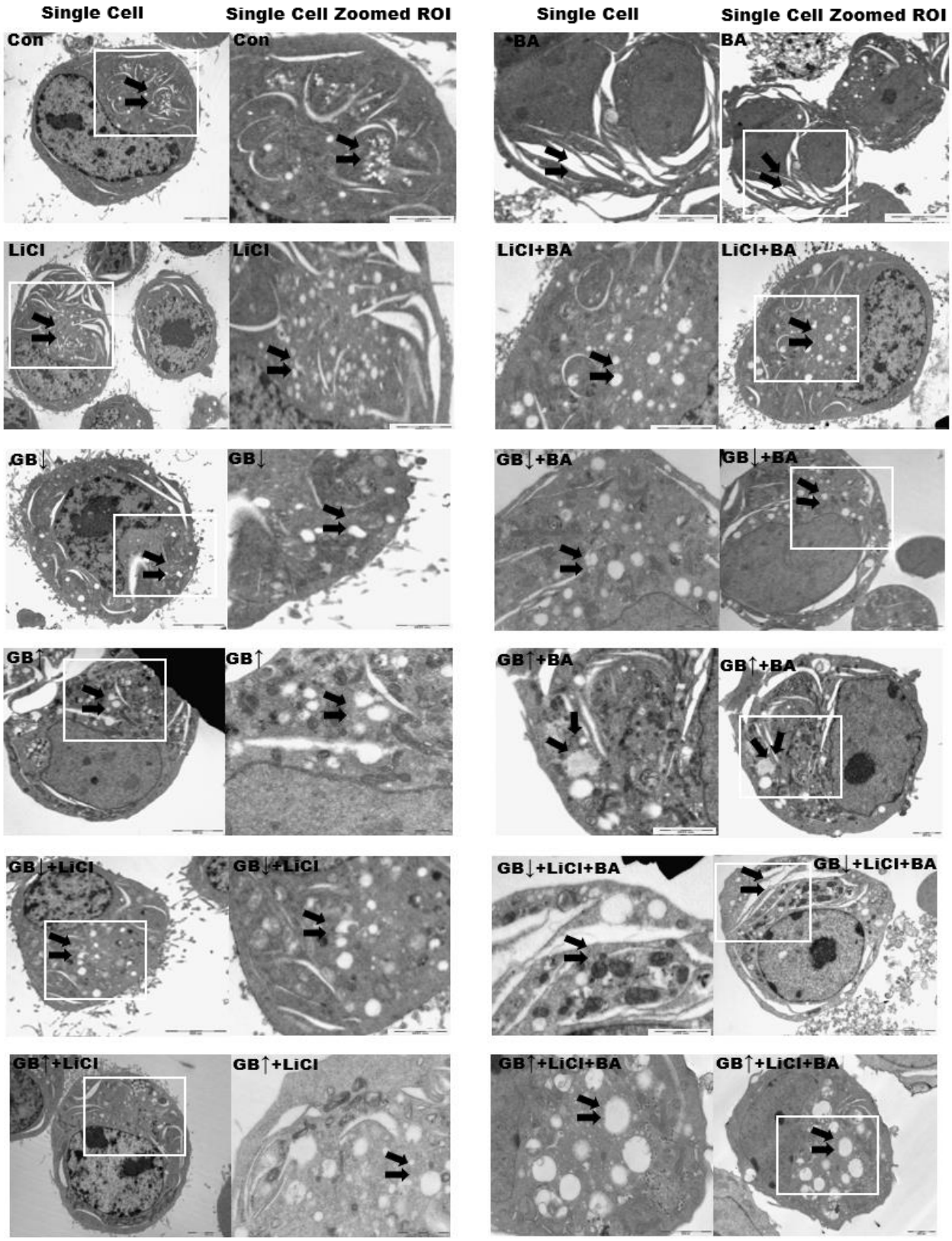

Figure 3.3.3: Representative Transmission electron micrographs of N2aswe cells (Con) that were treated with LiCl, GB low (↓:10µg/ml), GB high (↑:200µg/ml), GB low (↓:10µg/ml) + LiCl, GB high (↑:200µg/ml) + LiCl, for 24 hrs and subsequently treated without (left) or with BA (right) (5mM, 48 hrs). First panel represent Single cell and second panel represent single cell zoomed ROI. Arrows indicate structures of interest. Scale bar =5000 nm.

Section 3.4 The effect of Gingko Biloba treatment on the clearance of amyloidogenic proteins under neurotoxic conditions

Western blot analysis was performed to assess whether GB treatment, both in the presence and absence of LiCl, has an effect on the protein expression levels of APP, BACE and Aβ, which are involved in amyloid processing (Kellett and Hooper, 2009).

As shown in Figure 3.4 A The results indicate a significant increase in APP protein levels in cells treated with BA compared to control cells [1.43 ± 0.24 ($p<0.05$)]. Similarly, the results indicate a significant increase in BACE [0.68 ± 0.06 ($p<0.05$)] and Aβ [0.66± 0.05 ($p<0.05$)]. protein levels in cells treated with BA compared to control cells (Fig 3.4 B & C). These results indicate that the increase in APP due to the overexpression also translate in increased BACE protein levels as well as a significant increase in Aβ protein synthesis in cells treated with BA compared to control cells. Importantly, the results indicate a significant reduction in APP protein levels following 24 hrs treatment of LiCl [0.77 ± 0.13 ($p<0.05$)], GB low (↓:10µg/ml) [0.68 ± 0.14 ($p<0.05$)], GB high (↑:200µg/ml) [0.77 ± 0.17 ($p<0.05$)], GB low (↓:10µg/ml) + LiCl [0.41 ± 0.08 ($p<0.05$)], GB high (↑:200µg/ml) + LiCl [0.66 ± 0.30 ($p<0.05$)] compared to cells only treated with BA (5 mM, 48 hrs) (Fig 3.4 B & C). Similarly, the results indicate a significant decrease in BACE and Aβ protein levels following 24 hrs treatment of GB low (↓:10µg/ml) [0.25 ± 0.02 ($p<0.05$)], GB high (↑:200µg/ml) [0.32 ± 0.05 ($p<0.05$)] in the presence and absence of LiCl [0.38 ± 0.01 ($p<0.05$)] prior to BA exposure compared to cells only treated with BA (5 mM, 48 hrs (B&C). However, no concentration dependent difference in the clearance of the proteins is observed. All autophagy inducing drugs appear to clear the proteins of interest relatively equally.

(A)

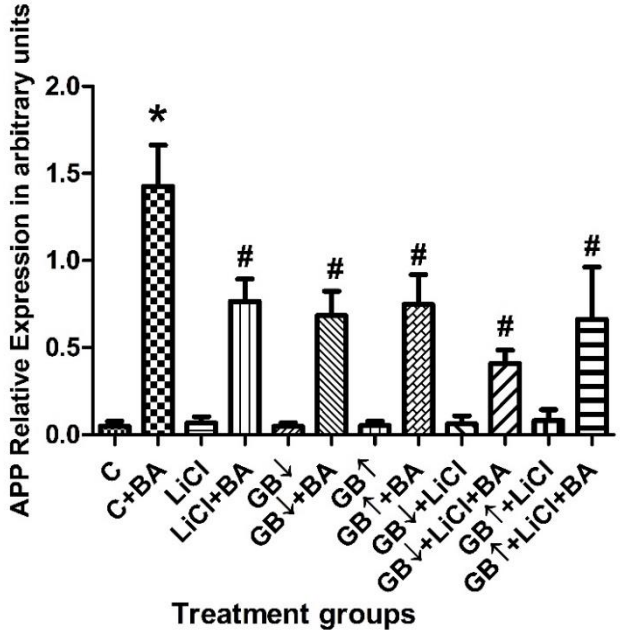

(B)

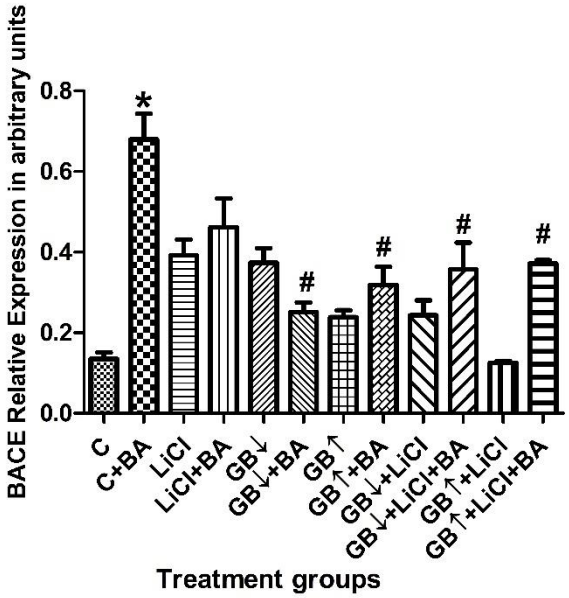

(C)

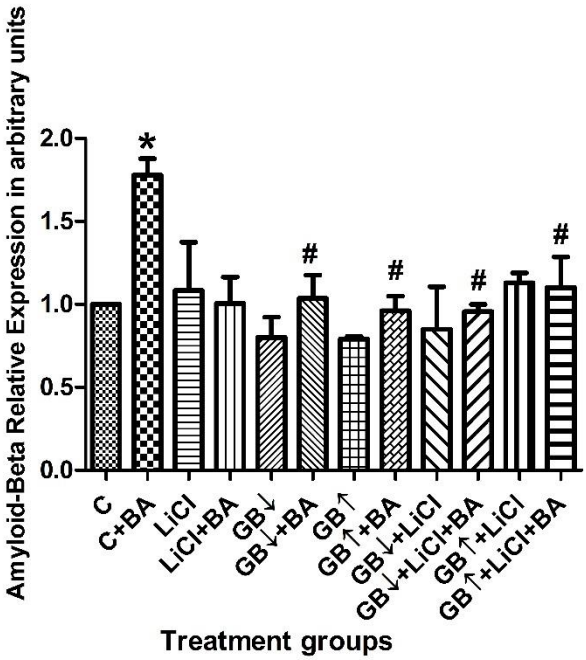

(D)

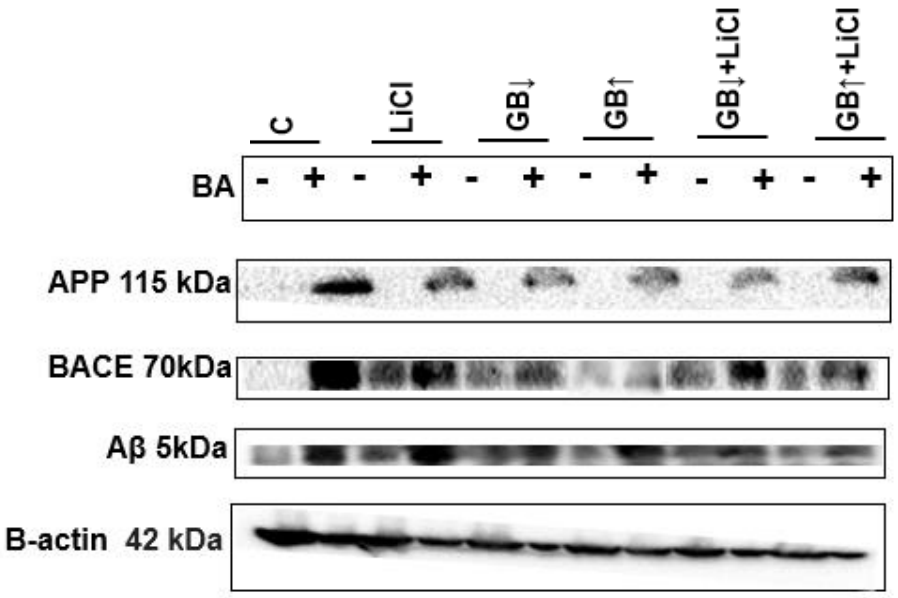

Figure 3.4: Relative protein expression levels of **(A)** APP and **(B)** BACE **(C)** Aβ in N2aswe cells (C) following treatment with LiCl, GB low (↓:10µg/ml), GB high (↑:200µg/ml), GB low (↓:10µg/ml) + LiCl, GB high (↑:200µg/ml) + LiCl, for 24 hrs and subsequently treated without or with Butyric acid (BA;5 mM; 48 hrs). Beta-actin (β-actin) was used as a loading control. All data are expressed as mean ± SEM (* $p < 0.05$ vs C, # $p < 0.05$ vs C+BA). (D) A representative blot for each protein is shown.

Section 3.5 The effect of Gingko biloba treatment on apoptosis onset under neurotoxic conditions

Both cytochrome-c and cleaved-caspase-3 play immediate roles in the induction and execution of cell death via apoptosis. An increase in the relative expression of both proteins is indicative of active apoptosis. Western blot analysis of cytochrome-c and cleaved-caspase 3 protein expression levels was performed to assess the potential protective role of GB supplementation in the context of APP overexpression.

A significant increase in cytochrome-c [3.12 ± 0.67 ($p<0.05$)] and cleaved-caspase 3 [3.26 ± 0.83 ($p<0.05$)] protein expression following 48 hrs of butyric acid (BA, 5mM) treatment was observed when compared to control (Fig 3.5 A&B). This indicates that APP overexpression indeed leads to the release of cytochrome-c. Notably, a significant decrease in cytochrome-c protein levels was observed in 24 hrs pre-treatment with LiCl [2.62 ± 0.61 ($p<0.05$)], GB low (↓:10µg/ml) [2.47 ± 0.30 ($p<0.05$)] and GB high (↑:200µg/ml) in the presence [2.21 ± 0.65 ($p<0.05$)] and absence of LiCl [2.40 ± 0.68 ($p<0.05$)] before 48 hrs BA (5 mM,48 hrs) treatment compared to cells only treated with BA. These results indicate protective effects of all the treatment interventions, in the context of APP-induced neuronal toxicity. However, relatively unchanged cleaved caspase-3 expression was observed following 24 hrs pre-treatment with LiCl [0.55 ± 0.13], GB low (↓:10µg/ml) [0.33 ± 0.18] and GB high (↑:200µg/ml) in the presence [0.60 ± 0.13] and absence of LiCl [0.60 ± 0.24] before 48 hrs BA (5 mM,48 hrs) treatment compared to cells only treated with BA (Fig 3.5 B).

(A)

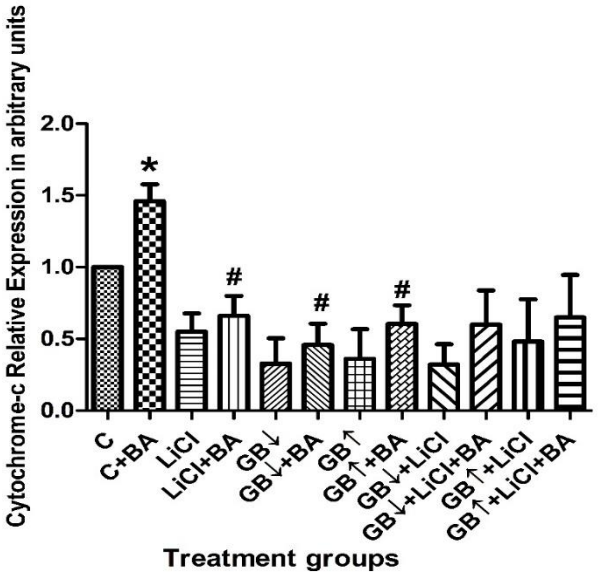

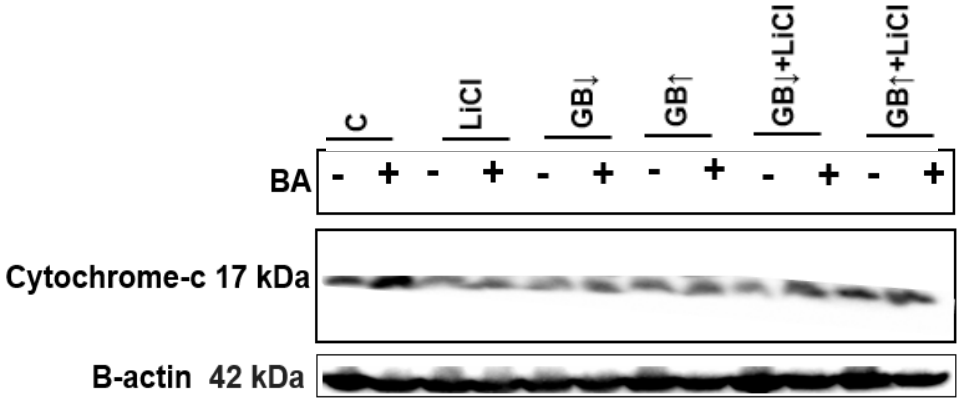

(A.1)

(B)

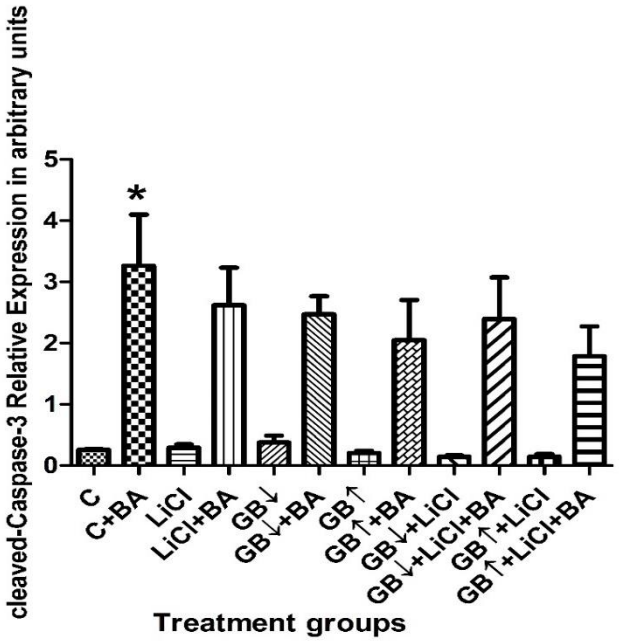

(B.1)

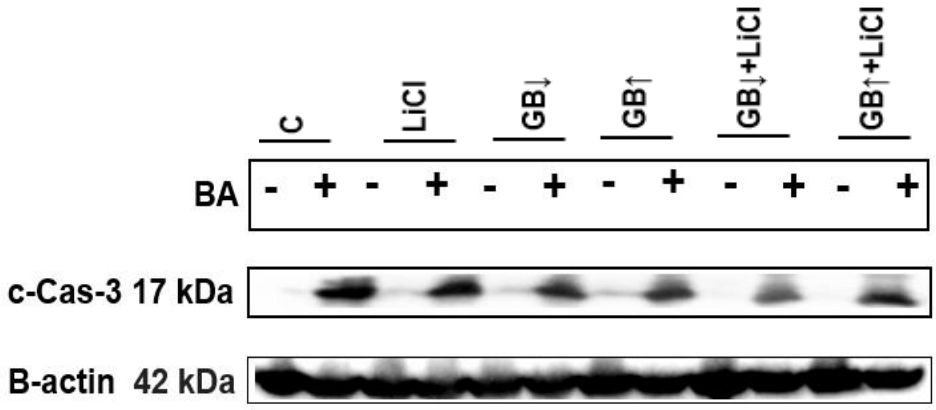

Figure 3.5: Relative protein expression levels of **(A)** Cytochrome-c and **(B)** Cleaved-Caspase-3 in N2aswe cells following treatment LiCl, GB low (↓:10µg/ml), GB high (↑:200µg/ml), GB low (↓:10µg/ml) + LiCl, GB high (↑:200µg/ml) + LiCl, for 24 hrs and subsequently treated without or with Butyric acid (BA;5 mM; 48 hrs. Beta-actin (β-actin) was used as a loading control. All data is expressed as means ± SEM (* p<0.05 vs C, # p <0.05 vs C+BA. (n=3). (A.1 & B.1) A representative blot is shown.

Section 3.6 The effect of Gingko Biloba treatment on mitochondrial fission and fusion dynamics

Western blot analysis of MNF1 and DRP1 protein expression levels were performed to assess whether GB supplementation enables the preservation of mitochondrial function in the context of APP overexpression. MNF1 is a protein primarily responsible for the regulation of the fusion events and is localized on the outermost mitochondrial membrane. DRP1 is prominently found in the cytoplasm, however, the fragmentation of mitochondria is promoted by the interaction of DRP1 with the outer membrane of mitochondria (Fig 3.6.1 A). The results revealed that LiCl [1.30 ± 0.04 (p<0.05)] and GB low (↓:10µg/ml) [1.37 ± 0.07 (p<0.05)] & GB high (↑:200µg/ml) [1.47 ± 0.31 (p<0.05)] in the presence of LiCl significantly increased the protein expression of MNF1. Interestingly, combination treatment of GB high (↑:200µg/ml) + LiCl (10mM) [1.55 ± 0.03 (p<0.05)] showed significantly increased more MNF1 protein levels compared to cells treated with GB (↑200µg/ml) only. This suggests that GB high (↑:200µg/ml) in the presence of LiCl favours the fusion state of a mitochondrial network as compared to GB-treated cells only. Exposure to butyric acid (BA, 48 hrs, 5 mM) led to a significant decrease in MNF1 protein levels in control cells [0.67 ± 0.03 (p<0.05)]. Importantly however, pre-treatment with LiCl, GB low (↓:10µg/ml) [0.65 ± 0.04], GB high (↑:200µg/ml) [0.68 ± 0.4], GB low (↓:10µg/ml) + LiCl [0.67 ± 0.35], GB high (↑:200µg/ml) + LiCl [0.72 ± 0.04] for 24 hrs followed by BA exposure, and had no effect on MFN1 expression compared to BA-treated cells.

Exposure to both GB concentrations (10µg/ml) [0.52 ± 0.08 ($p<0.05$)] & GB high (200µg/ml) [0.47 ± 0.10 ($p<0.05$)] and a combination treatment of GB low (↓:10µg/ml) +LiCl [0.05 ± 0.20 ($p<0.05$)] caused a significant decrease in DRP1 protein expression compared to control (Fig 3.6.1B). We hypothesised that exposure to butyric acid (BA, 48 hrs, 5nM) would significantly increase the protein expression of DRP1, however, this was not the case. Surprisingly, untreated cells displayed relatively greater although non-significant protein expression of DRP1 compared to BA-treated cells [0.56 ± 0.09]. Importantly, pre-treatment with GB low (↓:10µg/ml) [0.32 ± 0.10 ($p<0.05$)] and GB high (↑:200µg/ml) [0.29 ± 0.05 ($p<0.05$)] in the absence and presence of LiCl followed by BA treatment caused a significant decrease in DRP1 protein expression compared to BA treated cells.

(A)

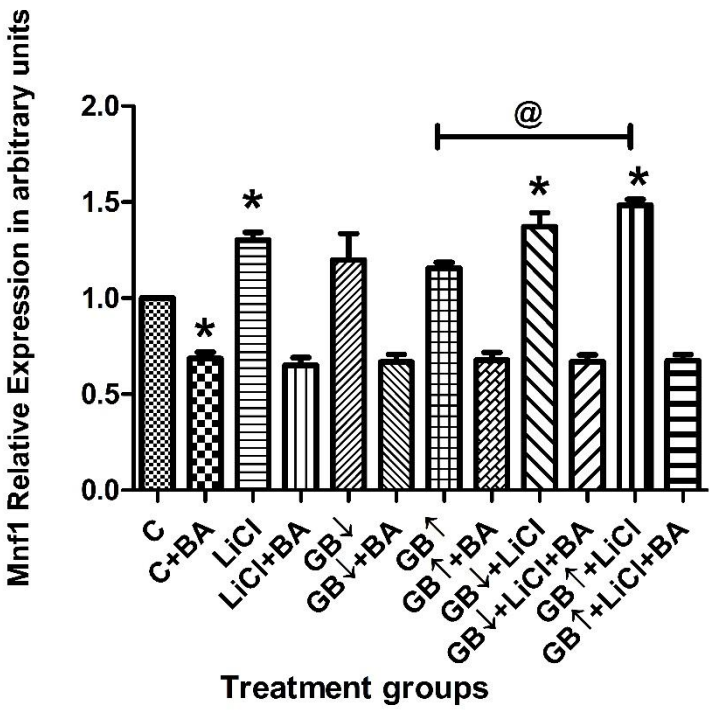

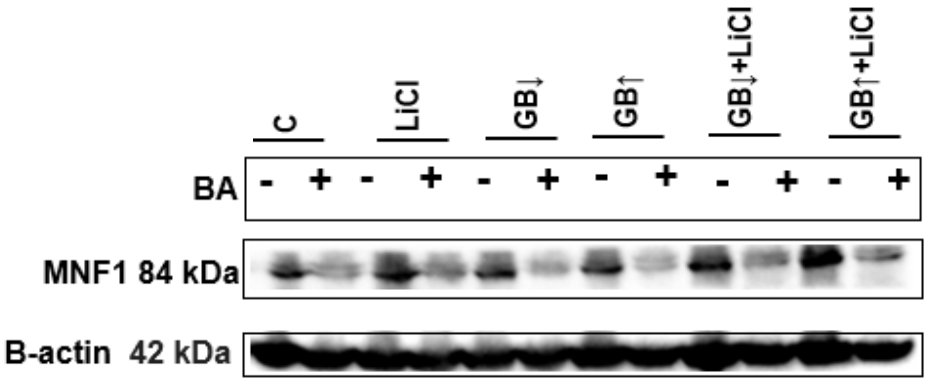

(A.1)

(B)

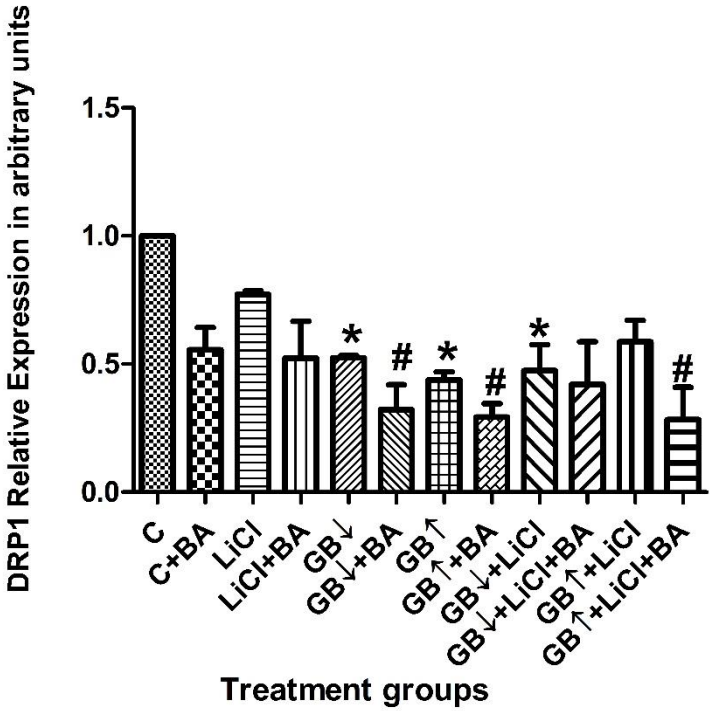

(B.1)

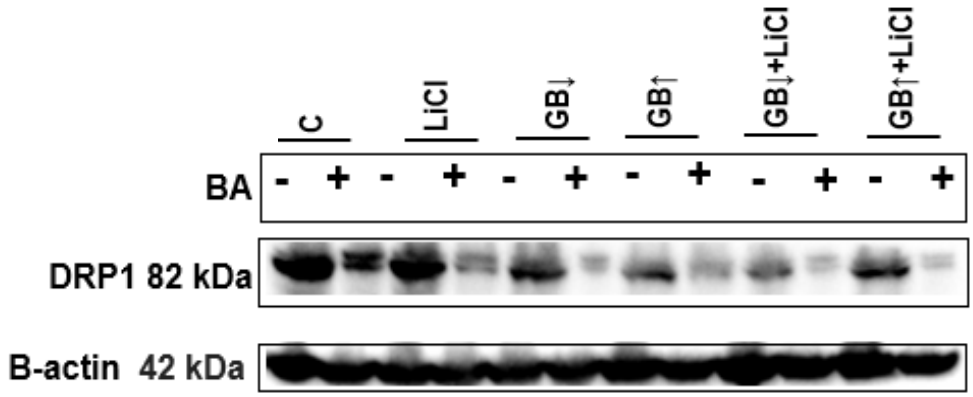

Figure 3.6.1: Relative protein expression levels of (A) MNF1 (B) DRP1 in N2aswe cells following treatment with LiCl, GB low (↓:10 µg/ml), GB high (↑:200 µg/ml), GB low (↓:10 µg/ml) + LiCl, GB high (↑:200µg/ml) + LiCl, for 24 hrs and subsequently treated without or with Butyric acid (BA;5 mM; 48 hrs). Beta-actin (β-actin) was used as a loading control. All data are expressed as means ± SEM (* p<0.05 vs C, # p <0.05 vs C+BA, @ p <0.05 vs GB high (↑:200 µg/ml). (A.1 & B.1) A representative blot is shown.

3.6.2 The effect of Gingko biloba treatment on mitochondrial morphology

The function of cells can, at least in part, be assessed by the network organization or morphology of mitochondria. A network of elongated, fused mitochondria is usually associated with healthy viable cells (Chan, 2006). Staining cells with Tetra-methyl-rhodamine-ethyl-esther TMRE revealed that control cells displayed elongated mitochondria that form a highly interconnected network. A 24-hr supplementation with all treatment groups including: LiCl (10 mM, GB low (↓:10 µg/ml), GB high (↑:200 µg/ml) and combination treatments GB low (↓:10 µg/ml) + LiCl, GB high (↑:200 µg/ml) + LiCl, displayed elongated fused mitochondria, very similar to control cells.

On the other hand, cells subjected to butyric acid (BA, 5mM, 48 hrs) treatment exhibited a complete loss of network connectivity, portrayed by the fragmented mitochondrial morphology. Cells subjected to 24 hrs pre-treatment with all treatment groups including: LiCl (10 mM), GB low (↓:10µg/ml), GB high (↑:200 µg/ml) and combination treatments GB low (↓:10 µg/ml) + LiCl, GB high (↑:200 µg/ml) + LiCl, prior to BA exposure exhibited a network of both fused and fragmented mitochondria; however, a larger degree of mitochondrial connectivity and a reduction in fragmented mitochondria was evident compared to BA-only treated cells (Figure 3.6.2).

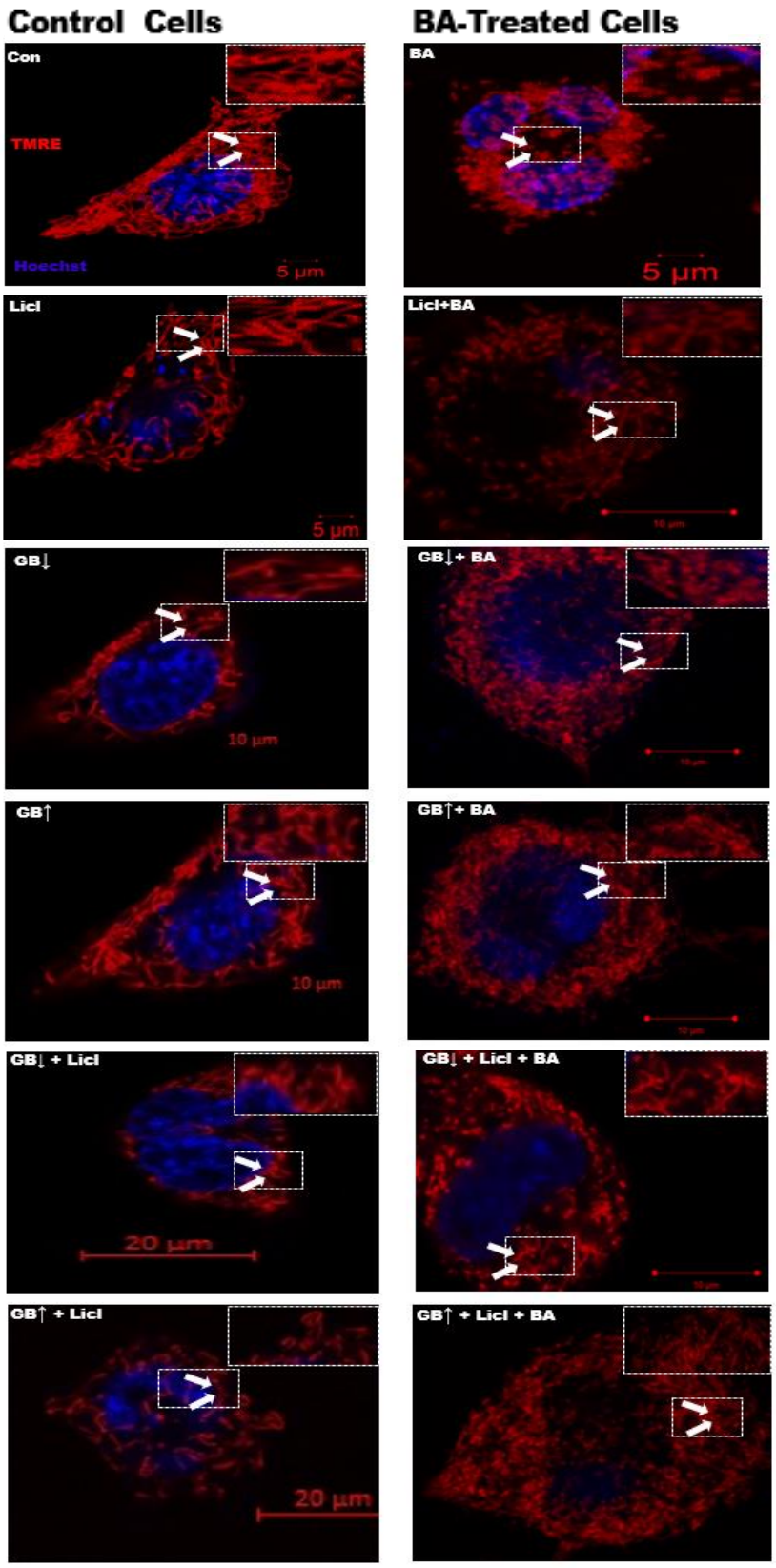

Figure 3.6.2: Representative micrographs of N2aswe cells stained with TMRE at control conditions (Con), with LiCl, GB low (↓:10µg/ml), GB high (↑:200µg/ml), GB low (↓:10µg/ml) + LiCl, GB high (↑:200µg/ml) + LiCl, for 24 hrs and subsequently treated without (left) or with Butyric acid (BA, 5mM, 48 hrs) (right) . Red = TMRE, blue = Hoechst. Scale bar = 5 µm/10µm/20µm. Arrowheads indicate mitochondria morphology (fused vs fragmented network).

Section 3.7 Autophagy activity (flux) under neurotoxic conditions

In order to assess the effects of the treatment interventions on autophagy activity, i.e. the rate of protein degradation through autophagy (autophagy flux), cells were treated with saturating concentrations bafilomycin. Protein expression of p62 is shown to increase upon BafA1 treatment, suggesting that the autophagic process is indeed active under the examined conditions (Fig 3.7 A). Significantly increased p62 protein levels were observed for the GB high (↑:200µg/ml) + BA + BafA1 [1.87 ± 0.68 ($p<0.05$)] treatment group compared to its corresponding BafA1 negative group, indicating upregulation of autophagy activity under this treatment condition. A significant increase p62 protein levels was also observed when cells were exposed to GB high (↑:200µg/ml) [1.89 ± 0.68 ($p<0.05$)] followed by BA and BafA1 treatment, in comparison with control and GB low (↓:10µg/ml) treated cells followed by BA and BafA1 treatment, respectively. This further suggests that autophagy flux is highest when cells are exposed to GB high (↑:200µg/ml) and again highlights the dose-dependent modulation of GB on autophagy flux. In this context, a combination treatment of GB high (↑:200µg/ml) + LiCl [1.93 ± 0.20 ($p<0.05$)] followed by BA and BafA1 treatment, displayed a increase in p62 protein levels compared to control and LiCl treated cells followed by BA and BafA1 treatment respectively. These results, therefore, in the case of neuronal damage, suggest that a combination treatment also further enhances the autophagic flux compared to exposure to one drug only.

(A)

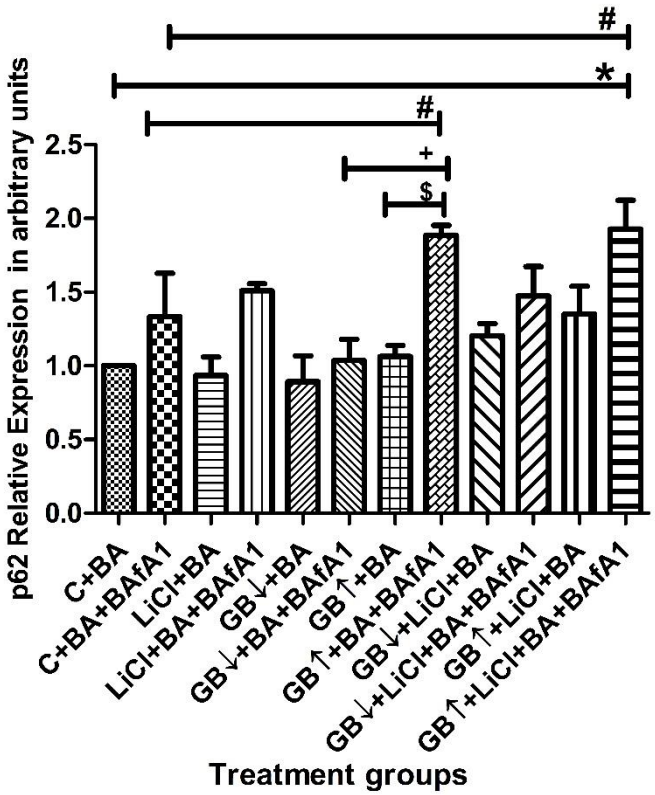

(A.1)

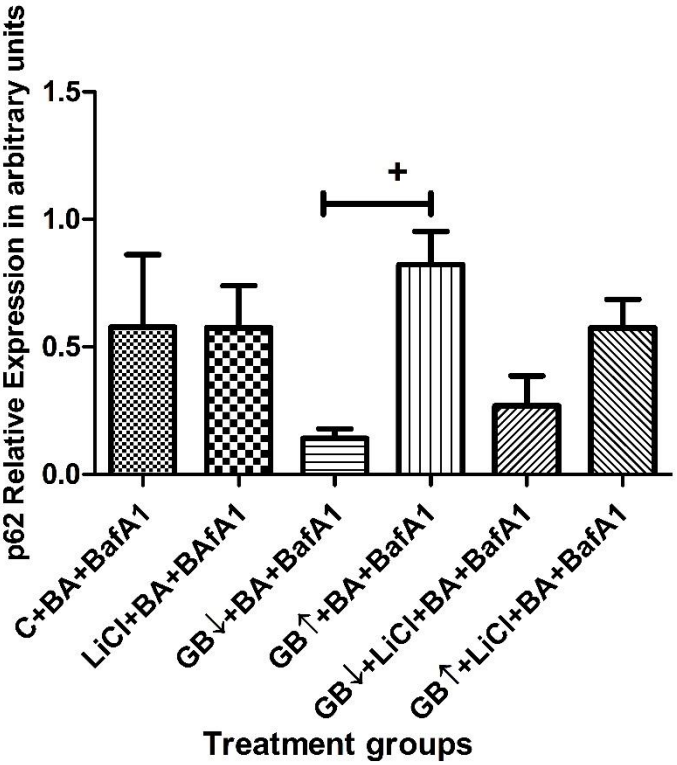

(A.2)

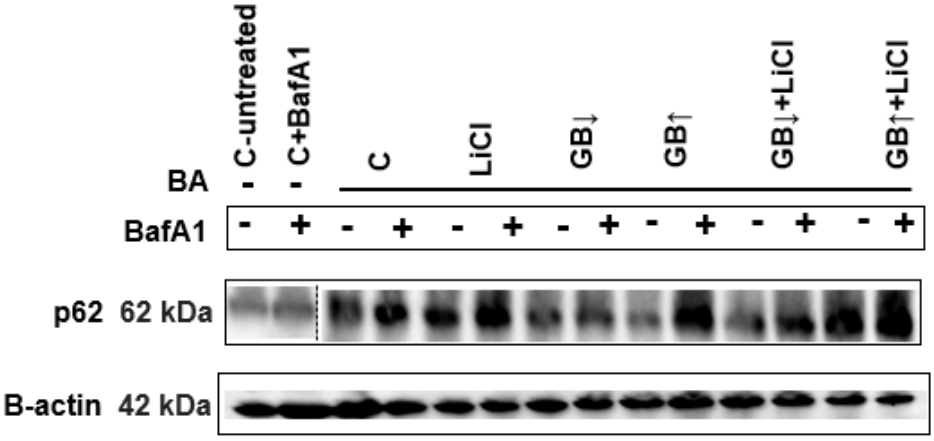

Figure 3.7 A: Relative protein expression levels of p62 and p62 Net Flux in N2aswe cells following treatment with medium (C), LiCl, GB low (↓:10µg/ml), GB high (↑:200µg/ml), GB low (↓:10µg/ml) + LiCl, GB high (↑:200µg/ml) + LiCl, for 24 hrs and subsequently treated with Butyric acid (BA;5 mM; 48 hrs) followed by Bafilomycin A1 (BafA1, 400nM, 4hrs). Beta-actin (β-actin) was used as a loading control. All data are expressed as means ± SEM (* p <0.05 vs C+BA, # p <0.05 vs C+BA+BafA1, + vs GB low (↓:10µg/ml) +BA+BafA1), $ p<0.05 vs its relative control) (n=3). (A.2) A representative blot is shown.

These results are supported by the LC3-II protein expression data (Fig 3.7 B), which demonstrated that LC3-II protein levels significantly increased when the cells were treated with GB high (↑:200µg/ml) + BA + BafA1 [2.25 ± 0.25 ($p<0.05$)], compared to its corresponding BafA1 negative group. This result indicates an increase in the LC3 abundance and autophagosome pool size, hence suggesting upregulation of autophagy under these treatment conditions. Furthermore, a significant increase in LC3-II protein levels was observed when the cells were exposed to GB high (↑:200µg/ml) [2.25 ± 0.20 ($p<0.05$)] followed by BA and BafA1 treatment, compared to control cells treated with BA (hence basal autophagy) This further suggests that autophagy flux is highest when cells are exposed to GB high (↑:200µg/ml) as compared to GB low (↓:10µg/ml). Overall, our findings suggest that high autophagy flux can be achieved and is crucial to decrease proteotoxicity by favoring the degradation of accumulated protein aggregates.

(B)

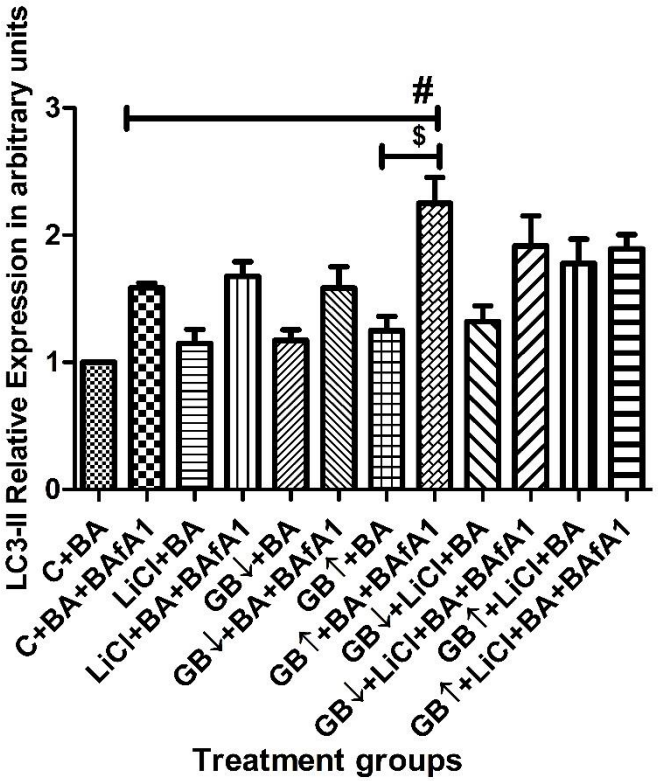

(B.1)

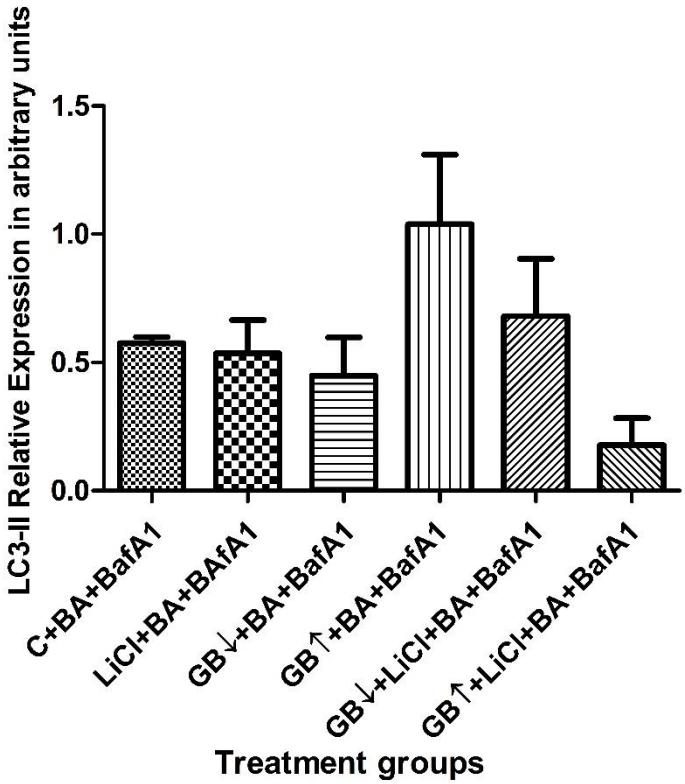

(B.2)

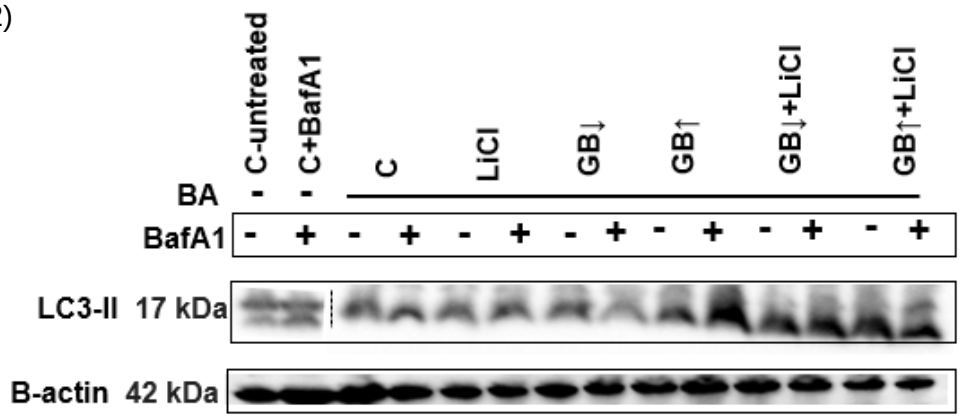

Figure 3.7 B: Relative protein expression levels of LC3-II and LC3-II Net Flux in N2aswe cells following treatment with medium (C), LiCl, GB low (↓:10µg/ml), GB high (↑:200µg/ml), GB low (↓:10µg/ml) + LiCl, GB high (↑:200µg/ml) + LiCl, for 24 hrs and subsequently treated with Butyric acid (BA;5 mM; 48 hrs) followed by Bafilomycin A1 (BafA1, 400nM, 4hrs). Beta-actin (β-actin) was used as a loading control. LC3-II blot shows the concersion of LC3-I to LC3-II. All data are expressed as means ± SEM (# p-value <0.05 vs C+BA+BafA1, $ p <0.05 vs its relative control, + vs GB low (↓:10µg/ml) +BA+BafA1). (n=3). (B.2) A representative blot is shown.

Section 3.8 The effect of Gingko Biloba treatment on autophagy flux and APP processing

3.8.A Inhibition of autophagy leads to the accumulation of APP

Western blot analysis was performed to assess whether GB's dose dependent effect on autophagic activity translates in distinct, flux dependent removal of APP and Aβ. In the previous section, our results demonstrated that GB reduces the protein expression APP, BACE and Aβ, which are all involved in the amyloidogenic pathway. We hypothesise that the clearance of these proteins is facilitated through the autophagy process. In order to assess this hypothesis, cells were treated with bafilomycin to determine whether the particular proteins are targeted and degraded through the autophagy pathway. Upon bafilomycin treatment, cargo targeted for degradation by the autophagy system would accumulate. Under basal conditions, control cells treated with BA (5mM, 48 hrs) and post-treated with BafA1 displayed a decrease in APP protein expression [0.70 ± 0.03 ($p<0.05$)] compared to cells only treated with BA (Fig 3.8 A), suggesting that indeed autophagy is involved APP processing.

Our results indicate that treatment with BafA1 caused strong trends of elevated APP protein levels in most treatment conditions besides GB low (↓:10µg/ml) [0.56 ± 0.41] (Figure 3.8 A). In addition, exposure to GB high (↑:200µg/ml) [0.70 ± 0.03 ($p<0.05$)] prior to BA and BafA1 treatment caused a significant increase in APP protein levels compared to control and GB low (↓:10µg/ml) conditions This further supports a GB concentration-dependent modulation of autophagy activity and hence degradation of target proteins. Accordingly, a decrease in APP protein levels, when treated with GB high (↑:200µg/ml) [0.70 ± 0.03] prior to BA exposure, appears to be significantly increased in the presence of GB high (↑:200µg/ml), BA and BafA1 compared to cells treated with GB high (↑:200µg/ml) and BA. This further suggest that APP is targeted as cargo for autophagy degradation. Since GB high (↑:200µg/ml) has the highest autophagy and is therefore clearing APP the strongest, inhibiting its autophagy leads to APP accumulating in a most robust manner (Fig 3.8 A).

(A)

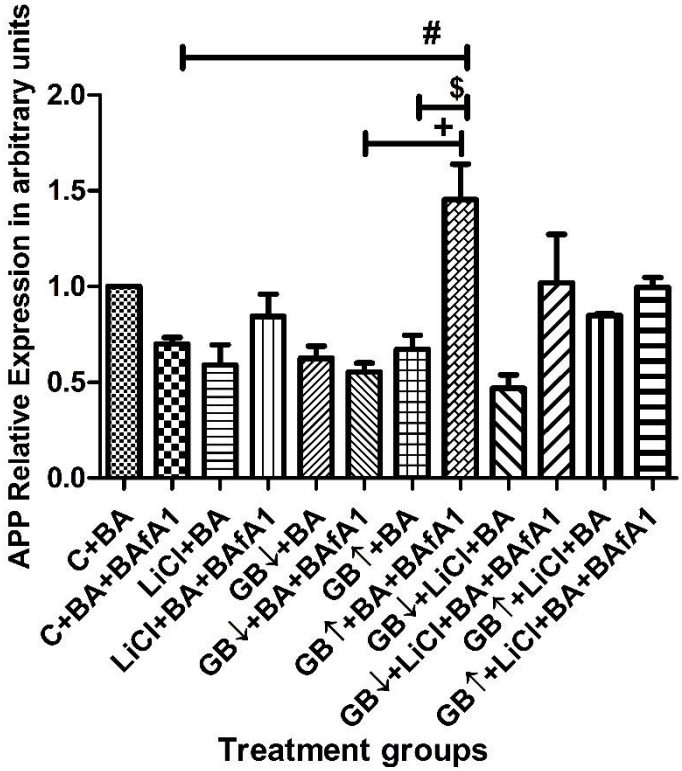

(A.1)

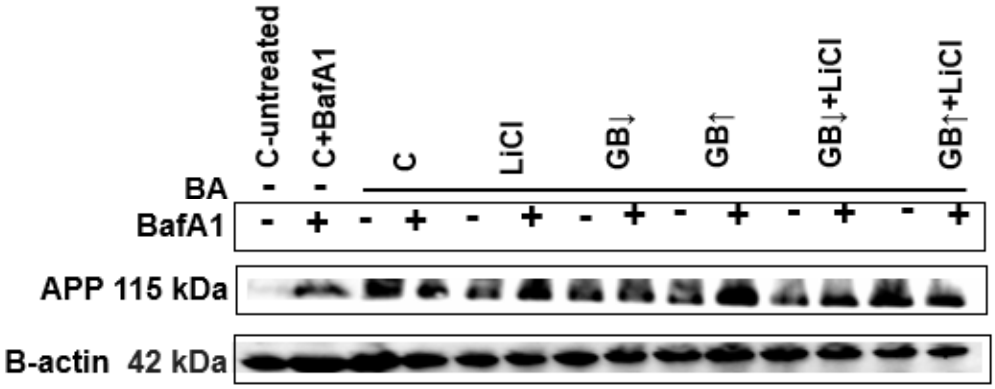

Figure 3.8 A: Relative protein expression levels of APP in N2aswe cells (C) following treatment with LiCl, GB low (↓:10µg/ml), GB high (↑:200µg/ml), GB low (↓:10µg/ml) + LiCl, GB high (↑:200µg/ml) + LiCl, for 24 hrs and subsequently treated with Butyric acid in the presence and absence of BafA1 (BA;5 mM; 48 hrs). Beta-actin (β-actin) was used as a loading control. All data are expressed as means ± SEM (# $p<0.05$ vs C+BA, \$ $p<0.05$ vs its relative control, + $p<0.05$ vs GB low (↓:10µg/ml) +BA+BafA1). (n=3). (A.1) A representative blot is shown.

3.8.B Inhibition of autophagy leads to the accumulation of BACE

Similar to the effect observed of autophagy on APP processing under basal conditions, cells treated with BA (5mM, 48 hrs) [0.80 ± 0.05] and post-treated with BafA1 displayed a decrease in BACE protein expression. Our results (Fig 3.8 B) indicate that treatment with BafA1 caused strong trends of accumulation in BACE protein levels in most treatment conditions, although this effect was non-significant (Figure 3.8 B). Exposure to GB high (↑:200µg/ml) [1.38 ± 0.21 ($p<0.05$)] prior to BA and BafA1 treatment caused the most robust increase in BACE protein levels compared to control and GB low (↓:10µg/ml) conditions [1.05 ± 0.157]. Interestingly, exposure to GB high (↑:200µg/ml) in the presence of LiCl showed a significant increase in BACE when co-treated with BA+BafA1, compared to control cells treated with BA and BafA1 and GB high (↑:200µg/ml) and BA. This further supports the notion of a GB concentration-dependent modulatory effect on autophagy and hence degradation of target protein. This further suggest that BACE is targeted as cargo.

(B)

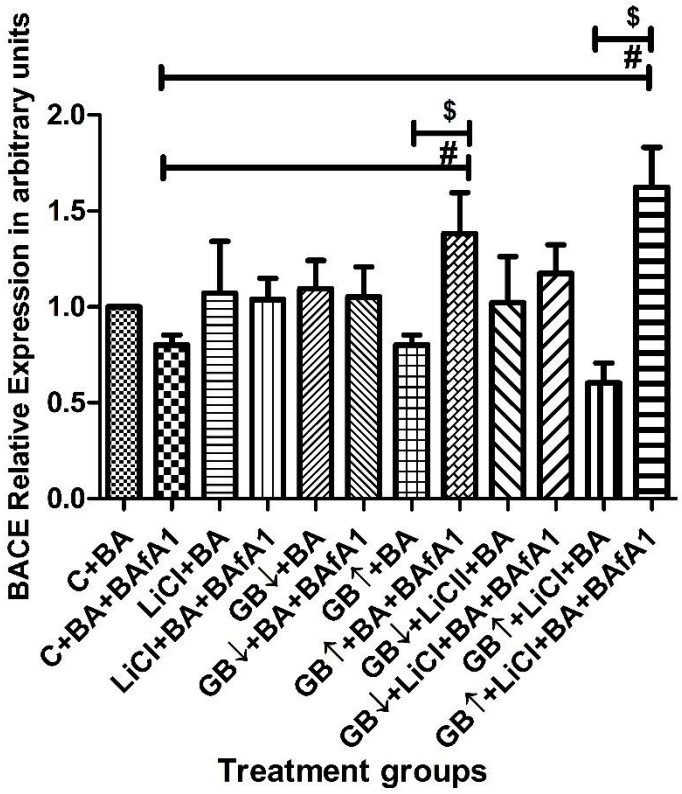

(B.1)

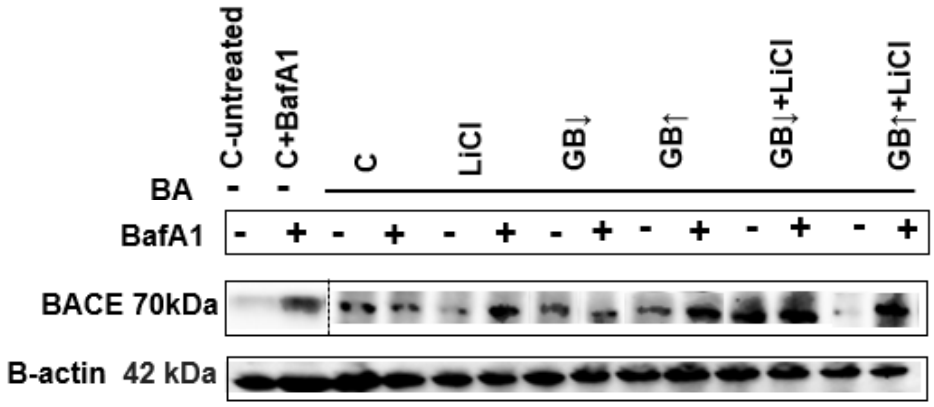

Figure 3.8 B: Relative protein expression levels of BACE in N2aswe cells (C) following treatment with LiCl, GB low (↓:10µg/ml), GB high (↑:200µg/ml), GB low (↓:10µg/ml) + LiCl, GB high (↑:200µg/ml) + LiCl, for 24 hrs and subsequently treated with Butyric acid in the presence and absence of BafA1 (BA;5 mM; 48 hrs). Beta-actin (β-actin) was used as a loading control. All data are expressed as means ± SEM (# $p<0.05$ vs C+BA, $ $p<0.05$ vs its relative control, + $p<0.05$ vs GB low (↓:10µg/ml) +BA+BafA1). (n=3). (B.1) A representative blot is shown.

3.8.C Inhibition of autophagy leads to the accumulation of Aβ

Since Aβ is the product of APP cleavage by BACE, the protein expression of BACE is expected to translate in the protein expression of Aβ. Thus, a decrease in BACE following BA exposure would also result in a decrease in Aβ protein expression. To our surprise, no significant changes were observed in the protein expression of Aβ, however, strong trends of increased Aβ protein expression can be observed with exposure to BafA1 particularly under conditions of GB high (↑:200µg/ml) and both in the presence [0.42 ± 0.2] and absence [0.52 ± 0.1] of LiCl.

(C)

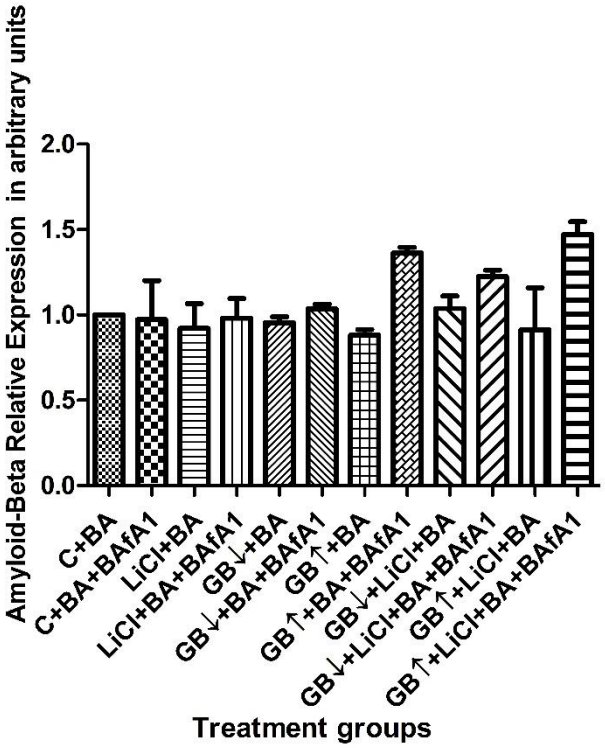

(C.1)

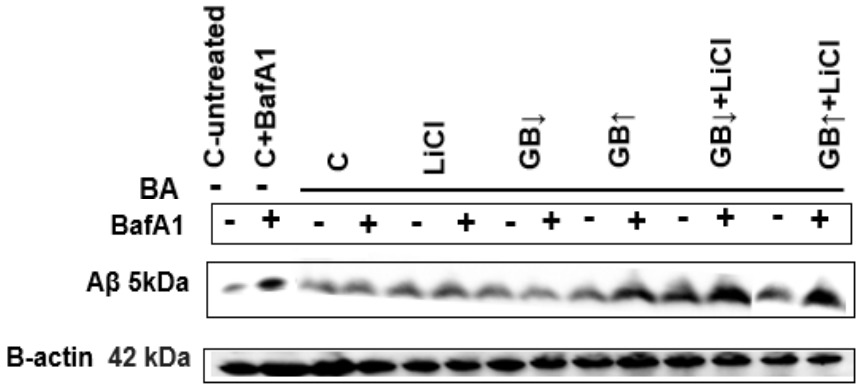

Figure 3.8 C: Relative protein expression levels of Aβ in N2aswe cells (C) following treatment with LiCl, GB low (↓:10µg/ml), GB high (↑:200µg/ml), GB low (↓:10µg/ml) + LiCl, GB high (↑:200µg/ml) + LiCl, for 24 hrs and subsequently treated with Butyric acid in the presence and absence of BafA1 (BA;5 mM; 48 hrs). Beta-actin (β-actin) was used as a loading control. All data are expressed as means ± SEM (# p-value <0.05 vs C+BA, $ p-value <0.05 vs its relative control, +p<0.05 vs GB low (↓:10µg/ml) +BA+BafA1). (n=3). (C.1) A representative blot is shown.

Section 3.9 The effect of Gingko Biloba treatment on autophagy and apoptosis

3.9.A The role of Autophagy inhibition on cell death onset

In the following section we aimed to assess whether the observed neuroprotective effects of GB treatment were dependent on the modulation of autophagy. We subsequently aimed to assess how the modulation of autophagy by GB, when blocking autophagy, would affect cell death susceptibility. Thus, western blot analysis was performed to assess the protein expression of cytochrome-c and cleaved-caspase-3. Cytochrome-c protein expression was significantly increased in cells exposed to GB high (↑:200µg/ml) [1.401 ± 0.52 ($p<0.05$)] followed by BA and BafA1 treatment compared to cells treated BA + BafA1 and with GB low (↓:10µg/ml) followed by BA and BafA1 treatment. These results further demonstrate the dose-dependent effect of GB on autophagy and its protective role. Moreover, these results suggest that since GB high (↑:200µg/ml) caused the highest autophagy flux, when its autophagy activity is inhibited, the onset of apoptosis will increase, as shown by the increased cytochrome-c release. This suggests how highly dependent these cells are on high autophagy activity to delay the onset of cell death. Thus, autophagy has a protective effect in these conditions.

(A)

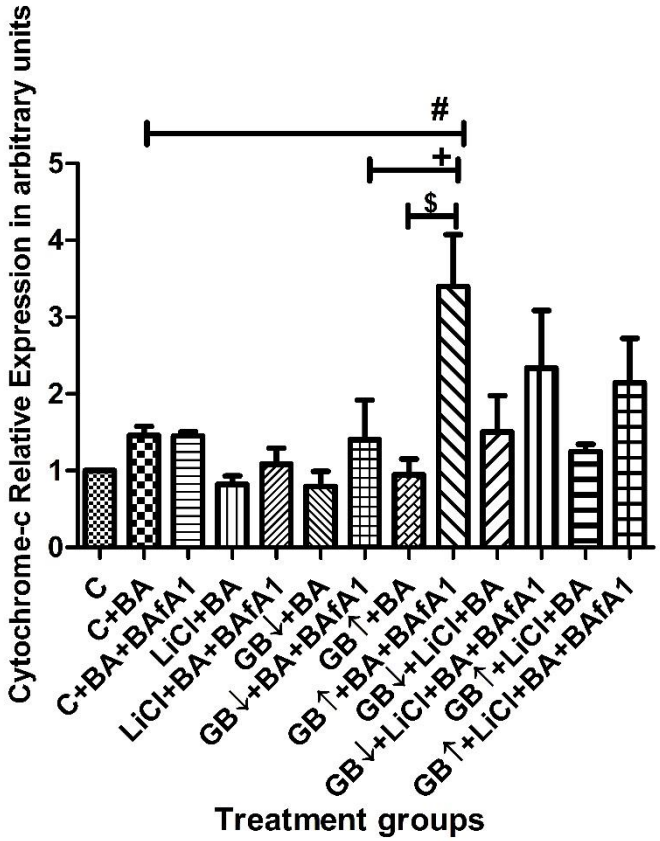

(A.1)

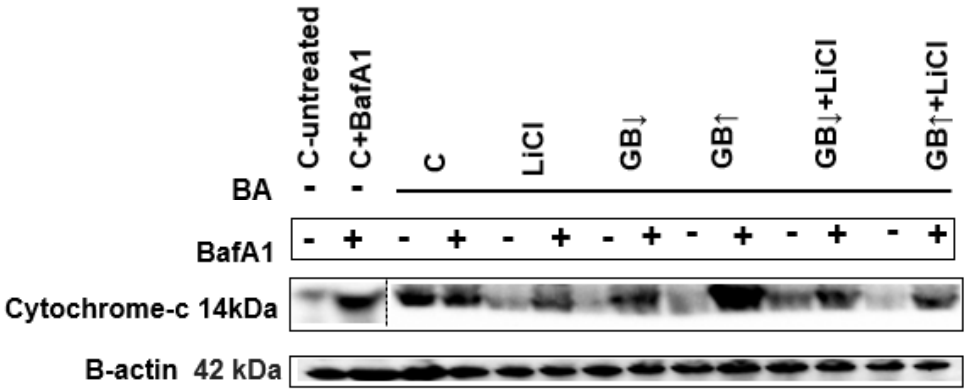

Figure 3.9 A: Relative protein expression levels of cytochrome-c in N2aswe cells following treatment with medium (Con), LiCl, GB low (↓:10µg/ml), GB high (↑:200µg/ml), GB low (↓:10µg/ml) + LiCl, GB high (↑:200µg/ml) + LiCl, for 24 hrs and subsequently treated with Butyric acid (BA;5 mM; 48hrs) followed by Bafilomycin A1 (BafA1, 400nM, 4 hrs). Beta-actin (β-actin) was used as a loading control. All data are expressed as means ± SEM (# p <0.05 vs C+BA, $ p<0.05 vs its relative control, +p<0.05 vs GB low (↓:10µg/ml) +BA+BafA1). (n=3). A representative blot is shown.

3.9 B The role of Autophagy on oxidative stress

In order to further measure neuronal injury, 4-Hydroxynonenal (4HNE) was utilized, to assess lipid peroxidation. 4HNE has been shown to increase during states of oxidative stress which is a result of increased cellular stress events that in turn cause higher rates of lipid peroxidation. The neuroprotective role of GB high (↑:200µg/ml) and its associated high autophagy flux was further demonstrated through western blot analysis of 4HNE. 4HNE protein expression was significantly increased when cells were treated with GB high (↑:200µg/ml) + BA+ BafA1 [1.90 ± 0.81 ($p<0.05$)] compared to cells exposed to GB low (↓:10µg/ml) +BA+ BafA1 and control cells treated with BA and BafA1 respectively. These results suggest that, when the upregulation of autophagy by GB is high (↑:200µg/ml), yet autophagosome fusion is inhibited, the cells manifest in high lipid peroxidation. Moreover, these findings demonstrate how highly dependent cells are on high autophagy activity to resist cellular stress. Furthermore, pre-treatment with LiCl [1.50 ± 0.10 ($p<0.05$)] and GB high (↑:200µg/ml) [1.90 ± 0.81 ($p<0.05$)] prior to BA + BafA1 exposure presented with an increase in 4HNE protein levels, in comparison to their relative BafA1 negative groups

(B)

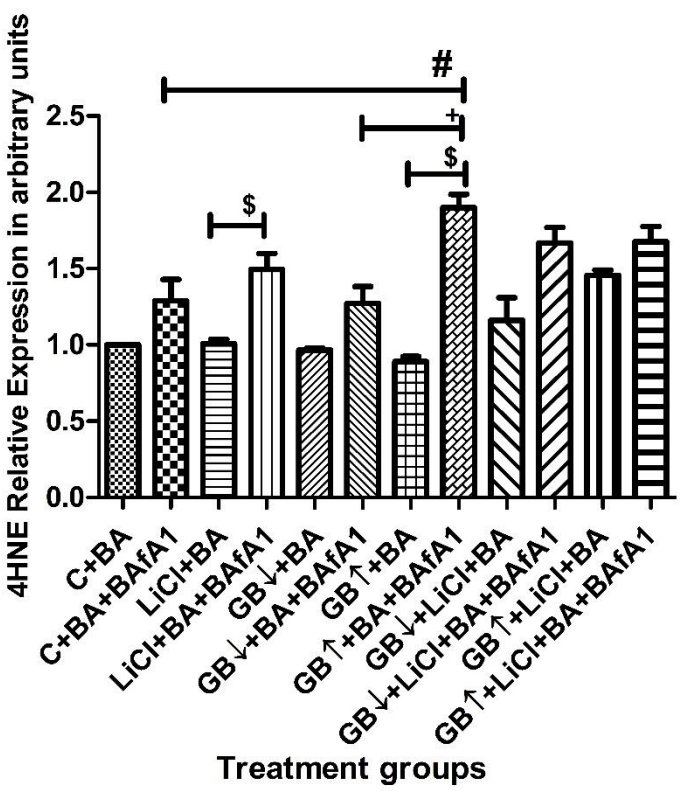

(B.1)

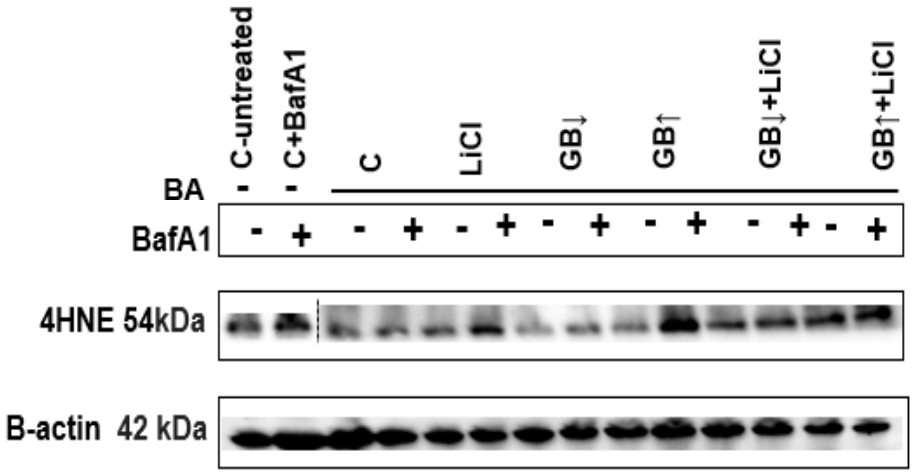

Figure 3.9 B: Relative protein expression levels of 4HNE in N2aswe cells following treatment with medium (C), LiCl, GB low (↓:10µg/ml), GB high (↑:200µg/ml), GB low (↓:10µg/ml) + LiCl, GB high (↑:200µg/ml) + LiCl, for 24 hrs and subsequently treated with Butyric acid (BA;5 mM; 48 hrs) followed by Bafilomycin A1 (BafA1, 400nM, 4 hrs). Beta-actin (β-actin) was used as a loading control. All data are expressed as means ± SEM (* p-value <0.05 vs C+BA+BafA1, $ p-value <0.05 vs its relative control, + vs GB low (↓:10µg/ml) +BA+BafA1). (n=3). A representative blot is shown.

Section 3.10 The compositional analysis of GB

The Liquid chromatography–mass spectrometry (**LC-MS**) **Q-TOF** technique was utilized to identify the specific components including, terpene lactones and flavonoid glycosides present in GB. The table 3.10 below represents a summary of the compounds identified in the GB extract used in the study:

Table 3.10: The Liquid chromatography–mass spectrometry of GB

Name	Formula	Retention Time	Mass (g/mol)
Ginkgolide A	$C_{20}H_{24}O_9$	19.49	408.1425
Ginkgolide B	$C_{20}H_{24}O_{10}$	14.5	424.1374
Ginkgolide C	$C_{20}H_{24}O_{11}$	1409	440.1317
Ginkgolide J	$C_{20}H_{24}O_{10}$	19.5	424.1362
Bilobalide	$C_{15}H_{18}O_8$	13.7	326.1001
Kaempferol-3-[6'''-*p*-coumaroylglucosyl-β-(1→4)-rhamnoside]	$C_{36}H_{36}O_{17}$	19.5	740.1957
Kaempferol 3-(2G-rhamnosylrutinoside)	$C_{33}H_{40}O_{19}$	19.7	740.218
Kaempferol 3-*O*-glucoside	$C_{21}H_{20}O_{11}$	13.94	448.101
Luteolin 3'-*O*-glucoside	$C_{21}H_{20}O_{11}$	16.1	448.101
Isorhamnetin 3-*O*-rutinoside	$C_{28}H_{32}O_{16}$	16.1	624.168
Kaempferol 3-*O*-rutinoside	$C_{27}H_{30}O_{15}$	16.1	594.1583
Kaempferol-3-*O*-β-D-glucorhamnoside	$C_{27}H_{30}O_{15}$	14.74	594.1584
Rutin	$C_{27}H_{30}O_{16}$	15.6	609
Quercetin-3-o-robinobiside	$C_{15}H_{10}O_7$	14.2	609

Our results reveal the presence of major active components in Ginkgo biloba extract including: a) flavonoid glycoside (Kaempferol and glucose glycoside) and b) Ginkgolides A, B, C and J, Bilobalide which are terpene lactones.

CHAPTER 4: DISCUSSION

Autophagy is a vital process in cellular survival, as it is essential for organelle and long-lived protein turnover. As such, it is widely accepted that autophagy impairment is a major contributing factor in the development of AD (Nixon, 2007). This impairment is associated with a rise in the vulnerability of the cell to undergo cell death (Ntsapi et al., 2018). Conversely, autophagy inhibition has been shown to modulate APP processing and causes the deposition of Aβ (Pickford et al., 2008). The implication of the presence of Aβ has been shown to become toxic when its levels increase above physiological levels, due to the imbalance in production and clearance, as evidenced in AD. The modulation, in particular the increase of autophagic activity is therefore thought to be a promising therapeutic strategy aimed towards the alleviation of Aβ-associated neurotoxicity in AD, which is often accompanied by extensive mitochondrial and lysosomal damage (Nixon, 2007). Although significant insight has been gained regarding AD pathology, limited progress has been made in the development of pharmaceutical therapeutics that modify or reverse the debilitating effects of this disease. Currently, all approved treatment options for AD are primarily symptomatic, these include acetylcholine inhibitors, as well as N-methyl-D-aspartate (NMDA)-receptor antagonist, which address symptoms but not the underlying cause or defect (Anand et al., 2014). Despite advances in unravelling the biological underpinnings of AD pathology, to date there are still no disease-modifying therapies available for those affected.

Gingko biloba (GB) and lithium chloride (LiCl) have been reported to be neuroprotective in the context of neurodegenerative diseases (Kanowski, et al., 1996; Baldessarini et al., 1999). These neuroprotective effects include the preservation of synaptic plasticity (Hong et al., 1997), enhancing mitochondrial function (Forlenza et al., 2012), inhibition of apoptosis, decreasing the deposition of Aβ (Su et al., 2004) and improving cognitive defects (Fornai et al., 2008). Some of these beneficial effects have been translated into the clinical context through supplementation with GB (EGb 761), which was shown to improve the neuropsychiatric symptoms in dementia patients when compared to a placebo group (Schneider et al., 2005). Even though some countries readily prescribe GB and LiCl to individuals suffering from AD, their mechanism of action remains largely unclear. Both these drugs have shown promising autophagy modulating properties (Liu et al., 2015; Sarkar et al., 2005) and thereby play a role in the removal of toxic protein aggregates. However, this role has not been fully explored for translation to a clinical level, largely due to limited knowledge around the ranges of drug concentration that affect and control autophagy finely

The aim of the proposed study was therefore to investigate the effect of both GB and LiCl as a single or combination treatment intervention on the modulation of autophagy activity, and the mitigation of Aβ proteotoxicity in an *in vitro* model of AD. We hypothesized that treatment with GB will exhibit a dose dependent effect on autophagic activity, and this effect will be further enhanced through combination treatment with LiCl. This effect may then translate in the distinct removal of APP and Aβ, preserving lysosomal function and mitochondrial integrity.

4.1 Gingko biloba pre-treatment confers neuroprotection against Aβ proteotoxicity

The N2aswe cell line has extensively been utilized to study disease pathologies related to Aβ mediated neurotoxicity (Park et al., 2016b). The early accumulation of extracellular Aβ peptides in AD susceptible neurons of the brain has been shown to be the main contributor to the pathogenesis of AD (Hardy and Higgins, 1992). We hypothesized that GB would have a concentration dependent effect on the cellular viability of APP overexpressing N2aswe cells, and that this effect would be further potentiated in the presence of LiCl. In an attempt to assess the neuroprotective role of GB against Aβ mediated proteotoxicity, WST1 assays were utilized. Our results indicate that the use of 5 mM of BA for 48 hrs significantly reduced the relative reductive capacity of cells compared to control conditions (Fig 3.1.4). Since BA induces the expression of APP, and hence enhanced production of Aβ, our results indicate that 48 hrs expression of APP impacts the viability of the cells. Importantly, this Aβ induced reduction in cellular viability was markedly suppressed by 24 hrs exposure to LiCl 10 mM, GB 10 µg/ml & 200 µg/ml and a combination treatment of GB↓ (10 µg/ml) + LiCl 10 mM prior BA exposure. Indeed, the comparison of concentrations is however poorly described, and we observed protective effects with both low and high concentrations of GB in the context Aβ proteotoxicity. Our results revealed that both GB and LiCl confer neuroprotective properties. This is consistent with current literature findings which have demonstrated that pre-treatment with GB extract (EGb761) increased the cell viability of oxygen and glucose-deprived human neuroblastoma cells (Ba and Min, 2015). Conversely, 24 hr pre-treatment with 3 mM of LiCl has been shown to increase the cell viability of rat pheochromocytoma cells which were exposed to Aβ peptide for 24 hrs (Wei et al., 2000). This led to a suppression in Aβ-induced loss of redox activity. Together with our results, these findings suggest that both GB and LiCl are neuroprotective under proteotoxic conditions. The possible mechanism underlying LiCl's neuroprotective role is potentially by increasing the activity of Bcl-2 which in turn regulates cell survival by inhibiting apoptotic genes such as p53 and Bax protein (Wei et al., 2000). Interestingly, administration of both combination treatment of GB↓10 µg/ml & GB↑200 µg/ml with LiCl also demonstrated an additive protective effect compared to BA-only treated cells

(Fig 3.1.4). However, this effect was only significant under GB↓10 µg/ml + LiCl conditions and was not markedly higher compared to the scenario when cells were exposed to the single treatments. To our best knowledge, this is the first time that these two drugs have been administrated in combination, in which case our findings warrant further investigation in the future. Thus, pre-treatment with GB in the presence and absence of LiCl prior to Aβ aggregate accumulation would potentially ameliorate Aβ-induced cytotoxicity. This is important because the early accumulation of extracellular Aβ peptides in AD susceptible neurons of the brain has been shown to be the main contributor to the pathogenesis of AD (Hardy and Higgins, 1992).

4.2 Gingko biloba treatment and LiCl modulate autophagic flux

To elucidate potential mechanisms underlying the neuroprotective effects of LiCl and GB, we measured the protein levels of p62 and LC3-II in the presence and absence of BafA1. It is known that the administration of an autophagy inhibitor such as Bafilomycin A1 (BafA1) translates to elevated levels of LC3-II in association with increased p62 protein levels, since fusion of autophagosomes and lysosomes is inhibited (Mizushima and Yoshimori, 2007).. We hypothesised that the protective role of both LiCl and GB was brought about through their respective modulatory role on autophagy. We further hypothesized that GB would exhibit a concentration-dependent effect on autophagy, an effect that would further be potentiated in the presence of LiCl.

The expression of LC3-II is indicative of the abundance of autophagosomes, whereas an increase in p62 protein levels measures functional autophagy, following BafA1 treatment. Our results reveal that BafA1 had no effect in control cells, displayed by the non-significant changes in LC3-II and p62 protein expression compared to BafA1 untreated cells (Fig 3.2.1 A &B). This suggests that these cells have a relatively low basal autophagy flux. The non-significant increase in p62 levels following BafA1 treatment could be explained by the fact that p62 is also required for the selective binding of ubiquitinated tagged proteins and marks the proteins for degradation by either the UPS system or the autophagy system (Ding et al. 2007). Therefore, blocking autophagy may result in cellular compensation through the UPS process.

However, treatment with both concentrations of GB in the presence and absence of LiCl lead to a robust accumulation of autophagosomes (LC3-II levels) compared to their respective BafA1 negative group and control cells only treated with BafA1. Similarly, an elevation of p62 protein levels was demonstrated when the cells were exposed to GB high (↑:200 µg/ml) in the presence of BafA1, compared to its corresponding BafA1 negative group. This effect was enhanced when GB high (↑:200 µg/ml) was combined with LiCl (Fig 3.2.1B). Taken together,

these results indicate that GB, in the presence and absence of LiCl, upregulates autophagy and induces autophagy above basal autophagy levels. This is consistent with current literature that demonstrated that GB dietary supplementation results in robust autophagic induction, as revealed by an increase in LC3-II protein levels and beclin1 expression in the brains of APP-transgenic mice (Liu et al., 2015). Similarly, in microglia cells, the protein expression of LC3-II and beclin1 was elevated and associated with decreased p62 levels following GB EGb761 treatment, suggesting that GB treatment upregulates autophagy activity. In contrast, another GB extract (EGb1212), consisting of a greater quantity of bilobalide and ginkgolide B, has been reported to inhibit autophagy in the ischemic brain (Yin et al., 2013). These data suggest that the different components found in GB influence the overall modulation of GB on autophagy. Moreover, these data demonstrate that indeed autophagic activity may differ, depending on the drug concentration used. This may have important implications in drug screening as well as in treatment intervention approached, allowing to match autophagy dysfunction with a most suitable autophagy enhancing drug. A reverse transcription-polymerase chain reaction assay study demonstrated that Lewis lung cancer cells exposed to different concentrations of GB exocarp extracts (10, 20 and 40 mg/ml) displayed a significant upregulation in ATG 5 mRNA (Cao et al., 2017). Moreover, the higher concentration of GB exocarp extracts (20 and 40 mg/ml) markedly increased Beclin1 mRNA. Since the upregulation of ATG 5 and Beclin1 is associated with high autophagy activity, these data suggest that higher concentration of GB exhibit indeed a greater effect on the modulation of autophagy activity. These findings highlight that a concentration-dependent modulation of GB on autophagy indeed exists, as we had proposed. This study further demonstrates that GB exocarp extracts elevated the protein expression of p-AMPK and p-mTOR through western blot analysis, which could potentially be the underlying mechanism by which GB upregulates autophagy (Cao et al., 2017). However, these parameters were not investigated in this present study and thus warrant further investigation. Although a recent study showed that GB exocarp extracts increase the abundance of autophagosomes in Lewis lung cancer cells using TEM analysis (Cao et al., 2017), little is known about the effect of GB's on autophagic flux. Autophagic flux is defined as the rate of protein degradation through the entire autophagy pathway (du Toit et al., 2014; Klionsky et al., 2016) and can only be investigated using an autophagy inhibitor such as BafA1 (Mizushima and Yoshimori, 2007). Thus, to our best knowledge, this is the first time that the extent of autophagic flux modulation in response to GB treatment is presented.

Although LiCl treatment on its own did not significantly increase the pool size of autophagosomes following BafA1, a strong trend of increased LC3-II protein expression was demonstrated (Fig 3.2.1 A). This is consistent with a study that demonstrated that N2aswe

cells exposed to LiCl for 24 hrs manifested in an increased amount of LC3-II protein levels (Heiseke et al., 2009). Moreover, the abundance of LC3-II protein levels in the presence of BafA1 was larger, indicating that LiCl indeed upregulates autophagic activity above basal levels. The underlying mechanism by which LiCl upregulates autophagy is suggested to be through its inhibitory action on inositol monophosphatase (IMPase), which results in the depletion of free inositol (Sarkar et al., 2005). On the other hand, we believe that since LiCl has an inhibitory effect on GSK3β, which results in the activation of mTORC1 and the consequent suppression of autophagy, this could potentially counteract the upregulation of autophagy by LiCl through IMpase inhibition (Sarkar et al., 2008). This may serve as an indication for our findings, revealing a non-significant induction of autophagy by LiCl. Another study also showed that LiCl (10 mM) induced autophagy in COS-7 cells but did not increase the accumulation of LC3-II in neuronal cells (Tsvetkov et al., 2009).

Given that both GB and LiCl upregulate autophagy, we found that a combination treatment of GB and LiCl manifested in an upregulation of autophagy, in which GB high (↑:200 µg/ml) + LiCl had a larger increase in the accumulation of autophagosomes, compared to GB low (↓:10 µg/ml) + LiCl (Fig 3.2.1). Although we hypothesized that the extent of autophagic flux modulation, in response to GB treatment in the presence of LiCl, would confer additive protective effects, this was not confirmed in the study. To our surprise, the response of LC3-II protein levels in the presence of BafA1 was similar when the cells were exposed to both low and high concentration of GB alone or in the presence of LiCl (Fig 3.2.1 A). Our results differ from a study that investigated the combination effect of LiCl and rapamycin (Sarkar et al., 2005). This study showed that co-treatment with rapamycin and LiCl revealed greater reduction of pathological prion proteins in murine neuroblastoma cells compared to cells treated with either drug on its own (Sarkar et al.,2005). Furthermore, this effect was due to enhanced autophagy flux of the combinatorial treatment.

Corresponding fluorescence microscopy of p62 was employed to further characterise the extent of GB modulation of autophagy flux. Our results revealed a low abundance of p62 aggregates under normal conditions, which remained unaltered when exposed to GB in the presence or absence of LiCl (Fig 3.2.2). Indeed, low p62 expression under normal conditions is indicative of high protein degradation through autophagy, which is common in neurons (Mizushima and Yoshimori, 2007). As expected, treated with BafA1 resulted in a marked increase in p62 aggregates compared to untreated cells (Fig 3.2.2). Importantly, fluorescence micrographs demonstrated that exposure to GB high (↑:200 µg/ml) and a combination treatment of GB high (↑:200 µg/ml) + LiCl 10 mM in the presence of BafA1 presented with the highest abundance of p62 compared to control cells treated with BafA1 and GB low (↓:10 µg/ml) in the presence of BafA1. These results further suggest that GB

may have a dose-dependent effect on the abundance of p62 and hence, an effect on the functional activity of autophagy.

4.3 Gingko biloba treatment preserves lysosome function

The internalization of Aβ has been described to cause instability of lysosomes (Zuroff et al., 2017). Therefore, we proposed that GB treatment in the presence or absence of LiCl would preserve lysosome function under Aβ-induced cytotoxicity. Since LAMP2a is a specific lysosomal membrane associated protein, we assessed whether its protein expression correlates with the abundance of lysosomes with intact membranes (Eskelinen, 2006).

Although no significant changes were observed in the expression levels of LAMP2a, strong trends can be observed (Fig 3.3.1). Firstly, it is apparent that exposure to LiCl and GB reduces the protein levels of LAMP2a (Fig.3.3.1). Our results differ from a study that used the mono-dansyl-cadaverine staining method to detect the generation of acidic vacuoles (including lysosomes) in cells, showing that the fluorescence intensity of untreated cells was weaker and displayed fewer acidic vacuoles (Cao et al., 2017). However, exposure to GB exocarp extracts resulted in enhanced mono-dansyl-cadaverine fluorescence intensity and prominent aggregated particles. Thus, the authors concluded that GB treatment increased the activation and generation of acidic vacuoles (Cao et al., 2017). Since our results reported that LiCl and GB induce autophagy (Fig 3.2.1), and it is known that lysosomes are the organelles that carry out the cargo degradation, it could be plausible that these lysosomes are rapidly fusing with autophagosomes to form auto-lysosomes. Moreover, it is possible that both LiCl and GB also target chaperone-mediated autophagy. This notion is supported by a study that showed that LAMP2a levels directly correlate with the activity of the proteolytic pathway, particularly chaperone-mediated autophagy (Kaushik and Cuervo, 2015). On the other hand, it can be argued that the reduction of LAMP2a protein expression observed in our study, when exposed to GB and LiCl, potentially resulted from a reduction in lysosomal pool size or biogenesis compared to control conditions. However, we doubt that this is the case in our scenario, as LAMP2a does not directly correlate to the biogenesis state of lysosomes and the high rate of degradation through the autophagy-lysosomal-pathway following GB treatment would not be possible. Indeed, lysosomal vesicles have been shown to be vital in the functional execution of protein/organelle degradation through the autophagy pathway (Settembre et al., 2015). Our TEM micrographs (Fig 3.3.3) support the notion that both GB and LiCl treatment increase the size and number a vaculaor structures which we believe represent autophagosomes, lysosomes and autolysosomes.

Secondly, and of particular interest, treatment with BA revealed an elevation in LAMP2a protein levels (Fig 3.3.1). Since BA induces the overexpression of APP and thus, enhanced

production of Aβ, we believe that the increase in LAMP2a could have been as a result of Aβ accumulation in the lysosomes, resulting in the destabilization of lysosomes and consequently inhibiting the cathepsin enzymes in lysosomes necessary to degrade Aβ. The TEM micrographs support this notion, revealed by disrupted vaculoar structures following BA treatment (Fig 3.3.3). In support of this notion, suppression of lysosomal enzymes has previously been reported to trigger the accumulation of Aβ within the lysosomal lumen (Zheng et al., 2006). However, it is also plausible that Aβ damaged the lysosomal membrane and caused subsequent rupture, resulting in the leakage of cellular contents, including the cathepsins from the lysosomal lumen into the cytosol (Boya and Kroemer, 2008). A decrease in LAMP2a in response to BA could also be expected in this regard. However, for future studies and to fully elucidate the role of the damaged lysosome pool in comparison to healthy lysosomes, the protein expression of Galectin-3, which is reported to accumulate in damaged lysosomes, could be compared with the protein expression of LAMP2a (Maejima et al., 2013). Interestingly, it has been reported that damaged lysosomes themselves can be targeted for autophagy degradation (Maejima et al., 2013). We therefore suggest that GB in the presence and absence of LiCl would attenuate the damages caused by BA exposure, potentially by inducing the degradation of these damaged lysosomes through lysophagy.

Pre-treatment with GB high (↑:200 µg/ml) prior to BA exposure caused a decrease in LAMP2a expression, whereas pre-treatment with LiCl, GB low (↓:10 µg/ml) both GB (low↓:10 µg/m + (↑:200 µg/ml) in the presence of LiCl revealed an elevation in LAMP2a protein expression (Fig 3.3.1). The reduction in LAMP2a expression in response to GB high (↑:200 µg/ml) prior to BA exposure potentially suggests that GB high (↑:200 µg/ml) decreases the damaged lysosomes as a result of BA treatment and hence, preserves the functioning of lysosomes. This notion can also be supported by GB high (↑:200 µg/ml) associated high autophagy flux (Fig 3.2.1), sequestering damaged lysosomes robustly, potentially through lysophagy. Therefore, Aβ triggers lysosomal damage, which in turn leads to an increase in LC3-II expression, suggesting that lysosomal rupture contributes to the induction of autophagy (Maejima et al., 2013). However, we suggest that further experiments like confocal microscopy analysis could be conducted to study the colocalization of LC3 and LAMP1, which would reveal the possibility of damaged lysosomes being selectively targeted by the autophagy process (Maejima et al., 2013). It might be conceivable that GB sequesters damaged lysosomes in an autophagy dependent manner and hence prevents the release of the cytosolic contents which could trigger events such as apoptosis. However, before a therapeutic strategy can be implemented, it is important that the steps and extent of autophagy dysfunction is fully identified. Merely increasing autophagy initiation may be detrimental if the clearance by lysosomes is defective. Therefore, a treatment intervention

would have to improve any defects in the lysosomes and re-establish the acidification of lysosomes, followed by the stimulation of autophagy. In this context, since LiCl and GB (low↓:10 µg/ml) displayed the same LAMP2a expression as BA-treated cells, this would suggest that their autophagic activity is not high enough to sequester the damaged lysosomes. Overall, induction of autophagy by GB in the presence and absence of LiCl prior to Aβ aggregate accumulation would potentially ameliorate Aβ-induced lysosomal damage.

To further validate the effect of GB in the presence and absence of LiCl on lysosomal function, acridine orange (AO) stain was employed (Fig 3.3.2). AO binds to DNA which fluoresces green but emits red fluorescence in acidic vesicular organelles (AVOs), including lysosomes, endosomes and autolysosomes. Since lysosomes are the most acidic organelles in cells, we employed AO as a rapid staining technique to assess the acidic compartments, particularly lysosomes (Thomé et al., 2016). It is important to highlight a major weakness when assessing lysosomal function using AO stain, which is the fact that AO associates with all acid compartments and hence is unable to differentiate between functional and non-functional lysosomes or endosomes and other acidic vacuoles.

Lysosomal detection using AO staining revealed similar findings to that observed using LAMP2a western blot analysis (Fig 3.3.1). Under control conditions, untreated control cells displayed a clear abundance of lysosomal acid compartments (LAC), whereas exposure to GB and LiCl displayed the same morphology as the untreated control cells, although a relative decrease in LAC was demonstrated (Fig 3.3.2). Treatment with BA revealed a marked reduction in LAC compared to control condition, indicating that BA treatment contributes to the deacidifcation of organelles. These results suggest that BA exposure resulted in the damage of lysosomes or decrease in lysosome function. However, to fully elucidate the difference between damaged and healthy lysosomes, we propose that additional analyses are conducted such as antibody-based fluorescence microscopy against LAMP2a which can be used as a lysosomal marker and Galectin-3 antibody which can be used as a marker for damaged lysosomes (Maejima et al., 2013). Furthermore, the uses of GFP-Galectin-3 transfected cells to could be used to better assess the distribution of damaged versus healthy lysosomes. Similarly, to the results revealed with western blot analysis, pre-treatment with LiCl prior to BA exposure caused a robust increase in LAC compared to BA-only treated cells. In this context, it is possible that LiCl increases the biogenesis and lysosomal pool size which regulates many cellular processes. In fact, literature has shown that LiCl induces lysosomal dependent processes such as the Wnt/*β*-catenin signalling and increases the degradation by cathepsin H (Kishimoto and EItoi, 2013). However, pre-treatment with GB in the absence and presence LiCl prior to BA exposure did

not alter the LAC abundance. This may indicate that these cells maintained the overall LAC volume in the cytoplasm even under BA exposure.

4.4 Gingko biloba treatment clears amyloidogenic proteins under neurotoxic conditions

The ability of compounds or drugs to clear toxic protein aggregates in the context of neurodegeneration has received major attention. Exposure to both, high and low concentrations of GB manifested in a significant reduction of APP, BACE and Aβ prior to BA treatment (Fig 3.4. A, B &C). These findings suggest active clearance of the amyloidogenic proteins by both GB concentrations. Although statistically there are no GB dose-dependent differences in the reduction of amyloidogenic proteins between the low treatment groups, the immunoblot data reveal that GB high (↑:200 µg/ml) reduces BACE protein levels robustly more than GB low (↓:10 µg/ml). These data further point to a concentration-dependent clearance of BACE by GB, where the highest GB concentration clears the amyloidogenic proteins strongest. This is in line with a study that performed Aβ aggregation assays in response to different concentrations of GB [EGB 761 (1- 100 µg/ml)] (Luo et al. 2002). This study reported that the anti-Aβ aggregation properties of GB (EGB 761) was only evident at the highest concentration (GB 100 µg/ml) by directly inhibiting the generation of Aβ fibrils (Luo et al. 2002). Unfortunately, however, no autophagy assessment was performed. Another study showed that a duration of 5 months and not 2 months of treatment with GB (EGb 761) decreased phosphorylated-tau protein levels in a tau-mutant transgenic mouse (Qin et al., 2018). Since tau phosphorylation is known to be a downstream effect of Aβ pathology, this finding suggests that long-term treatment with GB is more beneficial in ameliorating AD pathology. We believe that other protein expression tests such as ELISA should be conducted to more finely assess these observed differences. In the brain tissue of transgenic mice, chronic treatment with EGb761 (300 mg/kg) has been shown to differentially influence protein levels involved in the processing and metabolism of APP (Augustin et al., 2009). The same study also revealed that long-term EGb761 dietary supplementation leads to a significant decrease in human APP levels in the cortex and hippocampus region, which could indicate a role for APP to be molecularly targeted by EGb761. Overall, our results demonstrated that GB results in the clearance of amyloidogenic proteins.

Exposure of cells to 24 hrs LiCl significantly decreased the protein levels of APP, suggesting that LiCl affects the general synthesis of APP by supressing the expression of APP (Fig 3.4 A). Our results are however conflicting, since another study demonstrated that the protein expression of APP and CTFß (C99) was unaltered by 24 hrs LiCl (10 mM) treatment, suggesting that LiCl does not influence ɣ-secretase activity (Esselmann et al., 2004). Our

results further demonstrate that LiCl reduces the expression of BACE and Aβ (Fig 3.4 B &C). This finding is of importance since Aβ has been shown to increase the activity of GSK3β, which leads to an increase in phosphorylation of tau and apoptotic cell death, further exacerbating AD pathology (Diniz et al., 2013). Thus, since it is generally acknowledged that LiCl Inhibits GSK3β, treatment with LiCl would potentially abolish Aβ mediated cell death and tau hyper-phosphorylation. Moreover, our findings are consistent with a study showing that LiCl inhibits the generation of Aβ peptide in neuronal cells and animal models that overexpress APP (Phiel et al., 2003). Notably, the combination treatment of GB and LiCl also leads to a reduction in APP, BACE and Aβ protein expression. However, the combination treatments did not necessarily manifest an additional clearance effect compared to the single treatments. This can be explained, at least in part, by the fact that administrated in isolation, GB and LiCl resulted in a reduction of the amyloidogenic proteins. Overall, induction of autophagy by GB in the presence and absence of LiCl prior to Aβ aggregation would potentially ameliorate Aβ-induced cytotoxicity. Therefore, if autophagy is induced by GB in the presence and absence of LiCl, prior to the manifestation of cellular stress, it may indeed act against Aβ-mediated cytotoxicity and display neuroprotective effects. Our results support this notion.

4.5 Gingko biloba treatment prevents Aβ induced apoptosis

The release of cytochrome-c from mitochondria is a vital step in the generation of the apoptosome, which in turn initiates the apoptosis caspase cascade. As a result, assessment of cytochrome-c can serve as an indication for the engagement of the upstream apoptotic machinery (Galluzzi et al., 2017), while assessment of caspase-3 is indicative of the execution step of apoptosis, since caspase-3 is a key effector protease. Our results presented a marked increase in cleaved caspase-3 and cytochrome-c after BA exposure, signifying induction of apoptosis (Fig 3.5 A & B). This is line with a study that showed a similar activation of caspase 3 and release of cytochrome-c following exposure to BA (Luo et al., 2002). This data supports the notion that the activation of apoptosis is due to the enhanced synthesis of Aβ in the N2aswe mutant cells. Our TEM data also support this notion, demonstrated by the disruption of the nuclear integrity and loss of regular cytoplasmic content. Indeed, nuclei fragmentation, membrane blebbing, chromosomal DNA cleavage, and cell shrinkage are characteristics of apoptosis (Fig 3.3.3) (Edinger and Thompson, 2004). However, exposure to both GB and LiCl significantly reduced the release of cytochrome-c and slightly decreased the cleavage of caspsase-3 (Fig 3.5 A & B). It is thus reasonable to conclude that both GB and LiCl impact the apoptotic machinery upstream of cytochrome-c release and fail, at the time point of investigation, to alter the pro-apoptotic caspase cascade, demonstrated by the non-significant effect on protein expression of

cleaved-caspase-3. Since cytochrome-c is initially released, followed by caspase 3 activation, hence, the effects we observe may indicate the cascade events of apoptosis. Later time points may be utilized in future work to confirm this. These findings further suggest that both GB and LiCl play a role in the preservation of the mitochondrial membrane potential. This is consistent with the finding that PC12 cells treated with GB (EGB 761) resulted in the prevention of cytochrome-c release from the mitochondria and fragmentation of DNA (Smith et al., 2002). Smith et al also found that GB (EGB 761) significantly inhibited the cleavage and activation of caspase-3, whereas in our study GB treated cells slightly suppressed the cleavage of caspase-3. GB Extract (EGB71) has also been shown to block apoptosis through the apoptosis-inducing factor signal transduction pathway and transcription Bcl-2 anti-apoptotic protein (Ba and Min, 2015). Luo et al. (2002) demonstrated that 48 hrs exposure to EGb761 prior to the induction of APP expression by BA, apoptosis was attenuated in neuroblastoma Swedish cells (Luo et al., 2002). LiCl has been shown to increase the activity of Bcl-2 which in turn regulates cell survival by inhibiting apoptotic genes such as p53 and Bax protein (Wei et al., 2000). Moreover, since LiCl increases the activity of Bcl-2, this protein to able to prevent the release of cytochrome-c and thereby prevent apoptosis. These findings raise the possibility that both LiCl and GB prevent the induction of the apoptosis cascade at multiple levels and cellular pathways.

4.6 Gingko biloba treatment preserves mitochondrial fission and fusion dynamics

It is well established that Aβ protein aggregates impair mitochondrial function (Diana et al., 2008). For this reason, we aimed to assess the effect of GB treatment in the presence and absence of LiCl treatment on mitochondrial fission and fusion dynamics. When the mitochondria are healthy, an equilibrium exists between the fusion and fission state, which enables their intracellular movement (Laura et al., 2014). Interestingly, under control conditions, our cells appear to favour a fission state revealed by the higher protein expression of DRP1 compared to MNF1 (Fig 3.6.1 A & B). However, TMRE micrographs demonstrated that morphologically, the cells display a mitochondrial network that is highly fused, yet, DRP1 levels are high. These data indicate strongly that protein levels that control mitochondrial equilibrium states between fission and fusion do not by themselves dictate a particular morphology. Although this result was unexpected, they are, however, in accordance with a study that reported that fibroblasts collected from AD sporadic patients expressed less DRP1 levels and displayed a network of elongated mitochondria (Wand et al., 2008). We believe that these cells were under conditions where the removal of damaged mitochondria was achieved through the fission process. During this process, damaged mitochondria are separated into smaller fragments, thereby making it more likely for these

organelles to be targeted for degradation through autophagy, in a process referred to as mitophagy (Laura et al., 2014). Importantly, under control conditions, we found that exposure to LiCl and GB favored the fusion state of the mitochondrial network and decreased the expression of DRP1 fission protein, indicating that these treatment interventions promote healthy functioning mitochondria (Fig 3.6.1B). This effect was however only statistically significant when the cells were exposed to LiCl and GB +LiCl. This is important since in sporadic AD, the impairment of mitochondria is reported to be the primary event that causes the deposition of Aβ (Swerdlow et al., 2010). Hence, the preservation of mitochondria by GB and LiCl is important to prevent Aβ deposition. In addition, these findings raise the possibility that LiCl greatly impacts the functioning of mitochondria. Since mitochondrial fusion favours the distribution of ATP in metabolically active cells (Westermann, 2010), this could also suggest that LiCl favours the production of ATP. This finding is of importance, since mitochondrial function is necessary for cellular metabolism, as sustained ATP synthesis is integral part to maintaining normal cellular function, cellular viability and homeostasis.

Exposure to BA significantly reduced the protein expression of MNF1 compared to control cells which corresponded to the marked increase in the protein levels of DRP1 (Fig 3.6.1 A&B). These results indicate the induction of the APP transgene, resulting in the overexpression of Aβ, negatively impacting the functioning of mitochondria. This is consistent with a study reporting that neuroblastoma cells overexpressing APP displayed mitochondria that were predominantly fragmented with reduced DRP1 and OPA1 levels (Wang et al., 2008). This is also in accordance with a study that investigated the effect of Aβ on the mitochondria of neuroblastoma cells expressing APP and PS1 assessed using a Mitosensor (Luo et al., 2002). This study demonstrated that cells treated with BA predominately fluoresced green, indicating mitochondria undergoing apoptosis, whereas untreated cells fluoresced red indicative of mitochondria that are healthy and functional (Luo et al., 2002). Thus, this study demonstrated that BA induces Aβ-mediated damage to mitochondria. Under Aβ proteotoxicity, pre-treatment with LiCl and GB seemed to have minor effects on the fusion state of the mitochondrial network, however, the fission state was drastically reduced compared to BA only conditions. This is important, since a decrease in fission would also indicate and lead to an increase in fusion. Indeed, observations in literature suggest that supplementation with GB in neuroblastoma cells amends the performance of mitochondrial oxidative phosphorylation and attenuates Aβ toxicity (Eckert, 2012). GB was also reported exert protective effects by enhancing the production of ATP in these neurons.

The functionality of cells can be assessed by the network organization or morphology of mitochondria. Elongated, fused mitochondrial networks are associated with healthy viable

cells, while fragmented morphology is usually associated with stressed cells (Chan, 2006). Thus, the study of mitochondrial network dynamics is critical, since the morphology of mitochondria is associated with crucial cellular activities (Fig 3.6.2). Under control conditions, treatment with GB in the presence and absence of LiCl displayed a similar morphology (fused elongated mitochondria) compared to untreated cells. These results indicate that GB and LiCl do not alter the normal mitochondrial network organization (Fig 3.6.2) but only effect the diseased/proteotoxic state.

In contrast, exposure to BA displayed a dominant state of fragmented mitochondria, suggesting that BA favours the fission state of the mitochondrial network (Fig 3.6.2). This is consistent with another study that demonstrated that neuronal cells exposed to conditioned media from cells overexposing mutant APP lead to elevated mitochondrial fission states (Wang et al., 2008). Several studies have demonstrated that cells deficient in fusion proteins (i.e. MNF1) are susceptible to apoptotic cell death, and such cells display mitochondria that favour the fission state, hence extensive fragmentation (Lee et al., 2004). Moreover, Aβ protein aggregates have been shown to impair mitochondrial function (Diana et al., 2008). Rhein et al. (2010) showed that neuroblastoma cells overexpressing APP, displayed a strong decrease in the mitochondrial electron transport chain coupling and the respiratory capacity. However, we observed that GB treatment in the presence and absence of LiCl prior to BA exposure improved the morphology of mitochondria by displaying a mitochondrial population that is more fused and elongated (Fig 3.6.2). These findings suggest that GB and LiCl rescue and preserve the functionality of mitochondria. This is in accordance with a study demonstrating that neuronal cells supplemented with GB EGb761 were protected from hydrogen peroxide induced toxicity (Shi et al., 2010). Exposure to GB has been shown to enhance energy homeostasis and reduce the levels of ROS in neuroblastoma cells overexpressing APP (Rhein et al., 2010). Taken together, these results suggest that GB and LiCl have regulatory effects on mitochondria and their function.

4.7 Robust autophagy flux is vital under neurotoxic conditions to maintain cellular homeostasis

In an attempt to validate that autophagy is essential to maintain cellular functions and degrade toxic proteins such as Aβ and damaged organelles, we assessed how GB in the presence and absence of LiCl modulates autophagy during APP overexpression. Treatment with BA and BafA1 resulted in an increase in p62 and LC3-II protein levels compared to BA-only treated cells (Fig 3.7 A & B). This result suggests that autophagy is still functional even in the context of APP overexpression. In accordance with Nixon et al. (2005), an elevation of large autophagic vacuoles appeared to accumulate in dystrophic neurites in an electron

microscopy study on post mortem human brain samples from patients with AD. Our results, however, indicate that the presence of autophagic vesicles is indeed reflective of a still functional autophagy flux.

We observed that treatment with GB high (↑:200 µg/ml) followed by BA and BafA1 exposure manifested in a significant elevation of p62 and LC3-II protein expression compared to its relative BafA1 negative group and cells exposed to only BA and BafA1 (Fig 3.7 A &B). These results suggest that GB high (↑:200 µg/ml) induces autophagy in the context of APP overexpression and additionally upregulates autophagy beyond the basal autophagy of the cells under APP overexpression. This result suggests that treatment with GB (↑:200 µg/ml) leads to the highest autophagy flux, which is still functional even under APP overexpression. Importantly, cells treated with GB (↑:200 µg/ml) followed by BA and BafA1 treatment, resulted in a significant increase in p62 protein levels compared to cells treated with GB low (↓:10 µg/ml) followed by BA and BafA1 treatment. This is in accordance with a recent study by Qin et al. (2018) reporting that treatment with 5 g/ml of GB (EGb761), but not at a lower concentration (2.5 g/ml), significantly increased the protein level of LC3B-II in the cell lysate.

4.8 Inhibition of autophagy leads to the accumulation of amyloidogenic proteins

Under normal physiological conditions, generated and aggregated Aβ can be targeted for degradation by the autophagy system. However, defects in this system result in the accumulation of Aβ since it will no longer be removed. Moreover, the accumulation of Aβ within autophagosome vesicles has been reported to be exacerbated by the defective clearance of autophagosomes containing APP in AD, thereby inducing Aβ neurotoxicity and resulting in neuronal impairment (Yu et al., 2005). Therefore, in this sense, the ability of GB in the presence and absence of LiCl to enhance autophagy would be neuroprotective by facilitating the removal of Aβ aggregates.

In order to elucidate whether the amyloidogenic proteins, including APP, BACE and Aβ, are targeted by autophagy, western blot analysis was conducted to evaluate how the suppression of the autophagy pathway would impact the processing of APP in the presence and absence of BafA1 treatment. We anticipated that the elevation of APP, BACE and Aβ in response to BA exposure would be further increased when autophagy was inhibited with BafA1 treatment, and thereby suggesting that the turnover of these proteins is mediated by autophagy. To our surprise, the protein expression of APP, BACE and Aβ decreased in the presence of BA and BafA1 treatment compared to cells only treated with BA (Fig 3.8 A, B and C). These findings suggest that the basal autophagy of these cells is too low to degrade the accumulated amyloidogenic proteins, which are clearly generated in excess when

overexpressed. The system may hence be overloaded with protein cargo. However, it could also suggest that basal autophagy is not fully functional during APP overexpression, thereby being unable to clear APP, BACE and Aβ sufficiently. This is, however, unlikely the case, since we observed that LC3-II and p62 protein levels were increased during APP overexpression and inhibition of autophagosome turnover. Another study also demonstrated that APP protein levels were unaltered in beclin deficient AD transgenic mice (Pickford et al., 2008). However, others have reported that during APP overexpression, the accumulation of Aβ has been shown to increase mTOR signalling, which in turn may further increase Aβ accumulation by blocking autophagy (Caccamo et al., 2017). It has also been reported that autophagic vacuoles may be a source of Aβ production and that autophagic vacuoles accumulate in AD brains and in APP/PS1 transgenic mice, thus suggesting that an increase in autophagy may in fact lead to a further accumulation of Aβ (Boland et al., 2008; Yu et al., 2005). In contrast, other, and most reports show that autophagy protects neurons from Aβ toxicity (Hung et al., 2009; Pickford et al., 2008).

Pickford et al. (2008), showed that increasing autophagy by overexpressing beclin-1, a key protein involved in autophagy induction, reduces Aβ deposits in a transgenic model of AD. Since GB (↑:200 µg/ml) yielded the highest upregulation of autophagy in the context of APP overexpression (Fig. 3.8 A & B), we hypothesised that it would therefore clear APP, BACE and Aβ the strongest, and hence the inhibition of autophagy would cause these proteins to accumulate most. Indeed, exposure to GB (↑:200 µg/ml) plus BA and BafA1 presented with a significant increase in APP and BACE protein expression and a non-significant increase in Aβ protein levels compared to cells treated with BA and BafA1 (Fig 3.8). Thus, these aggregate-prone proteins are distinct confirmed autophagy substrates. Interestingly, in an *in vitro* study of Huntingtin disease, treatment with BafA1 did not influence the expression of polyglutamin aggregates and protein levels of LC3-II, when treated with GB (EGb761) in HEK293 cells expressing htt Q103 (soluble polyQ proteins) (Stark and Beh, 2014). The authors suggest that autophagy had no impact on polyglutamin aggregate levels.

Importantly, cells treated with GB (↑:200 µg/ml) followed by BA and BafA1 treatment resulted in an increase in APP protein levels compared to cells treated with GB low (↓:10 µg/ml) followed by BA and BafA1 treatment. These results suggest that GB (↑:200 µg/ml) clears APP through autophagy stronger than GB low (↓:10 µg/ml), suggesting a concentration dependent effect of GB on protein clearance via autophagy. These findings are consistent with another study reporting that 0.5 g/ml of rapamycin was insufficient to completely abolish p70S6K phosphorylation and significantly reduced mTOR activity, and that the biggest decrease in Aβ levels was detected when rapamycin was used at a much higher concentration (50 g/ml) (Caccamo et al., 2010). Interestingly, in our study, the protein

expression of Aβ remained unaltered even in the presence of BafA1, although exposure to GB (↑:200 µg/ml) in the absence and presence of LiCl and GB low (↓:10µg/ml) only in the presence of LiCl displayed a trend of increased Aβ protein levels. This is consistent with a study showing that although rapamycin was successful in decreasing intracellular Aβ42 levels, this effect was abolished in the presence of an autophagy inhibitor and in the presence of 3-methyladenine (autophagy inhibitor) (Xue et al., 2013). Overall, our results suggest that APP, BACE and Aβ are targeted by the autophagic machinery, serving as substrates for protein degradation through autophagy. Moreover, we have shown that GB ameliorates Aβ pathology by increasing autophagy. Thus, our data support the theory that an increase in autophagy may have a beneficial effect in AD pathogenesis.

4.9 Autophagy upregulation by GB attenuates Aβ mediated cell death

The role of autophagy in chronic neurodegeneration appears to be complex. Autophagy, when too high and highly active for too long, represents a bona fide programmed cell death pathway, and could thereby theoretically contribute to neuronal loss in chronic neurodegeneration (Mok et al., 2007). In fact, autophagy has been implicated as a mechanism of neurodegeneration in prion disease (Sikorska et al., 2004). However, since autophagy is most often protective (Hara et al., 2006; Komatsu et al., 2006), we hypothesized that the inhibition of autophagy by BafA1 would result in the elevation of cytochrome-c release during APP overexpression. To our surprise, exposure to BA results in a degree of cell death which was, however, not augmented by BafA1 exposure (Fig 3.9 A). However, a trend of increased cytochrome-c protein expression was displayed when autophagy was inhibited by BafA1, suggesting that the cells are dependent on the autophagy pathway to delay the onset of cell death. Exposure to GB high (↑:200 µg/ml) during APP overexpression in the presence of BafA1, resulted in more release of cytochrome-c compared to cells treated with BA and BafA1 (Fig 3.9 A). Importantly, this effect was also apparent in cells treated with GB low (↓:10 µg/ml) during APP overexpression in the presence of BafA1. Taken together, these results suggest that autophagy induction by GB high (↑:200 µg/ml) is essential to prevent the trigger of apoptosis This is consistent with studies that reported that impairment of autophagy is associated with neuronal death and neurological abnormalities (Hara et al., 2006; Komatsu et al., 2006). Hence, autophagy is essential for maintenance of normal CNS functions. Therefore, if autophagy is induced by GB in the presence and absence of LiCl, before the manifestation of cellular stress, it acts against Aβ-mediated cytotoxicity and displays neuroprotective effects.

4.10 The role of autophagy in oxidative stress

Since it is a generally acknowledged phenomenon that oxidative stress is linked to AD, and since GB displays well established anti-oxidative properties, we propose that GB would relay neuroprotective effects by attenuating oxidative stress (i.e. lipid peroxidation) (Chan et al., 2007). Aβ targets microglia to induce a neuro-inflammatory response, and modulates its own metabolism (Huang and Mucke, 2012). Therefore, exposure to BA would indeed initiate oxidative stress and cytotoxicity, and subsequently increase peroxidation of proteins. In fact, exposure to BA caused an increase in 4HNE protein expression which was further augmented when autophagy was inhibited (Fig 3.9 B). Pre-treatment with LiCl and GB high (↑:200 µg/ml) showed a degree of oxidative stress which was further elevated in the presence of BafA1. Importantly, GB high (↑:200 µg/ml) together with BA and BafA1 revealed increased 4HNE protein expression compared to GB low (↓:10 µg/ml) plus BA and BafA1 treatment. These results signify that during the high autophagy induction by GB high (↑:200 µg/ml) manifestation of cellular stress is involved, likely acting against Aβ-mediated cytotoxicity and displaying neuroprotective effects. This finding is consistent with a study that demonstrated that GB (EGB761) confers anti-oxidative properties in *in vitro* and *in vivo* models by directly attenuating ROS levels and increasing the resistance of model organisms to oxidative stress (Smith and Luo 2003; Wu et al., 2002). Additionally, work by Schindowski et al., (2001) demonstrates that treatment with EGb761 *in vivo* and *in vitro* model systems has anti-inflammatory and antioxidant properties and enhances cerebral blood flow. In AD transgenic mice, Aβ aggregation and oxidative stress induced by Aβ has been shown to be attenuated by EGb761 supplementation (Shi, 2010). Another study has shown how GB (EGb 761) dose-dependently (10-100µg/ml) protects hippocampal neurons against Aβ-induced toxicity (impacting ROS and apoptosis), with highest and complete protection at the highest dose (Bastianetto et al., 2000). Taken together, these results indicate that GB's neuroprotective role is partly related to its antioxidant properties, demonstrating its potential effect in Aβ-induced neurodegenerative diseases such as AD.

CHAPTER 5: SUMMARY AND CONCLUSION

Although research efforts have intensified in the last decade, AD remains greatly understudied and poorly documented, especially in the context of South Africa. Moreover, despite advances in unravelling the biological underpinnings of AD pathology, to date there are no disease-modifying therapies available for those affected. This highlights the substantial need for dedicated research efforts toward the development of better targeted AD therapeutic interventions that are strongly aligned with the molecular defect and may potentially modify the progression of the disease. Recently, the role of proteotoxicity and autophagy dysfunction in the context of neurodegeneration has received major attention. As such, defects within the autophagic system is associated with the onset of neurodegenerative diseases, including AD (Wong and Cuervo, 2010). However, the relationship between candidate drugs of interest and autophagy activity remains unclear. This study therefore aimed to investigate the effect of both GB and LiCl as a single or combined treatment intervention on the modulation of autophagy activity, and the effect on Aβ proteotoxicity in an *in vitro* model of AD. It was hypothesized that treatment with GB will exhibit a concentration-dependent effect on autophagic activity, which can be further enhanced through combination treatment with LiCl. This effect will translate in the distinct removal of APP and Aβ, by preserving lysosomal function and mitochondrial integrity.

Our results indicated that GB induces autophagy in the presence and absence of LiCl, moreover indeed in a concentration-dependent manner, specifically with GB (↑:200 µg/ml) displaying highest induction of autophagy. Although we hypothesized that this effect will be further enhanced through combination treatment with LiCl, this was not always the case. Thus, more research is required to study the interaction of these two drugs. The induction of autophagy by GB further translated in the clearing of APP, BACE and Aβ, thus preventing Aβ-induced toxicity, which has been shown to be the main contributor of AD pathology. The assessment of the mitochondrial network and its morphology revealed that exposure to LiCl and GB in combination with LiCl favoured fusion states. Indeed, healthy mitochondria present a morphology of equilibrium between the fusion and fission states, which enables their intracellular movement (Laura et al., 2014). We also observed that APP overexpression impairs mitochondrial and lysosomal function, which was improved by GB treatment in the absence and presence of LiCl. Although the effect of GB in the presence and absence of LiCl on lysosomes is not fully verified, our results suggest that through the modulation of autophagy, the lysosomal abundance is somewhat impacted by GB exposure. We suggest that more specific techniques be used to assess lysosomal function, specifically to differentiate between damaged and healthy lysosomes.

In addition, GB pre-treatment resulted in the attenuation of Aβ-induced apoptosis by reduction in the release of cytochrome-c, hence serving as a protective mechanism. We hypothesised that this protective mechanism was brought about through the upregulation of autophagy. This notion was supported, since the release of cytochrome-c and lipid peroxidation was stronger when autophagy was inhibited. Moreover, APP, BACE and Aβ aggregates were elevated when the induction of autophagy by GB (↑:200 μg/ml) was inhibited.

In conclusion, the results presented here provide a molecular basis for Aβ -induced cell death, showing that GB, and more specifically, GB in combination with LiCl, an FDA approved drug, reduces Aβ pathology, preserves lysosomal and mitochondrial function and thereby attenuates Aβ-induced cell death by upregulating autophagy. This finding may constitute a novel therapeutic approach to AD. In addition, even though both concentrations of GB result in a similar degree of protection, their effect on protein clearance through autophagy, and autophagy activity is different. We therefore recommend that the individuals suffering from AD, or those susceptible to AD, are supplemented with the dose of GB which provides the highest clearance, highest protection and highest flux, which we reported as GB (↑:200μg/ml). For example, consumption of two capsules instead of one capsule would be the most beneficial. Hence a suitably high, yet non-toxic concentration may be recommended as adjuvant treatment. This notion can be tested in patients by using patient derived cells, such as fibroblasts, to screen and choose the best suitable drug.

5.1 Summary diagram

5.1.1 Molecular defects in AD

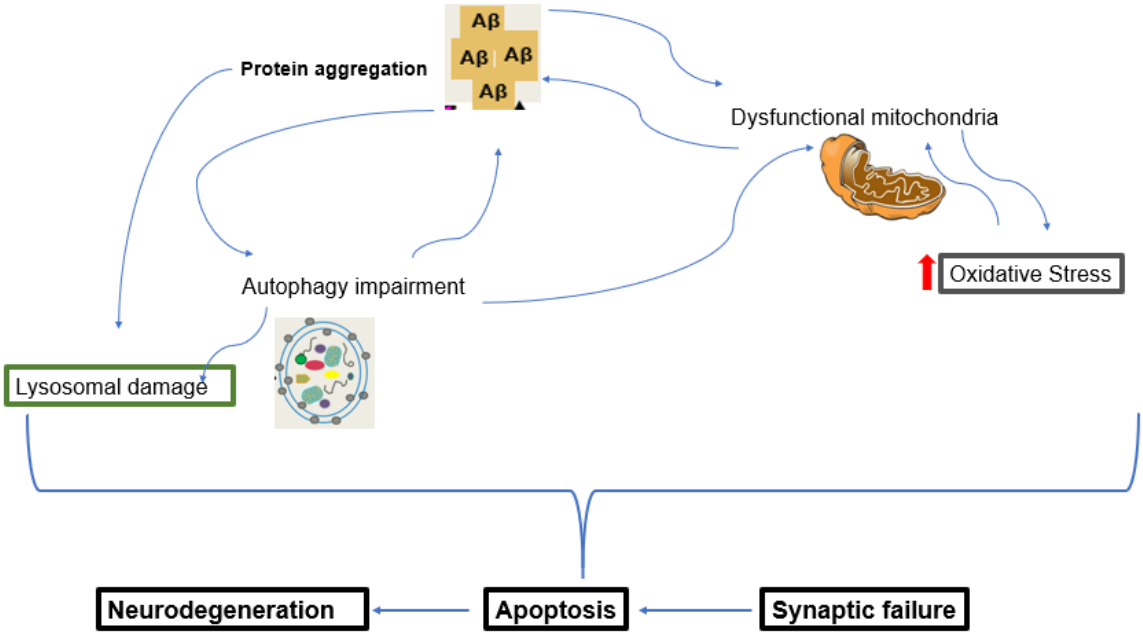

5.1.2 Proposed protective mechanism of GB in the presence and absence of LiCl.

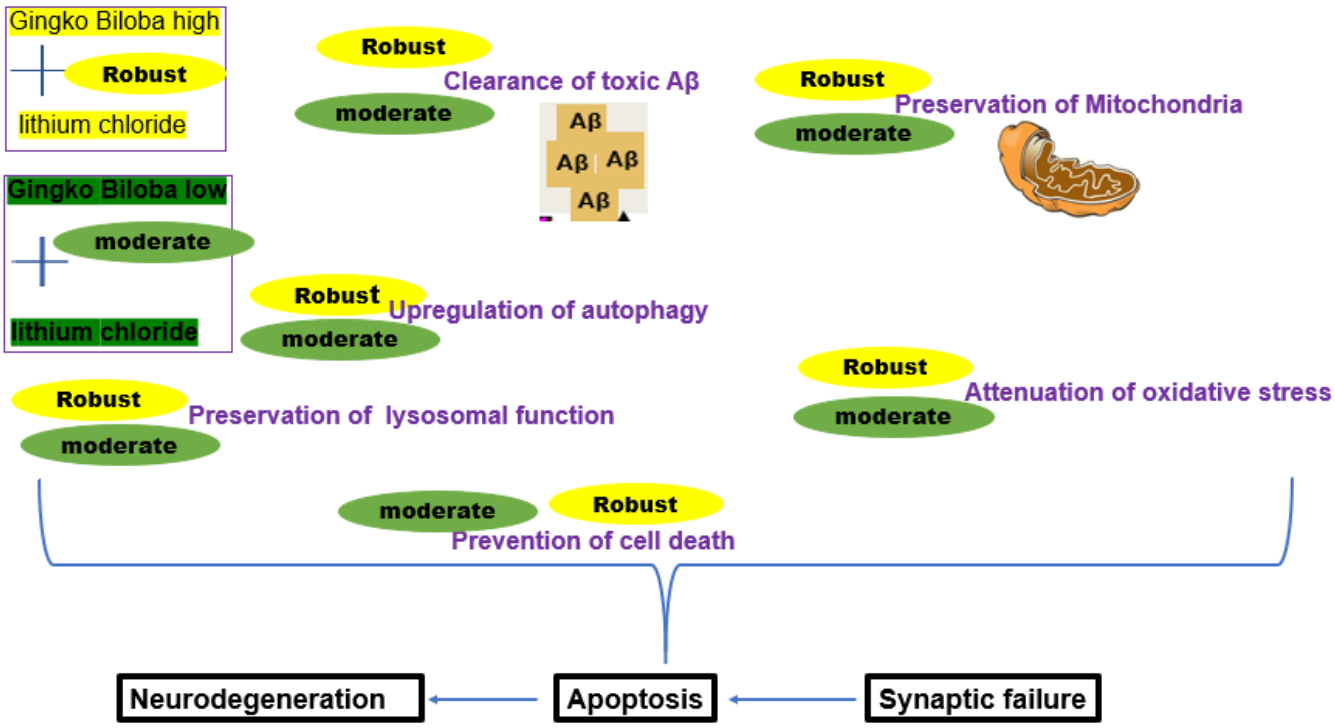

FUTURE RECOMMENDATIONS AND LIMITATIONS OF THE STUDY

It must be noted that the model system utilized is not without limitations. Firstly, the *in vitro* model of AD used in this study only represented late disease states, as APP overexpression was induced for 48 hrs. However, to better elucidate the scenario of the progression of AD, we propose that the investigation of early AD pathology (12 hrs APP overexpression) versus late AD pathology (48 hrs APP overexpression) be included, since this would have been better to mimic disease progression. However, the model system holds strength, as the deposition of Aβ peptide in the brain is an early event of AD progression and occurs years before AD symptoms manifest.

Although our study has demonstrated the importance of employing GB and LiCl supplements before any signs of AD may manifest, AD could be delayed or prevented by targeting Aβ peptide. Secondly, although a liquid chromatography–mass spectrometry was conducted in order to identify the composition of GB, we suggest that for further studies, each component is purified and assessed for its autophagy properties, as studies have shown that the different components of GB activate distinct pathways. Indeed, studies have demonstrated that the ginkgolides have several physiological properties (Yagmur et al., 2005). Moreover, we suggest that the molecular interaction between GB and LiCl be better evaluated, in order to more finely describe how their combination exerts protective effects. In addition, since extensive literature focused on the standardised GB leave extract EGb761, we suggest the assessment of the difference between the GB used in our study and the standard GB extract.

Although we believe that the GB used in our study, is a product available in health care and pharmacies in South Africa, mimics well what people indeed consume, and hence the results presented here are likely closely associated to what would be observed in an *in vivo* human response, caution should be taken when LiCl is administrated because it is also a mood disorder modulator (Baldessarini et al., 1999). Likewise, caution should be exercised with GB, as it is a platelet-activating factor antagonist which could have side effects for individuals with blood disorders (Yagmur et al., 2005). Ntsapi Although this study demonstrated that GB induces autophagy in the presence and absence of LiCl, the precise rate of autophagy, i.e. autophagic flux as described recently remains unclarified (du Toit et al., 2018). This could be done through a combination of life cell imaging and through TEM analysis, measuring the number of autophagosomes that are produced and then also quantifying the surface area of autolysosomes (Eskelinen et al., 2011). Alternatively, the GFP-LC3-RFP-LC3ΔG probe could be used, which is a fusion protein of GFP-LC3 and RFP-LC3 and was developed by Kaizuka et al. (2016) to better assess autophagic flux. We also recommend that the BafA1 incubation time to be longer, to allow more time for autophagosome accumulation to take place.

We also suggest that the defects in the autophagy-lysosomal pathway be localized, to precisely identify which step of the autophagy process the treatment intervention needs to target. For future studies, to fully elucidate the pool of damaged lysosomes versus healthy lysosomes, the protein expression of Galectin-3, which is reported to accumulate in damaged lysosomes, could be compared with the protein expression of LAMP2a protein levels (Maejima et al., 2013). In addition, in an attempt to elucidate the effect of APP over expression on mitochondria, additional mitochondrial parameters, such as mitochondrial respiration in response to APP overexpression, could be conducted. Finally, the assessment of changes in the shape, size, distribution and movement of mitochondria through life-cell time lapse analysis would provide additional context as to how APP overexpression impacts mitochondria.

REFERENCES

- Augustin, S., Rimbach, G., Augustin, K., Schliebs, R., Wolffram, S. and Cermak, R., 2009. Effect of a short-and long-term treatment with Ginkgo biloba extract on amyloid precursor protein levels in a transgenic mouse model relevant to Alzheimer's disease. *Archives of biochemistry and biophysics*, *481*(2): 177-182.
- Avila, J., Lucas, J.J., Perez, M.A.R. and Hernandez, F., 2004. Role of tau protein in both physiological and pathological conditions. *Physiological reviews*, *84*(2): 361-384.
- Bastianetto, S., Zheng, W.H. and Quirion, R., 2000. The Ginkgo biloba extract (EGb 761) protects and rescues hippocampal cells against nitric oxide-induced toxicity: involvement of its flavonoid constituents and protein kinase C. *Journal of neurochemistry*, *74*(6):2268-2277.
- Beck, S. and Stengel, J., 2016. Mass spectrometric imaging of flavonoid glycosides and biflavonoids in Ginkgo biloba L. *Phytochemistry*, (*130)*: 201-206.
- Behl, C., Davis, J.B., Klier, F.G. and Schubert, D., 1994. Amyloid β peptide induces necrosis rather than apoptosis. *Brain research*, *645*(1-2): 253-264
- Biswas, R., 2014. Regulation of silica-induced pulmonary inflammation.
- Boland B, Kumar A, Lee S, Platt FM, Wegiel J, Yu WH *et al*. Autophagy induction and autophagosome clearance in neurons: relationship to autophagic pathology in Alzheimer's disease. J Neurosci. 2008; (28, 27): 6926-6937.
- Boya, P. and Kroemer, G., 2008. Lysosomal membrane permeabilization in cell death. *Oncogene*, *27*(50): 6434.
- Caccamo A, Majumder S, Richardson A, Strong R and Oddo S. 2010; Molecular interplay between mammalian target of rapamycin (mTOR), amyloid-β, and Tau: effects on cognitive impairments. J Biol Chem, (285): 13107–13120.
- Cao, C., Su, Y., Han, D., Gao, Y., Zhang, M., Chen, H. and Xu, A., 2017. Ginkgo biloba exocarp extracts induces apoptosis in Lewis lung cancer cells involving MAPK signaling pathways. *Journal of ethnopharmacology*, (*198)*: 379-388.
- Chalecka-Franaszek, E., Chen, H. and Chuang, D.M., 1999. 5-Hydroxytryptamine2A receptor stimulation induces activator protein-1 and cyclic AMP-responsive element binding with cyclic AMP-responsive element-binding protein and Jun D as common components in cerebellar neurons. *Neuroscience*, *88*(3): 885-898.
- Criollo, A., Vicencio, J.M., Tasdemir, E., Maiuri, M.C., Lavandero, S. and Kroemer, G., 2007. The inositol trisphosphate receptor in the control of autophagy. *Autophagy*, *3*(4): 350-353.

- Cuervo, A.M., Bergamini, E., Brunk, U.T., Dröge, W., Ffrench, M. and Terman, A., 2005. Autophagy and aging: the importance of maintaining" clean" cells. *Autophagy*, *1*(3): 131-140.
- Ding, S., Dudley, E., Plummer, S., Tang, J., Newton, R.P. & Brenton, A.G. 2006. Quantitative determination of major active components in Ginkgo biloba dietary supplements by liquid chromatography / mass spectrometry. 2753–2760.
- Diniz, B.S., Machado-Vieira, R. and Forlenza, O.V., 2013. Lithium and neuroprotection: translational evidence and implications for the treatment of neuropsychiatric disorders. *Neuropsychiatric disease and treatment*, (*9*): 493.
- Dries, V.V., Stygelbout, V., Pierrot, N., Yilmaz, Z., Suain, V., De Decker, R., Buée, L., Octave, J.N., Brion, J.P. and Leroy, K., 2017. Amyloid precursor protein reduction enhances the formation of neurofibrillary tangles in a mutant tau transgenic mouse model. *Neurobiology of aging*, (*55)*: 202-212.
- Fontaine, S.N., Sabbagh, J.J., Baker, J., Martinez-Licha, C.R., Darling, A. and Dickey, C.A., 2015. Cellular factors modulating the mechanism of tau protein aggregation. *Cellular and molecular life sciences*, *72*(10): 1863-1879.
- Forlenza, O.V., De-Paula, V.D.J.R. and Diniz, B.S.O., 2014. Neuroprotective effects of lithium: implications for the treatment of Alzheimer's disease and related neurodegenerative disorders. *ACS chemical neuroscience*, *5*(6): 443-450.
- Forlenza, O.V., Diniz, B.S., Radanovic, M., Santos, F.S., Talib, L.L. and Gattaz, W.F., 2011. Disease-modifying properties of long-term lithium treatment for amnestic mild cognitive impairment: randomised controlled trial. *The British Journal of Psychiatry*, *198*(5): 351-356.
- Fornai, F., Longone, P., Cafaro, L., Kastsiuchenka, O., Ferrucci, M., Manca, M.L., Lazzeri, G., Spalloni, A., Bellio, N., Lenzi, P. and Modugno, N., 2008. Lithium delays progression of amyotrophic lateral sclerosis. *Proceedings of the National Academy of Sciences*, *105*(6): 2052-2057.
- Friedlander, R.M., 2003. Apoptosis and caspases in neurodegenerative diseases. *New England Journal of Medicine*, *348*(14): 365-1375.
- Funderburk, S.F., Marcellino, B.K. and Yue, Z., 2010. Cell "self-eating"(autophagy) mechanism in Alzheimer's disease. *Mount Sinai Journal of Medicine: A Journal of Translational and Personalized Medicine: A Journal of Translational and Personalized Medicine*, *77*(1): 59-68.

- Galluzzi, L., Baehrecke, E.H., Ballabio, A., Boya, P., Bravo-San Pedro, J.M., Cecconi, F., Choi, A.M., Chu, C.T., Codogno, P., Colombo, M.I. and Cuervo, A.M., 2017. Molecular definitions of autophagy and related processes. *The EMBO journal*, *36*(13), pp.1811-1836.
- Galluzzi, L., Bravo-San Pedro, J.M., Levine, B., Green, D.R. and Kroemer, G., 2017. Pharmacological modulation of autophagy: therapeutic potential and persisting obstacles. *Nature reviews Drug discovery*, *16*(7): 487.
- Gerenu, G., Liu, K., Chojnacki, J.E., Saathoff, J.M., Martínez-Martín, P., Perry, G., Zhu, X., Lee, H.G. and Zhang, S., 2015. Curcumin/Melatonin Hybrid 5-(4-Hydroxy-phenyl)-3-oxo-pentanoic Acid [2-(5-Methoxy-1 H-indol-3-yl)-ethyl]-amide Ameliorates AD-Like Pathology in the APP/PS1 Mouse Model. *ACS chemical neuroscience*, *6*(8): 1393-1399.
- Gervais, F.G., Xu, D., Robertson, G.S., Vaillancourt, J.P., Zhu, Y., Huang, J., LeBlanc, A., Smith, D., Rigby, M., Shearman, M.S. and Clarke, E.E., 1999. Involvement of caspases in proteolytic cleavage of Alzheimer's amyloid-β precursor protein and amyloidogenic Aβ peptide formation. *Cell*, *97*(3): 395-406.
- Hara T, Nakamura K, Matsui M, Yamamoto A, Nakahara Y, Suzuki-Migishima R *et al.* Suppression of basal autophagy in neural cells causes neurodegenerative disease in mice. Nature. 2006; 441, 7095: 885-889.
- Hardy, J., 1997. Amyloid, the presenilins and Alzheimer's disease. *Trends in neurosciences*, *20*(4):154-159.
- Hardy, J.A. and Higgins, G.A., 1992. Alzheimer's disease: the amyloid cascade hypothesis. *Science*, *256*(5054): 184-186.
- Hartl FU and Hayer-Hartl M. Converging concepts of protein folding in vitro and in vivo. Nat Struct Mol Biol. 2009; 16, 6: 574-581..
- Hyttinen, J.M., Amadio, M., Viiri, J., Pascale, A., Salminen, A. and Kaarniranta, K., 2014. Clearance of misfolded and aggregated proteins by aggrephagy and implications for aggregation diseases. *Ageing research reviews*, *18*: 16-28.
- Kabeya Y, Mizushima N, Ueno T, Yamamoto A, Kirisako T, Noda T *et al.* LC3, a mammalian homologue of yeast Apg8p, is localized in autophagosome membranes after processing. EBMO J. 2000; 19, 21: 5720-5728.
- Kellett, K.A. and Hooper, N.M., 2009. Prion protein and Alzheimer disease. *Prion*, *3*(4): 190-194.
- Kessing, L.V., Gerds, T.A., Knudsen, N.N., Jørgensen, L.F., Kristiansen, S.M., Voutchkova, D., Ernstsen, V., Schullehner, J., Hansen, B., Andersen, P.K. and

Ersbøll, A.K., 2017. Association of lithium in drinking water with the incidence of dementia. *JAMA psychiatry*, *74*(10): 1005-1010.

- Klionsky, D.J. and Ohsumi, Y., 1999. Vacuolar import of proteins and organelles from the cytoplasm. *Annual review of cell and developmental biology*, *15*(1), pp.1-32.
- Komatsu M, Waguri S, Koike M, Sou YS, Ueno T, Hara T *et al*. Homeostatic levels of p62 control cytoplasmic inclusion body formation in autophagy-deficient mice. Cell. 2007; 131: 1149–1163.
- Komatsu M, Waguri S, Ueno T, Iwata J, Murata S, Tanida I *et al.* Impairment of starvation-induced and constitutive autophagy in Atg7-deficient mice. J Cell Biol. 2005; 169, 3: 425-434.
- Lee JH, Yu WH, Kumar A, Lee S, Mohan PS, Peterhoff CM *et al*. Lysosomal proteolysis and autophagy require presenilin 1 and are disrupted by Alzheimer-related PS1 mutations. Cell. 2010; 141, 7: 1146-1158.
- Lee YJ, Jeong SY, Karbowski M, Smith CL and Youle RJ. Roles of the mammalian mitochondrial fission and fusion mediators Fis1, Drp1, and Opa1 in apoptosis. Mol Biol Cell. 2004; 15, 11: 5001-5011.
- Le Bars, P.L., Kieser, M. and Itil, K.Z., 2000. A 26-week analysis of a double-blind, placebo-controlled trial of the Ginkgo biloba extract EGb 761® in dementia. *Dementia and geriatric cognitive disorders*, *11*(4), pp.230-237.
- Lipinski MM, Zheng B, Lu T, Yan Z, Py BF, Ng A *et al*. Genome-wide analysis reveals mechanisms modulating autophagy in normal brain aging and in Alzheimer's disease. PNAS. 2010; 107, 32: 14164-14169.
- Lipton SA. Failures and successes of NMDA receptor antagonists: molecular basis for the use of open-channel blockers like memantine in the treatment of acute and chronic neurologic insults. NeuroRx. 2004; (1, 1): 101-110.
- Liu, X., Hao, W., Qin, Y., Decker, Y., Wang, X., Burkart, M., Schötz, K., Menger, M.D., Fassbender, K. and Liu, Y., 2015. Long-term treatment with Ginkgo biloba extract EGb 761 improves symptoms and pathology in a transgenic mouse model of Alzheimer's disease. *Brain, behavior, and immunity*, (*46*)121-131
- Lleó, A., 2007. Current therapeutic options for Alzheimer's disease. *Current genomics*, *8*(8): 550-558.
- Lockshin RA and Zakeri Z. Apoptosis, autophagy, and more. Int J Biochem. 2004; 36: 2405-2419.
- Loos B and Engelbrecht AM. Cell death. Autophagy. 2009; 5, 5: 590-603.
- Loos B, Engelbrecht AM, Lockshin RA, Klionsky DJ and Zakeri Z. The variability of autophagy and cell death susceptibility. Autophagy. 2013; 9, 9: 1270-1285.

- Mariño G, Pietrocola F, Eisenberg T, Kong Y, Malik SA, Andryushkova, A *et al*. Regulation of autophagy by cytosolic acetyl-coenzyme A. Mol Cell. 2014; 53, 5:710-725.
- Luo, J.L., Lu, F.L., Liu, Y.C., Shih, Y.C. and Lo, C.F., 2013. Fingerprint Analysis of Ginkgo biloba Extract and Ginkgo semen in Preparations by LC-Q-TOF/MS. *Journal of Food & Drug Analysis*, *21*(1).
- Luo, Y., Smith, J.V., Paramasivam, V., Burdick, A., Curry, K.J., Buford, J.P., Khan, I., Netzer, W.J., Xu, H. and Butko, P., 2002. Inhibition of amyloid-β aggregation and caspase-3 activation by the Ginkgo biloba extract EGb761. *Proceedings of the National Academy of Sciences*, *99*(19): 12197-12202.
- Maejima, I., Takahashi, A., Omori, H., Kimura, T., Takabatake, Y., Saitoh, T., Yamamoto, A., Hamasaki, M., Noda, T., Isaka, Y. and Yoshimori, T., 2013. Autophagy sequesters damaged lysosomes to control lysosomal biogenesis and kidney injury. *The EMBO journal*, *32*(17): 2336-2347.
- Melendez, A. and Levine, B., 2009. Autophagy in C. elegans. *WormBook*, *24*, pp.1-26.
- Mizushima N and Yoshimori T. How to interpret LC3 immunoblotting. Autophagy. 2007; 3, 6: 542-545.
- Mizushima N, Yamamoto A, Matsui M, Yoshimori T and Ohsumi Y. In vivo analysis of autophagy in response to nutrient starvation using transgenic mice expressing a fluorescent autophagosome marker. Mol Biol Cell. 2004; 15, 3: 1101-1111.
- Mizushima N, Yoshimori T and Levine B. Methods in mammalian autophagy research. Cell. 2010; 140, 3: 313-326.
- Mok, S.W., Riemer, C., Madela, K., Hsu, D.K., Liu, F.T., Gültner, S., Heise, I. and Baier, M., 2007. Role of galectin-3 in prion infections of the CNS. *Biochemical and biophysical research communications*, *359*(3): 672-678.

- Nixon RA. Autophagy, amyloidogenesis and Alzheimer disease. J Cell Sci. 2007; 120: 4081-4091.
- Nixon RA and Yang DS. Autophagy failure in Alzheimer's disease – locating the primary defect. Neurobiol Dis. 2011; 43, 1: 38-45.
- Nixon RA, Wegiel J, Kumar A, Yu WH, Peterhoff C, Cataldo A, *et al.* Extensive involvement of autophagy in Alzheimer disease: and immune-electron microscopy study. J Neuropathol Exp Neurol. 2005; 64, 2: 133-122.
- O'Brien RJ and Wong PC. Amyloid precursor protein processing and Alzheimer's disease. Annu Rev Neurosci. 2011; 34: 185-204.

- Ntsapi, C., Lumkwana, D., Swart, C., du Toit, A. and Loos, B., 2018. New insights into autophagy dysfunction related to amyloid beta toxicity and neuropathology in Alzheimer's disease. In *International review of cell and molecular biology* (336): 321-361. Academic Press.
- Ntsapi, C., Swart, C., Lumkwana, D. and Loos, B., 2016. Autophagic Flux Failure in Neurodegeneration: Identifying the Defect and Compensating Flux Offset. In *Autophagy in Current Trends in Cellular Physiology and Pathology*. IntechOpen.
- Paillard, T., Rolland, Y. and de Souto Barreto, P., 2015. Protective effects of physical exercise in Alzheimer's disease and Parkinson's disease: a narrative review. *Journal of clinical neurology*, *11*(3): 212-219.
- Pagani, Lucia & Eckert, Anne. (2011). Amyloid-Beta Interaction with Mitochondria. International journal of Alzheimer's disease. 2011. 925050. 10.4061/2011/925050.
- Paradis, E., Douillard, H., Koutroumanis, M., Goodyer, C. and LeBlanc, A., 1996. Amyloid β peptide of Alzheimer's disease downregulates Bcl-2 and upregulates Bax expression in human neurons. *Journal of Neuroscience*, *16*(23): 7533-7539.
- Park, H.K., Chu, K., Jung, K.H., Lee, S.T., Bahn, J.J., Kim, M., Lee, S.K. and Roh, J.K., 2009. Autophagy is involved in the ischemic preconditioning. *Neuroscience letters*, *451*(1): 16-19.
- Parr, C., Carzaniga, R., Gentleman, S.M., Van Leuven, F., Walter, J. and Sastre, M., 2012. Glycogen synthase kinase 3 inhibition promotes lysosomal biogenesis and autophagic degradation of the amyloid-β precursor protein. *Molecular and cellular biology*, *32*(21): 4410-4418.
- Paz, I., Sachse, M., Dupont, N., Mounier, J., Cederfur, C., Enninga, J., Leffler, H., Poirier, F., Prevost, M.C., Lafont, F. and Sansonetti, P., 2010. Galectin-3, a marker for vacuole lysis by invasive pathogens. *Cellular microbiology*, *12*(4): 530-544.
- Phiel, C.J., Wilson, C.A., Lee, V.M.Y. and Klein, P.S., 2003. GSK-3α regulates production of Alzheimer's disease amyloid-β peptides. *Nature*, *423*(6938): 435.
- Pickford, F., Masliah, E., Britschgi, M., Lucin, K., Narasimhan, R., Jaeger, P.A., Small, S., Spencer, B., Rockenstein, E., Levine, B. and Wyss-Coray, T., 2008. The autophagy-related protein beclin 1 shows reduced expression in early Alzheimer disease and regulates amyloid β accumulation in mice. *The Journal of clinical investigation*, *118*(6): 2190-2199.
- Pierre, S.V., Lesnik, P., Moreau, M., Bonello, L., Droy-Lefaix, M.T., Sennoune, S., Duran, M.J., Pressley, T.A., Sampol, J., Chapman, J. and Maixent, J.M., 2008. The standardized Ginkgo biloba extract Egb-761 protects vascular endothelium exposed

to oxidized low density lipoproteins. *Cell Mol Biol (Noisy-le-grand)*, *54*(Suppl): OL1032-OL1042.

- Ravikumar B, Sarkar S, Davies JE, Futter M, Garcia-Arencibia M, Green-Thompson ZW *et al.* Regulation of mammalian autophagy in physiology and pathophysiology. Physiol Rev. 2010; 90: 1383-1435.
- Ravikumar, B., Vacher, C., Berger, Z., Davies, J.E., Luo, S., Oroz, L.G., Scaravilli, F., Easton, D.F., Duden, R., O'Kane, C.J. and Rubinsztein, D.C., 2004. Inhibition of mTOR induces autophagy and reduces toxicity of polyglutamine expansions in fly and mouse models of Huntington disease. *Nature genetics*, *36*(6): 585.
- Reagan-Shaw, S., Nihal, M. and Ahmad, N., 2008. Dose translation from animal to human studies revisited. *The FASEB journal*, *22*(3): 659-661.
- Renna, M., Jimenez-Sanchez, M., Sarkar, S. and Rubinsztein, D.C., 2010. Chemical inducers of autophagy that enhance the clearance of mutant proteins in neurodegenerative diseases. *Journal of Biological Chemistry*, *285*(15): 11061-11067.
- Rhein, V., Giese, M., Baysang, G., Meier, F., Rao, S., Schulz, K.L., Hamburger, M. and Eckert, A., 2010. Ginkgo biloba extract ameliorates oxidative phosphorylation performance and rescues Aβ-induced failure. *PloS one*, *5*(8): e12359.
- Rodríguez-Navarro, J.A., Rodríguez, L., Casarejos, M.J., Solano, R.M., Gómez, A., Perucho, J., Cuervo, A.M., de Yébenes, J.G. and Mena, M.A., 2010. Trehalose ameliorates dopaminergic and tau pathology in parkin deleted/tau overexpressing mice through autophagy activation. *Neurobiology of disease*, *39*(3): 423-438.
- Pickford F, Masliah E, Britschgi M, Lucin K, Narasimhan R, Jaeger PA *et al.* The autophagy-related protein beclin 1 shows reduced expression in early Alzheimer disease and regulates amyloid β accumulation in mice. J Clin Invest. 2008; 118, 6: 2190-2199.
- Pérez, M., WANDOSELL, F., Javier, D.N. and AVILA, J., 2003. Prion peptide induces neuronal cell death through a pathway involving glycogen synthase kinase 3. *Biochemical Journal*, *372*(1): 129-136.
- Rose, C., Menzies, F.M., Renna, M., Acevedo-Arozena, A., Corrochano, S., Sadiq, O., Brown, S.D. and Rubinsztein, D.C., 2010. Rilmenidine attenuates toxicity of polyglutamine expansions in a mouse model of Huntington's disease. *Human molecular genetics*, *19*(11): 2144-2153.
- Salminen, A., Kaarniranta, K., Kauppinen, A., Ojala, J., Haapasalo, A., Soininen, H. and Hiltunen, M., 2013. Impaired autophagy and APP processing in Alzheimer's disease: the potential role of Beclin 1 interactome. *Progress in neurobiology*, *106*, pp.33-54.

- Sarkar, S., Floto, R.A., Berger, Z., Imarisio, S., Cordenier, A., Pasco, M., Cook, L.J. and Rubinsztein, D.C., 2005. Lithium induces autophagy by inhibiting inositol monophosphatase. *J Cell Biol*, *170*(7): 1101-1111.
- Sarkar, S., Krishna, G., Imarisio, S., Saiki, S., O'Kane, C.J. and Rubinsztein, D.C., 2007. A rational mechanism for combination treatment of Huntington's disease using lithium and rapamycin. *Human molecular genetics*, *17*(2): 170-178.
- Sarkar, S., Ravikumar, B., Floto, R.A. and Rubinsztein, D.C., 2009. Rapamycin and mTOR-independent autophagy inducers ameliorate toxicity of polyglutamine-expanded huntingtin and related proteinopathies. *Cell death and differentiation*, *16*(1): 46.
- Scholey, A.B. and Kennedy, D.O., 2002. Acute, dose-dependent cognitive effects of Ginkgo biloba, Panax ginseng and their combination in healthy young volunteers: differential interactions with cognitive demand. *Human Psychopharmacology: Clinical and Experimental*, *17*(1): 35-44.
- Swerdlow, R.H., 2007. Mitochondria in cybrids containing mtDNA from persons with mitochondriopathies. *Journal of neuroscience research*, *85*(15):.3416-3428.
- Selkoe, D.J. 1998. The cell biology of precursor protein and presenilin in Alzheimer ' s disease. 8924(98):447–453.
- Napolitano, G., Johnson, J.L., He, J., Rocca, C.J., Monfregola, J., Pestonjamasp, K., Cherqui, S. and Catz, S.D., 2015. Impairment of chaperone-mediated autophagy leads to selective lysosomal degradation defects in the lysosomal storage disease cystinosis. *EMBO molecular medicine*, *7*(2): 158-174.
- Shimada, K., Motoi, Y., Ishiguro, K., Kambe, T., Matsumoto, S.E., Itaya, M., Kunichika, M., Mori, H., Shinohara, A., Chiba, M. and Mizuno, Y., 2012. Long-term oral lithium treatment attenuates motor disturbance in tauopathy model mice: implications of autophagy promotion. *Neurobiology of disease*, *46*(1): 101-108.
- Shin, J.Y., Yu, S.B., Yu, U.Y., Ahnjo, S.M. and Ahn, J.H., 2010. Swedish mutation within amyloid precursor protein modulates global gene expression towards the pathogenesis of Alzheimers disease. *BMB reports*, *43*(10): 704-709.
- Shuli, S., Yongmei, Z., Zhiwei, Z. and Zhijuan, J., 2001. β-Amyloid and its binding protein in the hippocampus of diabetic mice: effect of APP17 peptide. *Neuroreport*, *12*(15): 3317-3319.
- Singh, B., Kaur, P., Singh, R.D. and Ahuja, P.S., 2008. Biology and chemistry of Ginkgo biloba. *Fitoterapia*, *79*(6): 401-418.
- Smith, J.V. and Luo, Y., 2004. Studies on molecular mechanisms of Ginkgo biloba extract. *Applied microbiology and biotechnology*, *64*(4): 465-472.

- Son, S.M., Song, H., Byun, J., Park, K.S., Jang, H.C., Park, Y.J. and Mook-Jung, I., 2012. Accumulation of autophagosomes contributes to enhanced amyloidogenic APP processing under insulin-resistant conditions. *Autophagy*, *8*(12): 1842-1844.
- Spilman, P., Podlutskaya, N., Hart, M.J., Debnath, J., Gorostiza, O., Bredesen, D., Richardson, A., Strong, R. and Galvan, V., 2010. Inhibition of mTOR by rapamycin abolishes cognitive deficits and reduces amyloid-β levels in a mouse model of Alzheimer's disease. *PloS one*, *5*(4): e9979.
- Stambolic, V., Ruel, L. and Woodgett, J.R., 1996. Lithium inhibits glycogen synthase kinase-3 activity and mimics wingless signalling in intact cells. *Current biology*, *6*(12): 1664-1669.
- Stark, M. and Behl, C., 2014. The ginkgo biloba extract Egb 761 modulates proteasome activity and polyglutamine protein aggregation. *Evidence-Based Complementary and Alternative Medicine*, *2014*.
- Swaminathan, G., Zhu, W. and Plowey, E.D., 2016. BECN1/Beclin 1 sorts cell-surface APP/amyloid β precursor protein for lysosomal degradation. *Autophagy*, *12*(12): 2404-2419.
- Swart, C., Du Toit, A. and Loos, B., 2016. Autophagy and the invisible line between life and death. *European journal of cell biology*, *95*(12): 598-610.
- Swart, C., Haylett, W., Kinnear, C., Johnson, G., Bardien, S. and Loos, B., 2014. Neurodegenerative disorders: dysregulation of a carefully maintained balance?. *Experimental gerontology*, *58*: 279-291.
- Swart, C., Khoza, A., Khan, K., Roux, S.L. and du Plessis, A., 2017. Investigating Basal Autophagic Activity in Brain Regions Associated with Neurodegeneration using.
- Swart, C., Du Toit, A. and Loos, B., 2016. Autophagy and the invisible line between life and death. *European journal of cell biology*, *95*(12): 598-610.
- Sweeney, P., Park, H., Baumann, M., Dunlop, J., Frydman, J., Kopito, R., McCampbell, A., Leblanc, G., Venkateswaran, A., Nurmi, A. and Hodgson, R., 2017. Protein misfolding in neurodegenerative diseases: implications and strategies. *Translational neurodegeneration*, *6*(1): 6.
- Swerdlow, R.H., Burns, J.M. and Khan, S.M., 2014. The Alzheimer's disease mitochondrial cascade hypothesis: progress and perspectives. *Biochimica et Biophysica Acta (BBA)-Molecular Basis of Disease*, *1842*(8): 1219-1231.
- Tanaka, K.I., Fujita, N., Yoshioka, M. and Ogawa, N., 2001. Immunosuppressive and non-immunosuppressive immunophilin ligands improve H2O2-induced cell damage by increasing glutathione levels in NG108-15 cells. *Brain research*, *889*(1-2): 225-228.

- Tchantchou, F., Lacor, P.N., Cao, Z., Lao, L., Hou, Y., Cui, C., Klein, W.L. and Luo, Y., 2009. Stimulation of neurogenesis and synaptogenesis by bilobalide and quercetin via common final pathway in hippocampal neurons. *Journal of Alzheimer's Disease*, *18*(4): 787-798.
- Tchantchou, F., Xu, Y., Wu, Y., Christen, Y. and Luo, Y., 2007. EGb 761 enhances adult hippocampal neurogenesis and phosphorylation of CREB in transgenic mouse model of Alzheimer's disease. *The FASEB Journal*, *21*(10): 2400-2408.
- Tsang, C.K., Qi, H., Liu, L.F. and Zheng, X.S., 2007. Targeting mammalian target of rapamycin (mTOR) for health and diseases. *Drug discovery today*, *12*(3-4): 112-124.
- Uchiyama, Y., Koike, M., Shibata, M. and Sasaki, M., 2009. Autophagic neuron death. *Methods in enzymology*, *453*: 33-51.
- Ude, C., Schubert-Zsilavecz, M. and Wurglics, M., 2013. Ginkgo biloba extracts: a review of the pharmacokinetics of the active ingredients. *Clinical Pharmacokinetics*, *52*(9): 727-749.
- Underwood, B.R., Imarisio, S., Fleming, A., Rose, C., Krishna, G., Heard, P., Quick, M., Korolchuk, V.I., Renna, M., Sarkar, S. and García-Arencibia, M., 2010. Antioxidants can inhibit basal autophagy and enhance neurodegeneration in models of polyglutamine disease. *Human molecular genetics*, *19*(17): 3413-3429.
- Waldemar, G., Dubois, B., Emre, M., Georges, J., McKeith, I.G., Rossor, M., Scheltens, P., Tariska, P. and Winblad, B., 2007. Recommendations for the diagnosis and management of Alzheimer's disease and other disorders associated with dementia: EFNS guideline. *European Journal of Neurology*, *14*(1): e1-e26.
- Wang, S., Ouyang, B., Aa, J., Geng, J., Fei, F., Wang, P., Wang, J., Peng, Y., Geng, T., Li, Y. and Huang, W., 2016. Pharmacokinetics and tissue distribution of ginkgolide A, ginkgolide B, and ginkgolide K after intravenous infusion of ginkgo diterpene lactones in a rat model. *Journal of pharmaceutical and biomedical analysis*, *126*: 109-116.
- Wang, X., Su, B.O., Fujioka, H. and Zhu, X., 2008. Dynamin-like protein 1 reduction underlies mitochondrial morphology and distribution abnormalities in fibroblasts from sporadic Alzheimer's disease patients. *The American journal of pathology*, *173*(2): 470-482.
- Weikel, K.A., Cacicedo, J.M., Ruderman, N.B. and Ido, Y., 2016. Knockdown of GSK3β increases basal autophagy and AMPK signalling in nutrient-laden human aortic endothelial cells. *Bioscience reports*, *36*(5): e00382.

- Westrate, L.M., Drocco, J.A., Martin, K.R., Hlavacek, W.S. and MacKeigan, J.P., 2014. Mitochondrial morphological features are associated with fission and fusion events. *PLoS One*, *9*(4): e95265.
- White, E. and DiPaola, R.S., 2009. The double-edged sword of autophagy modulation in cancer. *Clinical cancer research*, *15*(17): 5308-5316.
- Wong, E. and Cuervo, A.M., 2010. Autophagy gone awry in neurodegenerative diseases. *Nature neuroscience*, *13*(7): 805.
- Wu, Y., Wu, Z., Butko, P., Christen, Y., Lambert, M.P., Klein, W.L., Link, C.D. and Luo, Y., 2006. Amyloid-β-induced pathological behaviors are suppressed by Ginkgo biloba extract EGb 761 and ginkgolides in transgenic Caenorhabditis elegans. *Journal of Neuroscience*, *26*(50): 13102-13113.
- Wurz, J., 2016. *The role of ketone bodies in autophagic flux, cellular energetics and injury-induced neurotoxicity* (Doctoral dissertation, Stellenbosch: Stellenbosch University).
- Xiao, Q., Wang, C., Li, J., Hou, Q., Li, J., Ma, J., Wang, W. and Wang, Z., 2010. Ginkgolide B protects hippocampal neurons from apoptosis induced by beta-amyloid 25–35 partly via up-regulation of brain-derived neurotrophic factor. *European journal of pharmacology*, *647*(1-3): 48-54.
- Xie, L., Kang, H., Xu, Q., Chen, M.J., Liao, Y., Thiyagarajan, M., O'Donnell, J., Christensen, D.J., Nicholson, C., Iliff, J.J. and Takano, T., 2013. Sleep drives metabolite clearance from the adult brain. *science*, *342*(6156): 373-377.
- Xiong, N., Jia, M., Chen, C., Xiong, J., Zhang, Z., Huang, J., Hou, L., Yang, H., Cao, X., Liang, Z. and Sun, S., 2011. Potential autophagy enhancers attenuate rotenone-induced toxicity in SH-SY5Y. *Neuroscience*, *199* :292-302.
- Xue, Z., Zhang, S., Huang, L., He, Y., Fang, R. and Fang, Y., 2013. Upexpression of Beclin-1-dependent autophagy protects against beta-amyloid-induced cell injury in PC12 cells. *Journal of Molecular Neuroscience*, *51*(1): 180-186.
- Yagmur, E., Piatkowski, A., Gröger, A., Pallua, N., Gressner, A.M. and Kiefer, P., 2005. Bleeding complication under Gingko biloba medication. *American journal of hematology*, *79*(4): 343-344.
- Yang, D.S., Kumar, A., Stavrides, P., Peterson, J., Peterhoff, C.M., Pawlik, M., Levy, E., Cataldo, A.M. and Nixon, R.A., 2008. Neuronal apoptosis and autophagy cross talk in aging PS/APP mice, a model of Alzheimer's disease. *The American journal of pathology*, *173*(3): 665-681.
- Yao, Z.X., Drieu, K. and Papadopoulos, V., 2001. The Ginkgo biloba extract EGb 761 rescues the PC12 neuronal cells from β-amyloid-induced cell death by inhibiting the

formation of β-amyloid-derived diffusible neurotoxic ligands. *Brain research*, *889*(1-2): 181-190.

- Yao, Z.X., Han, Z., Drieu, K. and Papadopoulos, V., 2004. Ginkgo biloba extract (Egb 761) inhibits β-amyloid production by lowering free cholesterol levels. *The Journal of nutritional biochemistry*, *15*(12):749-756.
- Yin, B., Liang, H., Chen, Y., Chu, K., Huang, L., Fang, L., Matro, E., Jiang, W. and Luo, B., 2013. EGB1212 post-treatment ameliorates hippocampal CA1 neuronal death and memory impairment induced by transient global cerebral ischemia/reperfusion. *The American journal of Chinese medicine*, *41*(06):1329-1341.
- Youmans, K.L., Tai, L.M., Kanekiyo, T., Stine Jr, W.B., Michon, S.C., Nwabuisi-Heath, E., Manelli, A.M., Fu, Y., Riordan, S., Eimer, W.A. and Binder, L., 2012. Intraneuronal Aβ detection in 5xFAD mice by a new Aβ-specific antibody. *Molecular neurodegeneration*, *7*(1):8.
- Yu, W.H., 2005. Cuervo AM, Kumar A, Peterhoff CM, Schmidt SD, Lee JH, Mohan PS, Mercken M, Farmery MR, Tjernberg LO, Jiang Y, Duff K, Uchiyama Y, Naslund J, Mathews PM, Cataldo AM, Nixon RA. *Macroautophagy–a novel Beta-amyloid peptide-generating pathway activated in Alzheimer's disease. J Cell Biol*, *171*: 87-98.
- Zhang, X., Chen, S., Song, L., Tang, Y., Shen, Y., Jia, L. and Le, W., 2014. MTOR-independent, autophagic enhancer trehalose prolongs motor neuron survival and ameliorates the autophagic flux defect in a mouse model of amyotrophic lateral sclerosis. *Autophagy*, *10*(4): 588-602.
- Zhou, X., Qi, Y. and Chen, T., 2017. Long-term pre-treatment of antioxidant Ginkgo biloba extract EGb-761 attenuates cerebral-ischemia-induced neuronal damage in aged mice. *Biomedicine & Pharmacotherapy*, *85*: 256-263.
- Zuroff, L., Daley, D., Black, K.L. and Koronyo-Hamaoui, M., 2017. Clearance of cerebral Aβ in Alzheimer's disease: reassessing the role of microglia and monocytes. *Cellular and Molecular Life Sciences*, *74*(12), pp.2167-2201.

Appendix

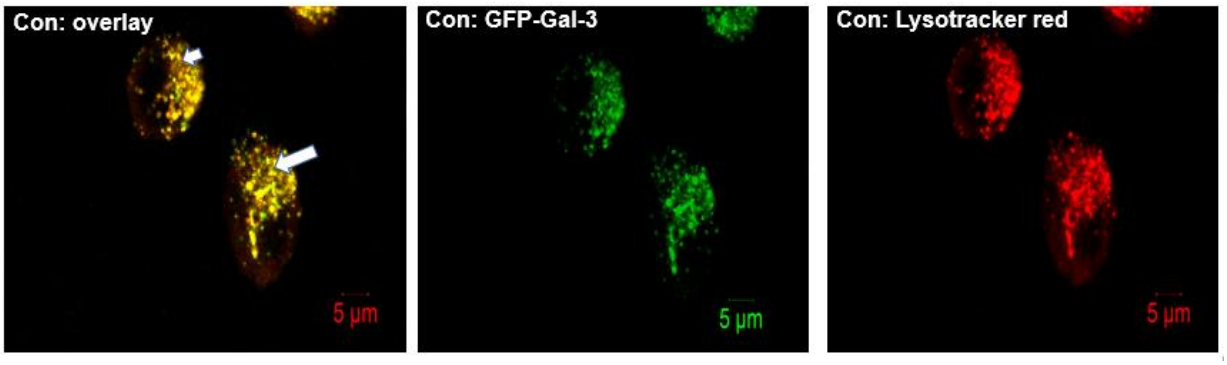

Supplementary results

Figure S1: Representative micrographs of N2a cells transfected with GFP-Galectin3 (GFP-Gal3) and counterstained with lysotracker red. Under control conditions (Con) and following treatment with Butyric acid (BA: 48H 5mM), Lithium chloride (Licl: 24 hrs 10 mM), Ginkgo biloba (GB 10ug/ml or 200ug/ml) or Butyric acid in the presence of Lithium chloride or Ginkgo biloba (BA + Licl: 48 H 5mM + Post-24H 10 mM). Red = Lysotracker, green = GFP-Galectin-3 . 60X magnification. Scale bar = 5 µm. Arrowheads indicate Gal3 positive lysosomes.

Protocols

Neuronal reductive capacity following ketone body treatment

With the guidance by literature, a dose response of Gingko biloba (GB) and lithium chloride (LiCl) was established. This was done to verify that the desirable concentration of both treatment groups was not toxic to the cells. Under control conditions, the reductive capacity was considered as 100% and no significant differences in cells treated with both GB and LiCl was yielded in comparison to control conditions.

Wst-1 assay

- The WST-1 should be warmed to 37 °C
- 5% of WST-1 of the well volume should be added to pre-warmed complete medium
- Discard the medium all the wells of 48-well plates
- Using a sterile P200 pipette tip, 200 µl of pre-warmed medium comprising of WST-1 should be placed in each well
- Plate should be wrapped in foil
- Incubate for 2 hrs at 37 °C (5% CO_2)
- The absorbance measured at 450 nm using a microplate reader

Transfection with ATeam indicator

- Seed cells at a density of 500 cells per well in NUNC 8-well chamber dishes
- Allow to adhere overnight
- Refresh the medium
- Make up **Mix 1** and **Mix 2** in two separate 0.5 ml eppies
- **Mix 1:** Add 1µL DNA (to obtain 800 ng DNA concentration), 100 µL serum-free medium, and 2 µL P3000 reagent to Eppendorf tube
- **Mix 2:** Add 1 µL lipofectamine and 100 µL serum-free medium to eppie (cold reagents)
- vortex both eppies Briefly
- Add **Mix 1** to **Mix 2** and vortex
- Incubate for 5 min at room temperature
- Add 50 µL of the transfection medium to each well
- Incubate for 48 hrs at 37 °C, 5% CO_2, refreshing medium 1 h after addition of the transfection medium to minimize exposure to the toxic transfection reagent
- Image cells 48 - 72 hrs after transfection
- Discard media
- Wash chamber twice with fresh media
- Add lysotracker (light sensitive) and fresh media
- Wrap 8-chamber plate with foil and incubate for 2H
- Add 2ul of Hoechst to each well in the 8-chamber plate for 10min (remember to cover with foil).

Compounds	EPPIE 1	EPPIE 2
GFP-galectin3	(1/773,8 ng/ul) X (800 DNA concentration) = 1ul	NA
P3000	1ul per well	NA
Serum free media	50ul per well	50ul per well
Lipofectamine	NA	0.5ul per well

Treatment	Working Concentration	Treatment volume	Media	Time
BA	5mM	22.85ul	50ml	48 H
LiCl	10mM	500ul	50ml	24H
BAF	400nM			
Lysotracker	75nM	0.0150ul in 200ul	(8-well chamber=200ul/well)	2H
Hoechst		1ul	(8-well chamber=200ul/well)	10min (before imaging)
Silica	250mg/ml			3Hrs
TMRE	500 nM			20min before imaging)

Seeding densities

Consumable	Cells per well	Media volume	Time
T-25			
T-75 (blots)	500000 cells		48 H treatment
24well-plate		500ul	
48well-plate	2500 cells	500ul	48 H treatment
96well plate	1000 cells	150ul	48H treatment
48well-plate	5000 cells	500ul	24H treatment
8-well chamber	500 cells	200ul	48 H treatment

Treatment	STOCK	Working Concentration
BA	10.94M	5mM
GB	(Current) 3150ug (2) 23000ug (3) 1388ug (4) 14620ug	100ug (low) 400ug (high)
LiCl	1M	10mM
BAF	200uM	400nM

Lysotracker (light sensitive)	1mM	75nM
Hoechst	0.5µg/ml	
Silica	500mg/ml	250mg/ml
TMRE	25mM	500 nM

Lysotracker : Media

- 0.075ul: 1000ul Media

Hoescht: Media

- 1ul:200ul Media

TMRE: Media

- 1ul:1000ul
- 1ul:1000ul
- Add 1ul of TMRE to 1000ul Media
- From this solution take 1ul and add it to another 1000ul of media

Conversions

- 1mM=1000000nM
- 1ml=1000ul
- 1ug=1000mg
- C1V1=C2V2
- 1um=1000nM

Media usage

Experiment	**Confluency treatment**	**Total Media**	**Treatment**	**Total treatment volume**
Western Blot	70%	(12 T-75 X 12ml) =144ml (three 50ml Tubes of media)	GB (400ug) GB (100ug) LiCl (10mM)	

PROTEIN EXTRACTION

Base Constituents

- Tris-HCl (buffering agent prevents protein denaturation)
- NaCl (salt prevents non-specific protein aggregation)
- NP-40 (non-ionic detergent to extract proteins; 10% stock solution in H2O) or use Triton X-100
- Na-deoxycholate (ionic detergent to extract proteins; 10% stock solution in H2O; protect from light)
- pH to 9.0. Boil, cool, pH again to 9.0. Repeat until colourless

RIPA Protease Inhibitors

- Phenylmethylsulfonyl fluoride (PMSF) (200 mM stock solution in isopropanol; store at room temperature)
- EDTA (calcium chelator; 100 mM stock solution in H2O, pH 7.4)
- Leupeptin (store frozen in aliquots, 1 mg/ml in H2O)
- Aprotinin (store frozen in aliquots, 1 mg/ml in H2O)
- Pepstatin (store frozen in aliquots, 1 mg/ml in methanol)

RIPA Phosphatase Inhibitors

- Activated Na3VO4 (200 mM stock solution in H2O; see Sodium Orthovanadate Activation Protocol)
- NaF (200 mM stock solution: store at room temperature)
- **Reminder:** Do not add phosphatase inhibitors when preparing lysates for phosphatase assays.

RIPA Trypsin Inhibitors

- Soyabean Trypsin Inhibitor (SBTI) (1 mg/ml in 0.01 M phosphate buffer, pH 6.5 with 0.15M NaCl- freeze aliquots at -20^{O}C)
- Benzamidine (200mM stock solution -dissolve in distilled H2O – store at -20^{0}C)

Procedure:

Prepare 100 ml modified RIPA buffer as follows:

- Add 790 mg Tris base to 75 ml distilled H2O. Add 900 mg NaCl and stir the solution until all solids are dissolved. Using HCl, adjust the pH to 7.4.
- Add 10 ml of 10% NP-40 to the solution.
- Add 2.5 ml of 10% Na-deoxycholate and stir until solution is clear.
- Add 1 ml of 100 mM EDTA to the solution. Adjust the volume of the solution to 100 ml using a graduated cylinder.
- Preferably, the remaining protease/ phosphatase inhibitors should be added to the solution on the same day you are running the assay Therefore, it is best to aliquot the buffer in **10ml aliquots without the protease inhibitors** and store at 2-8° C.

RIPA with inhibitors

On day of use, thaw the required amount of RIPA buffer and add the appropriate volume of protease/phosphatase inhibitor cocktail to the amount of RIPA buffer. If metalloproteases are present in the tissue, add an appropriate volume of 0.5M EDTA if not included in the cocktail itself. Halt Protease & Phosphatase Inhibitor Cocktail is supplied, ready- made and 10ul is added to 10ml RIPA on day of tissue lysis. A vial of 0.5M EDTA is also supplied and it is added if necessary, also 10ul/10ml RIPA buffer on day of use.

Causation: PMSF is extremely unstable in aqueous solutions, with a half-life of approximately 30 minutes, and it should be added immediately before use.

Preparation of RIPA Buffer (modified RadioImmunoPrecipitAtion buffer) per T-75 Flask

- PI → 42ul
- Sodium Orthovanadate (Na3VO4, 200 mM stock solution) → 5ul
- NaF 200 mM stock solution: store at room temperature)→ 5ul
- Phenylmethylsulfonyl fluoride (PMSF, 200 mM stock solution) → 10ul (add last to cocktail, just before adding the RIPA cocktail to cell)

Materials & equipment

- Ice (Remember to always put samples on ice)
- 1.5ml eppendorf tubes (18)
- Aluminium Foil
- Homogenising tubes
- Scalpel blade
- Fine tweezers (forceps)

- Tissue homogeniser
- Sonicator
- RIPA buffer

Sample preparation and Protein determination

Direct Detect Infrared Spectrometer protein determination

Description	
Catalogue Number	DDHW00010-WW
Trade Name	Direct Detect
Description	Direct Detect Spectrometer
Overview	The Direct Detect™ infrared (IR)-based quantification system is an innovative combination of software-controlled instrumentation and EMD Millipore Corporation's advanced membrane technology, optimized for the detection and quantification of proteins. Biomolecules are applied directly to a card-based hydrophilic polytetrafluoroethylene (PTFE) membrane that is transparent in most of the infrared spectral region. The Direct Detect™ system measures amide bonds in protein chains, accurately quantifying an intrinsic component of every protein without relying on amino acid composition, dye binding properties, or redox potential. Protein concentrations from 0.2 to 5 mg/mL can accurately be determined from a minimal sample volume (2 µL) without bio- or immuno-chemical staining. Sample analysis takes only minutes and in most cases can be performed directly from the buffered or native solution.
Applications	
Application	By measuring amide bonds in protein chains, the Direct Detect Spectrometer system accurately determines an intrinsic component of every protein without relying on amino acid composition, dye binding or redox potential.

Applications	
Key Applications	Protein Quantitation

Components of Direct Detect Infrared Spectrometer

Figure 1. Components supplied

1A	Direct Detect™ spectrometer
1B	Instrument power adapter with 4 power cord/plug configurations (EU, UK, US, Japan)
1C	Data cable (crossover cable for 10Base-T Ethernet standard, with RJ45 connectors)
1D	Dell® Netbook computer with Direct Detect™ software installed
1E	Computer power adapter with world-wide plug adapter
1F	Netbook stand
1G	Direct Detect™ Assay-free cards (package of 50)
1H	Direct Detect™ spotting tray
	Desiccant pack replacement (1, not shown)
	Torx® TX20 screw driver for replacing the IR source (not shown)
	Direct Detect™ Spectrometer Quick Start Card (not shown)

Direct Detect Spectrometer- Sample measuring

- Place the Assay-free cards on the spotting tray or another clean surface
- Designate one spot for blank measurement (the blank is the buffer (RIPA buffer) used to prepare the protein, but there is no protein in it). By default, the Direct Detect software designates position 1 as the blank
- Pipette 2µL of blank into the centre of spot designated as the blank position. Pipette 2µL of samples to be analysed into the centre of remaining spots
- Insert Assay-free card vertically into the instrument card holder with the instrument and card arrows aligned. The instrument will move the card up and down and sound a tone. The green light illuminates to confirm proper insertion

- Input samples details into software measurements set up screen. Select method (three calibration methods are preloaded), input sample names
- Click on the measure card button
- If the Dry sample card option is chosen (recommended), the indicator light will remain yellow until the sample is dry
- The sample concentration will appear on the screen, along with the statistical analysis and spectrum plot
- After all, four positions on the card have been read, the instrument will sound a tone. The second card will rise to the initial position and can be removed

Below is the figure representing exact protocol

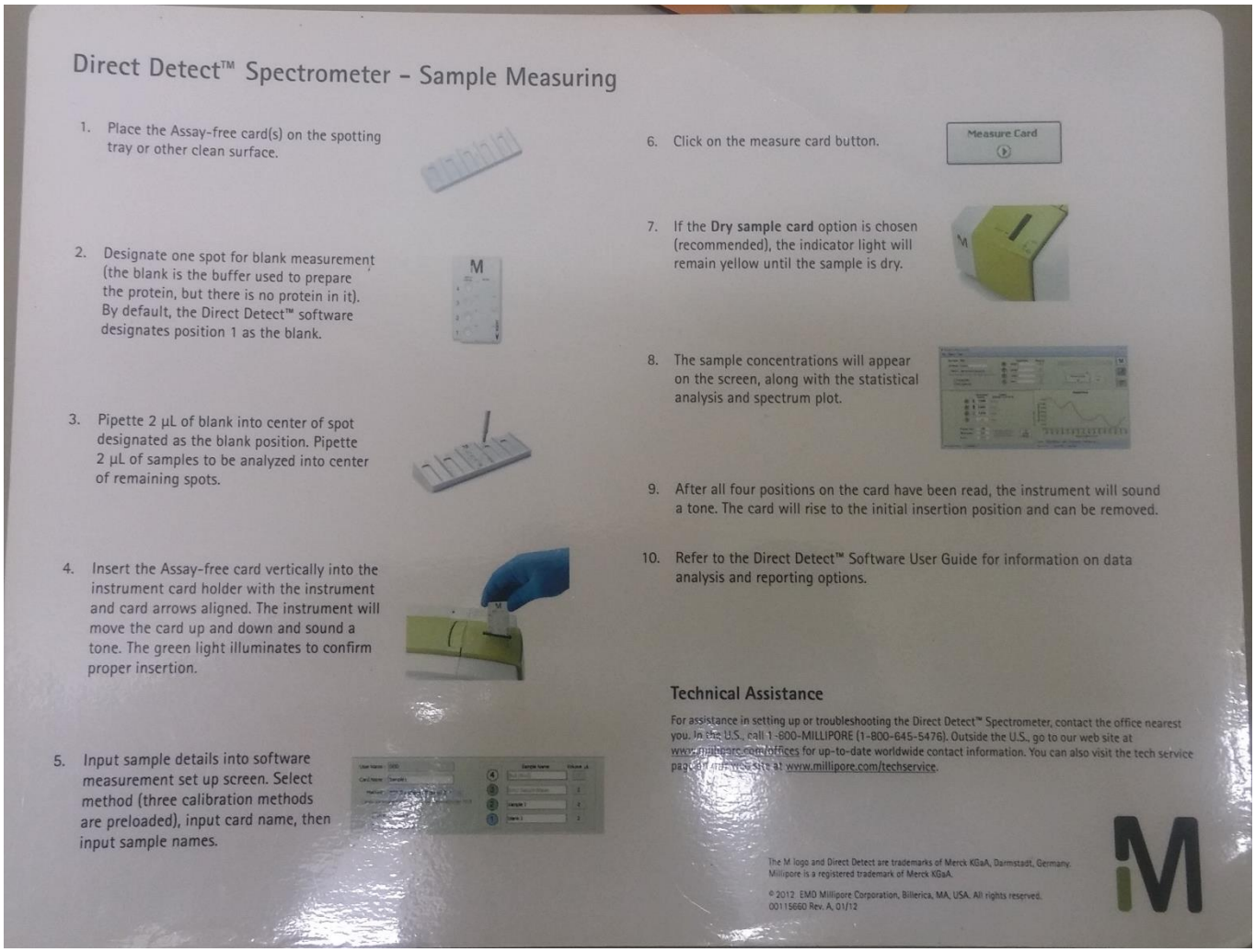

Direct Detect™ Spectrometer – Sample Measuring

1. Place the Assay-free card(s) on the spotting tray or other clean surface.

2. Designate one spot for blank measurement (the blank is the buffer used to prepare the protein, but there is no protein in it). By default, the Direct Detect™ software designates position 1 as the blank.

3. Pipette 2 µL of blank into center of spot designated as the blank position. Pipette 2 µL of samples to be analyzed into center of remaining spots.

4. Insert the Assay-free card vertically into the instrument card holder with the instrument and card arrows aligned. The instrument will move the card up and down and sound a tone. The green light illuminates to confirm proper insertion.

5. Input sample details into software measurement set up screen. Select method (three calibration methods are preloaded), input card name, then input sample names.

6. Click on the measure card button. (Measure Card)

7. If the **Dry sample card** option is chosen (recommended), the indicator light will remain yellow until the sample is dry.

8. The sample concentrations will appear on the screen, along with the statistical analysis and spectrum plot.

9. After all four positions on the card have been read, the instrument will sound a tone. The card will rise to the initial insertion position and can be removed.

10. Refer to the Direct Detect™ Software User Guide for information on data analysis and reporting options.

Technical Assistance

For assistance in setting up or troubleshooting the Direct Detect™ Spectrometer, contact the office nearest you. In the U.S., call 1-800-MILLIPORE (1-800-645-5476). Outside the U.S., go to our web site at www.millipore.com/offices for up-to-date worldwide contact information. You can also visit the tech service page at our web site at www.millipore.com/techservice.

00115660 Rev. A, 01/12

Sample Preparation

Laemmli's loading buffer

Solution A

- 38ml dH_2O
- 10ml 0.5M Tris (pH6.8) use HCl to pH.
- 8ml glycerol
- 16ml 10% SDS
- 4ml 0.05% (w/v) Bromophenol blue

Materials:

- Heat box (95°C)
- Syringe needle
- B-mercaptoethanol
- Ice and 1.5 mL
- eppendorf
- tubes
- Vortex
- Centrifuge

Protocol:

- Work out volume needed for samples (volume should be 40µg/µL) and then:
- Prepared in 2:1 ratio of protein sample + 3X Laemli's buffer (Sbuffer). Add Laemli's buffer should be added first followed by the protein sample (place tube on ice)
- Vortex the protein sample and the boil at 95°C for 5min
- Spin down samples for 10 seconds and place on ice
- Samples can now either be stored at -20°C for future use, or loaded onto the gels

Preparation of 12% BioRad Fast Cast Stain-Free gels according to instructions

- Assemble the gel casting stand using spacer and short plates
- Fill the gap between plates to the top with dH_2O using a disposable pipette
- Wait 5 min to check for leaks and readjust if necessary until watertight
- Remove the dH_2O by tipping the rig and use paper towel if necessary
- Make up the resolving and stacking gel according to the manufacturer's instructions
- Resolving gel (for one gel):

- Add 3 ml of both Buffer A and Buffer B into a small glass beaker
- 30 µl APS
- 3µl TEMED

- Stacking gel (for one gel):
  - Add 1 ml of Buffer A and Buffer B into a separate small glass beaker
  - 10 µl APS
  - 2 µl TEMED
- Mix the contents of both beakers thoroughly by swirling their contents
- Pour Resolver into the gel rig using a disposable pipette to approximately 1 cm from the top
- Pour the Stacker to the top using a new disposable pipette
- Insert the appropriate comb(s) gently, avoiding air bubbles
- Allow the gel(s) to set (30 min – 1 h)
- Use within three weeks
- Store at 4 °C and keep moist until use

Day 1

- Put on heat box (It takes 20min to reach 95°C)
- Before you start with the experiment verify if all the solutions are available in the lab
- Prepare 12% BioRad Fast Cast Stain-Free gels according to instructions
- (If it's not stain-free remember to add TCE)
- Gels can also be prepared in advance and kept in the fridge, by wrapping them in soaked paper towels and sealed in cling wrap
- Protein samples should be thawed on ice (NB proteins samples should always be on ice)
- Prepared in 2:1 ratio of protein sample + 3X Laemli's buffer (Sbuffer). Add Laemli's buffer should be added first followed by the protein sample (place tube on ice)
- Vortex the protein sample and the boil at 95°C for 5min
- Spin down samples for 10 seconds
- Assemble the gasket
- Gels should be assembled onto the gasket making sure the comb is facing inward
- Gasket should Fill the gasket with running buffer – check for leaks
- Carefully remove the combs and rinse out wells with P200 pipet (set to approx. 100 ul) and yellow tip
- Load ladder (4 ul BLUeye)
- Load samples

- Place gasket into tank and fill with running buffer (10x: dilute 900ml H_20 + 100ml running buffer). Re-fill gasket if necessary.
- Attach lid (black on black, red on red) and plug into power pack
- Run at 120 V for until you see blue dye runs down to bottom of the tank (this may take approximately 1h:45min
- When finished, activate the gel on ChemiDoc
- Gel activation protocol, 2.5 min
- Prepare for transfer (few min beforehand) on TurboBlot tray
- Place bottom part and roll out any bubbles
- Place the gel carefully on the bottom transfer pack
- Place top part of transfer pack
- Close with lid – be careful not to move lid while closing
- Transfer on TurboBlot according to desired settings
- Biorad defined LMWsetting generally works fine
- After transfer, disassemble stack
- Activate membrane on chemidoc
- Select Blots : Chemi : Stain-Free-Blot
- Mini-protein-gel
- Rinse in 100% methanol
- Air-dry membrane
- Becomes white
- Hold in fumehood for quicker drying
- Re-hydrate membrane in 100% methanol
- Until translucent, 10-15 sec
- Wash membrane in TBS-T 3x for 5 min
- Block membrane in 5% milk (prepared in TBS-T) for 1 hr with gentle shaking
- Wash membrane 3x for 5 min in TBS-T
- Incubate membrane on primary antibody O/N at 4°C
- Prepared in 50 ml centrifuge tube
- Dilute antibody in TBS-T to desired concentration, normally 1:1000
- 5ml TBS-T (5000ul) + 5ul primary AB
- Attach to rotators in walk-in fridge
- Make sure tube/s are straight and rotor is balanced

Day 2

- Retrieve membranes
- Stored primary antibody in fridge/freezer
- Wash membrane 3x 5 min in TBS-T
- Incubate membrane on secondary antibody for 1 hr at RT
- Prepared in 50 ml centrifuge tube
- Dilute antibody in TBS-T to desired concentration, normally 1:5000
- Place on roller in WB room
- Wash membrane 3x 5 min in TBS-T
- Develop
- Prepare minimum amount of ECL needed in eppie in 1:1 ratio
- Place membrane on Chemidoc and check position
- Add ECL to the desired area and roll to ensure even spread. Roll away excess ECL
- Expose using desired settings
- Place membrane on tray of Biorad Chemidoc, taking care to remove bubbles.

Image analysis:Image analysis on Chemi-Doc:

- Select “Image Lab” program from desktop on computer
- The start page will pop up – can choose an existing protocol or create a new one
- All protocol settings can be modified by selecting the item on the left under “Protocol Set Up”
- For self-poured gels: Select “Blot” and then select “Chemi” from drop down window.
- Next, set the imaging area to 12 x 9
- Specify the optimum exposure eg – “intense bands”
- Default colour is auto selected – you can change this if you want
- Select “Lane and Band Detection”
- Select either “Low” or “High” for intense or faint bands or use the “custom” slider to set exact sensitivity
- Select “Analyse MW” then select MW standard used, the lane it is in and the regression method (linear, semi-log)- if using Bio-Rad marker can analyse against this
- Generate a report: Specific output, then give a customised name and specify as to whether you want it printed or just displayed
- Get a protocol summary – if ok, save

- Load the gel into the imager and position it on the stage using the “position gel” button – this will show a live image of the gel’s position – can adjust by opening the **top door** of Chemi-doc (not the drawer where the gel is) -can adjust the zoom settings and position to get image exactly as you want it
- When happy with gel position, Click on “Run Protocol”
- Once protocol has run, the images and report will be displayed with all selected analyses applied
- Save the images wanted to an appropriate folder in documents.

Day 3

- Prepare Stripping Buffer
- 15g Glycine
- 10ml 10% SDS
- 10ml Tween-20
- 800ml dH_2O
- Set pH at 2.2 and adjust to final volume of 1l with dH_2O
- Stripping buffer protocol
- Wash membrane 2 x 10min with TBS-T
- Add stripping buffer and shake for 15min at RT
- Replace stripping buffer and shake for another 15min at RT
- Rinse membrane vigorously in TBS-T twice
- Wash membrane in TBS-T for ±15min
- Apply a final wash step of 3 x 5min in TBS-T
- Block membrane and continue with Ab probing

Base Constituents

- Tris-HCl (buffering agent prevents protein denaturation)
- NaCl (salt prevents non-specific protein aggregation)
- NP-40 (non-ionic detergent to extract proteins; 10% stock solution in H2O) or use Triton X-100
- Na-deoxycholate (ionic detergent to extract proteins; 10% stock solution in H2O; protect from light)